January 2015

Fabrication of Tissue Precursors Induced by Shape-changing Hydrogels

Olukemi O. Akintewe
University of South Florida, olukemi@mail.usf.edu

Fabrication of Tissue Precursors Induced by Shape-changing Hydrogels

by

Olukemi O. Akintewe

A dissertation submitted in partial fulfillment
of the requirements for the degree of
Doctor of Philosophy
Department of Chemical and Biomedical Engineering
College of Engineering
University of South Florida

Co-Major Professor: Ryan Toomey, Ph.D.
Co-Major Professor: Nathan Gallant, Ph.D.
Piyush Koria, Ph.D.
Mark Jaroszeski, Ph.D.
William Marshall, Jr., M.D.

Date of Approval:
June 30, 2015

Keywords: Micro-contact Printing, Cell Alignment, Poly-*N*-isopropylacrylamide, Temperature Responsive Hydrogel, Bioprinting

DEDICATION

I dedicate this to my family; the Ayodeji's and the Akintewe's

ACKNOWLEDGMENT

This dissertation would not have come to fruition without the efficient mentoring of my valuable advisors, Dr. Ryan Toomey and Dr. Nathan Gallant. Thank you for your sincere critiques and brilliant contributions to my research. I thank my committee members, Dr. Mark Jaroszeski, Dr. Piyush Koria and Dr. William Marshall Jr. for their proper guidance and intellectual support.

I acknowledge Alfred P. Sloan Foundation, NSF-LSAMP, UNCF-Merck Dissertation fellowship and McKnight doctoral fellowship for their financial support. The supported conferences, stipend, books and supplies were all put to great use. My deepest gratitude goes to Mr. Bernard Batson who provided relentless guidance and resources. Thank you for believing in me.

I thank my fellow graduate students from the Smart Materials Lab, Cellular Mechanotransduction and Biomaterials Lab, chemical engineering study mates, AAUW and the NSF Bridge to the doctorate fellows for those lunches, smiles and messages of encouragement and help.

The utmost gratitude goes to my life partner, Tunde Akintewe whose patience has being countlessly tested throughout this past 5 years. Thank you for being my greatest cheerleader. To my son, Toye thank you for your warm hugs and impressionable smiles. And to my parents, siblings and in-laws, I am thankful for your unwavering support and encouragement.

TABLE OF CONTENTS

LIST OF TABLES

LIST OF FIGURES

ABSTRACT

Scaffold based tissue reconstruction inherently limits regenerative capacity due to inflammatory response and limited cell migration. In contrast, scaffold-free methods promise formation of functional tissues with both reduced adverse host reactions and enhanced integration. Cell-sheet engineering is a well-known bottom-up tissue engineering approach that allows the release of intact cell sheet from a temperature responsive polymer such as poly-*N*-isopropylacrylamide (pNIPAAm). pNIPAAm is an ideal template for culturing cell sheets because it undergoes a sharp volume-phase transition owing to the hydrophilic and hydrophobic interaction around its lower critical solution temperature (LCST) of 32°C, a temperature close to physiological temperature. Compared to enzymatic digestion *via* trypsinization, pNIPAAm provides a non-destructive approach for tissue harvest which retains its basal surface extracellular matrix and preserves cell-to-cell junctions thereby creating an intact monolayer of cell sheet suitable for tissue transplantation.

The overall thrust of this dissertation is to gain a comprehensive understanding of how tissue precursors are formed, harvested and printed from interactions with shape-changing pNIPAAm hydrogel. A simple geometrical microbeam pattern of pNIPAAm structures covalently bound on glass substrates for culturing mouse embryonic fibroblast and skeletal myoblast cell lines is presented. In order to characterize the cell-surface interactions, three main investigations were conducted: 1) the mechanism of cell detachment; 2) the feasibility of micro-

contact printing tissue precursors onto target surfaces; and 3) the assembly of these tissues into three-dimensional (3D) constructs.

Detachment of cells from the shape-changing hydrogel was found to correlate with the lateral swelling of the microbeams, which is induced by thermal activation, hydration and shape distortion of the patterns. The mechanism of cell detachment was primarily driven by strain, which occurred almost instantaneously above a critical strain of 25%. This shape-changing pNIPAAm construct allows water penetration from the periphery and beneath the attached cells, providing rapid hydration and detachment within seconds. Cell cultured microbeams were used as stamps for micro-contact printing of tissue precursors and their viability, metabolic activity, local and global organization were evaluated after printing. The formation and printing of intact tissues from the shape-changing hydrogel suggests that the geometric patterning of pNIPAAm directs spatial organization through physical guidance cues while preserving cell functioning. Tissue precursors were sequentially assembled into parallel and perpendicular configurations to demonstrate the feasibility of constructing dense tissues with different organizations such as interconnected cell lines that could induce vascularization to solve perfusion issues in regenerative therapies. The novel approach presented in this dissertation establishes an efficient method for harvesting and printing of tissue precursors that may be applicable for the modular, bottom up construction of complex tissues for organ models and regenerative therapies.

CHAPTER 1: INTRODUCTION

This dissertation reports investigation of formation, release and printing of tissue precursors from shape changing surfaces that are thermally responsive to conditions close to physiological temperature.

1.1. Motivation

Tissue engineering is a promising approach to circumvent the shortage of organ donors needed to extend life. The use of autologous tissues for transplantation will provide an alternative to current therapy of organ transplantation that could lead to reduction in organ rejection or inflammatory response. Thus studies on development of functional tissues are of great importance in regeneration of diseased tissues or organ structures.

Cardiovascular diseases (CVD) in particular are the leading cause of death in the United States of America for both females and males. In 2014 alone, the mortality report indicated that more than 2150 Americans succumb to this disease daily; an average of 1 death every 40 seconds. By 2030, at least 40% of the U.S. population is projected to experience some form of CVD [1]. The American Heart Association's impact goal for 2020 is to reduce deaths from CVD by 20%. Thus far, there have not been any successful clinical trials for engineering replacement cardiovascular tissues.

The main challenge in tissue engineering is the ability to recapitulate the complex three-dimensional (3D) microarchitecture of the organs or tissues that would aid vascularization upon

implantation. An engineered 3D tissue construct should promote formation of vascular networks to aid prolific diffusion of nutrients and removal of metabolic waste. Also, the construct should be mechanically robust to sustain the continuous contractility function of a normal tissue or organ. Once implanted the engineered tissue should enhance or sustain the regular functionality of the diseased tissues.

1.2. Significance

This research provides understanding to the fundamental principles governing formation and assembly of 3D tissue precursors that could be further developed to closely represent the native tissues. The successful realization of this study provides a viable construct suitable for restoring functions of damaged tissues or organs that could overcome these key obstacles; vascular integration, diffusion, blood perfusion and new capillary formation in vivo thus revolutionize regenerative therapy.

The approaches developed in this study describe how a thermally responsive hydrogel is fabricated into patterned shape-changing structures and are used to direct cellular organization into tissue building blocks with defined shape and size while facilitating release and printing of tissues modules *via* a strain-induced detachment process which is driven by a thermal shift for only a short duration of 5 minutes.

1.3. Objectives, Hypothesis and Scope

The long-term goal of this research is to decrease the rates of those suffering from cardiovascular diseases by the development of a reliable method for generation of functional vascularized tissues. To accomplish this goal, the focus of this thesis project was to employ a temperature responsive hydrogel, poly-*N*-isoprylacrylamide to construct organized and multi-

layered tissue precursors that will aid regenerative repairs after transplantation. Towards this goal, the research objectives and hypotheses were three-fold.

1.3.1. Objective I and Scope

To establish a reliable and viable cell printing mechanism that demonstrates rapid fabrication of functional tissue precursors. Successful contact printing of cells on shape changing substrates depends on process variables: geometry, surface chemistry, time, pressure and temperature. The working hypothesis is that conformal contact between the target surface and stamp while in its swollen state will produce complete tissue detachment. To test this, the effects of the contact printing parameters were assessed and the corresponding cell morphology, organization and viability were evaluated. The scope of this study is to introduce a new method of fabricating tissues *in vitro* that would facilitate the production of robust tissues and also potentially reduce the long waiting list of organ donors.

1.3.2. Objective II and Scope

To investigate the biological effects of micro-contact printing on the developed micro-tissues that shows proper cell functioning. Cells are known to interact with adsorbed protein through their intercellular signal molecules. The two main interactions are the cell-to-cell communications and cell-to-extracellular matrix (ECM). The working hypothesis is that the duration and pressure applied during printing does not perturb cell normal activities such as adhesion or biochemical signaling. The scope of this study is to demonstrate that fabricated tissues via the novel printing method provide reliable functional tissues and also allows for scale-up production of complex tissues and organs.

1.3.3. Objective III and Scope

To construct multi-layered tissues modules by assembly of patterned cell stripes on top of each other or on monolayers of cell sheets. The working hypothesis is that stacking of tissue precursors may aid formation of 3D tissue constructs that can be used to promote development of vascular networks when cultured with various cell types. The scope of this study is to show that formation of capillaries with adequate perfusion can be developed by exploration of 3D tissue orientations through the combination of shape-changing hydrogel and a micro-contact printing technique. Neovascularization in engineered tissues is important for formation of new blood vessels to repair diseased tissues or organs.

1.4. Summary of Chapters

Chapters 1 and 2 provide the basis for conducting this research as it pertains to the relevant applications in tissue engineering. An overview of each aspect of the research from the research motivation, objectives, properties of the shape-changing hydrogel, cell and protein adhesion to current studies in engineering functional tissues using non-scaffold based platforms and *in vitro* tissue engineering is discussed.

Chapter 3 reports studies on how the shape-changing hydrogel was used to trigger rapid release of tissue precursors by employing a mechanically driven cell detachment mechanism. The data in this chapter has been published in Acta Biomaterialia and the copyrights permission from the publisher is displayed in appendix A. The results show that release of tissue modules occurred almost instantaneously depending on the cell seeding densities. A high cell seeding density induced a more rapid release due to the bonds formed between the cell-to-cell contacts. Complete tissue detachment occurred under 5 minutes. Mechanism of cell release studies suggested that release of tissue modules from shape-changing hydrogel is not a metabolic

activity but primarily driven by strain. An applied strain greater than 25% was observed to induce cell detachment even when the ATP was blocked. A LIVE/DEAD assay revealed that cell released from such dynamic surface is still viable for tissue formation.

Chapter 4 presents studies on the printing of tissue precursors from the shape-changing hydrogel structures by adapting micro-contact printing techniques. Effects of contact printing parameters, protein adsorbed on target surface, cell type, cytoskeleton examination, cell alignment and orientation studies were evaluated. The results reveal that printed tissues of 3T3 fibroblasts on target surfaces composed of human plasma fibronectin, collagen type 1 and poly-l-lysine individually demonstrated adequate cell viability with retained cell morphology, organization and pronounced focal adhesion complexes. Patterning of the shape-changing hydrogel composed of poly-*N*-isopropylacrylamide directed cellular organization while the applied compressive pressure during printing controlled cell viability.

Chapter 5 demonstrates the feasibility of stacking tissue precursors into multi-layered structures for construction of three-dimensional tissues for reconstructive tissue engineering and regenerative medicine. Patterned tissue precursors were assembled onto monolayer of cell sheet with orientations in parallel and perpendicular directions using either fibroblasts or myoblasts. Studies on how to improve the stacking resolution were investigated and discussed. The results suggest that maintenance of cellular organization in three-dimension configuration pose a challenge.

Chapter 6 presents overall research conclusions and provides directions for future studies in an attempt to accomplish the long-term goal of the research of developing robust tissues for treatments of cardiovascular diseases.

Finally, appendix B lists and describes the experimental methods and materials employed to execute the research objectives. The four main experimental procedures of this research were discussed in detail. Firstly, cell cultures of NIH/3T3 fibroblasts and C2C12 skeletal myoblasts were maintained frequently for cell attachment, release and print studies. Secondly, soft- and photolithography methods were used to fabricate and polymerize the shape-changing hydrogel arrays with defined beam width and spacing. Thirdly, a micro-contact printing technique was employed in transferring attached tissue precursors to target surfaces. And lastly, fluorescence microscopy was employed for imaging and analyses of the tissue modules to reveal information on cell morphology, organization and viability.

CHAPTER 2: BACKGROUND

2.1. Properties of Poly-*N*-isopropylacrylamide

Poly-*N*-isopropylacrylamide (pNIPAAm) polymers are classified as smart materials in that they respond to external stimuli such as temperature. Synthesis with other polymers or incorporation of other moieties attracts respond to other stimuli such as ions [2, 3], pH [4, 5] or magnetic fields [6, 7]. The response to temperature occurs around its lower critical solution temperature (LCST) of 32 °C in aqueous solution where a reversible phase transition point occurs. The LCST corresponds to the region in the phase diagram at which the enthalpy contribution of water, hydrogen bonding to the polymer chain becomes less than the entropic gain of the whole system and thus is largely dependent on the hydrogen bonding capabilities of the constituent monomer units [8].

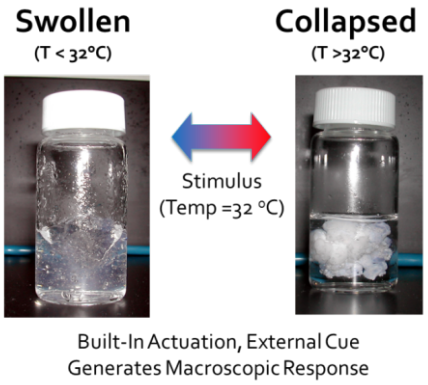

Figure 2-1: Macroscopic response of poly-*N*-isopropylacrylamide around its LCST.

Physical and chemical reaction of pNIPAAm to external stimulus occurs about its LCST. Environmental changes to a covalently cross-linked pNIPAAm can result into two main reversible physical structures; a swollen or collapsed structure (Figure 2.1). An aqueous solution of pNIPAAm heated above 32°C becomes hydrophobic due to the formation of intramolecular hydrogen bonding between the carboxyl and amide groups thus polymer precipitates out from solution resulting in a compact and collapsed state (Figure 2-2). Below the LCST, the intermolecular hydrogen bonding between water molecules and pNIPAAm is dominant leading to a completely soluble solution (a hydrophilic interaction) and thus results into a swollen state.

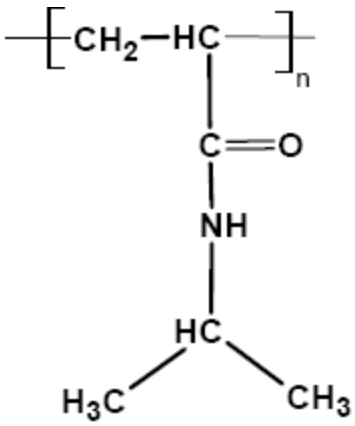

Figure 2-2: Structure of poly-*N*-isopropylacrylamide

2.1.1. Grafted pNIPAAm Surfaces for Cell Studies

Nanoscale thin grafted films of pNIPAAM coatings are typically prepared by electron beam polymerization (EBP) [9, 10], plasma polymerization [11, 12], surface-initiated atom transfer radical polymerization (ATRP) [13-16] or reversible addition fragmentation chain transfer polymerization (RAFT) [17] methods. The ability for cells to attach and detach on these

different methods of grafting deposition differs based on their molecular weights, film thickness, chain length and grafting densities. Typically, low densities and ultrathin films (< 30 nm) favors cell adhesion due to the shorter chain length. At this regime, hydration of the chains is limited which may limit the conformational collapse during the thermal shift thus promoting protein interaction with the basal substrate [18]. In contrast, high grafting densities, long chain length and increased thickness promote cell detachment. An increased hydrophilicity of the brushes is observed with decrease protein adsorption. In most of these grafting methods, film thickness above 45 nm impedes cell adhesion. Table 2-1 lists some of the grafting deposition techniques and their corresponding coating thickness and densities that are conducive for cell attachment.

Table 2-1: Grafted pNIPAAm films for cell adhesion

Grafting Method	**Densities mg/cm2**	**Dry thickness, nm**	**Contact Angle Swollen**	**Contact Angle Collapse**	**Release time (mins)**	**Ref.**
EBP	1.4-2.9	15.5- 29.3	n/a	n/a	90	[10]
Plasma polymerization	n/a	50 [9]	34	40	n/a	[11]
ATRP	0.2 - 0.3	10.9 - 30.4	37.81	44	60 - 120	[13]
RAFT	n/a	n/a	55.24	54.5	30	[17]

The hydrophillicity and hydrophobicity of the surface can be modified to improve cell adhesion and detachment by employing the RAFT method. Fabrication of grafted brushes with

carboxylate end groups yielded optimum bioadhesive surface with faster detachment, Table 2-1. Though high grafting densities exhibit more hydrophobic surfaces, cell detachment is predominantly dependent on the drastic conformation change that occurs during the temperature transition to the swollen state. Also detachment times vary depending on the grafting deposition technique and film thickness. As a result, contact angle alone is not sufficient to explain the mechanism of detachment from grafted surfaces.

Accelerated cell detachment is observed in confluent cell sheet compared to single cells or clusters. This behavior is attributed to a two-step detachment mechanism; passive and metabolic active processes. Upon temperature shift to the swollen state (T < LCST), the polymer hydrates instantaneously and the cell morphology is observed to change in the passive stage. In the metabolic active state, the cells detached as a sheet with simultaneous contraction in cell morphology and ECM [18]. Cell release studies indicate that a metabolism process facilitate detachment of cells. Treatment with sodium azide, an ATP inhibitor partially inhibited cell detachment suggesting that the mechanism on grafted surfaces is not solely by a reduction in cell-surface interactions from the spontaneous chain hydration but also driven by a metabolic process.

Primary metabolic driven processes could be limiting cell detachment from grafted pNIPAAm surfaces. Cell release requires long incubation periods ranging from 30 to 90 minutes with low temperature treatment of 4 or 20 °C depending on the cell type [10, 11, 21, 28, 29]. Duration of cell detachment from grafted surfaces of pNIPAAM is long due to the fact that water can only penetrate through the periphery of the cell sheet. However, the use of a porous membrane or incorporation of hydrophilic moiety like poly (ethylene glycol) has been shown to accelerate detachment time to 35 minutes [29, 30]. Slow detachment also occurs due to the

planar thin films. This planar geometry limits the extent of swelling needed to initiate a spontaneous cell release in shorter times.

2.1.2. pNIPAAM Shape-changing Surfaces

Shape-changing pNIPAAm hydrogels employ non-grafting techniques that induce an expansion in shape upon thermal reduction below the LCST. Fabrication techniques of these non-planar surfaces often involve UV crosslinking, solvent casting and dip coating [19-21]. Cell adhesion is delayed with this hydrogel due to the long chain length of the increased thickness which when hydrated produces a more hydrophilic surface impeding cell adhesion while favoring cell detachment. High degree of hydration and gel expansion occurs due to the increased thickness and chain length thereby inducing rapid cell detachment.

Methods to improve cell adhesion of shape-changing hydrogel involve copolymerization with hydrophobic monomers or coating the surface with a cell adhesion promoter. These cell adhesion molecules do not affect the rates of cell detachment [22]. Increase in hydrophobic chains enhanced the adsorption of cell adhesive proteins thereby promoting cell adhesion and proliferation.

Swelling instabilities of microscale surface confined pNIPPAAm hydrogels can yield rapid cell detachment almost instantaneously [19]. Additionally, these platforms can generate different geometrical patterns depending on the initial aspect ratio of the hydrogel. DuPont et. al report four swelling instabilities which are lateral differential swelling, surface creasing, local edge buckling and global buckling. Cell studies on these different geometrical patterns of pNIPAAm substrates could be used to build tissue precursors for tissue engineering applications. Mechanism of cell detachment from the differential lateral swelling geometry requires an applied strain of at least 25%. At T < LCST, cell released occurred nearly instantly from the hydrogel

arrays and complete detachment was observed in less than 5 minutes [23]. Thus, accelerated cell detachment is achievable with this platform however cell adhesion and proliferation is improved with initial protein adsorption on the surfaces. Application of shape-changing hydrogel should be further explored for formation of diverse tissue geometries that may closely mimic the microarchitecture of complex tissues to aid proper functioning.

The main difference between cell interactions on grafted films and shape-changing surfaces of pNIPAAm is tabulated in Table 2-2.

Table 2-2: Summary of grafted thin films and shape-changing hydrogel

pNIPAAm	Cell adhesion	Cell detachment time, mins	Cell detachment temp., °C	Mechanism of cell detachment	Pattern/tissue geometry
Grafted	Yes	30 - 90	4°C, 20°C	Metabolic	planar
Hydrogel	Yes*	3 - 5	25-29°C	Mechanical	Vast

* Improved with protein adsorption on surfaces.

2.2. Mechanism of Cell Adhesion on Synthetic Surfaces

Cell adhesion on synthetic surfaces is mediated by integrin binding, a family of heterodimeric adhesion transmembrane receptors that has extracellular domains which binds to ligands at the arginine-glycine-aspartic acid (RGD) peptide sites. Linkage of the integrin intracellular domain to actin cytoskeleton is responsible for proper cell functioning like proliferation, migration, viability and morphology. [24-29] Adhesion of cells occurs by expression of integrin receptors recognizable by the protein ligand. On synthetic surfaces, cell

adhesion molecules (CAM) composed of glycoproteins (extracellular proteins such as fibronectin, vitronectin, laminin, collagen) or chemically derived proteins (poly-*l*-lysine, poly-*d*-lysine) can be adsorbed on such surfaces to promote attachment providing that the attached cells express receptors for the choice of CAM. Tables 2-3 and 2-4 list the binding motifs of selected ligands and cell types with their respective integrin receptors.

The mechanism of cell attachment is different on glycoproteins and chemically derived proteins adsorbed surfaces. Naturally occurring proteins like fibronectin binds its divalent ions to the ECM of the cells [30, 31]. While positively charged ions of synthetically derived proteins like poly-l-lysine binds to the plasma membrane anions of cells via electrostatic interactions [32].

Attachment of cells on protein-adsorbed surfaces is also influenced by the design of target surface and the protein state. Cell adhesion can be dictated based on surface chemistry, surface energy, roughness, topography and wettability [31, 33-35]. While the protein type, concentration, conformation and orientation are also important factors for regulating cell attachment [36-39].

Cell adhesion on target surfaces composed of a monolayer of cells like stacked tissue sheets require a different binding mechanism. This adhesion occurs through formation of cell-to-cell contacts mediated by calcium dependent homophillic molecules called cadherins. The mechanism of cell-to-cell adhesion occurs via formation of tight junctions, desmosomes, adherens junctions and gap junctions. Each of these bonds is responsible for regulating unique cell functioning although not all these junctions are present in every cell type except for epithelial cells.

Table 2-3: Cells and their corresponding integrin receptors

Cell type	Integrin	Ref.
Fibroblasts	$\alpha_1\beta_1$	[40]
	$\alpha_2\beta_1$	
	$\alpha_3\beta_1$	
	$\alpha_5\beta_1$	
Myoblasts	$\alpha_2\beta_1$	[41, 42]
	$\alpha_3\beta_1$	
	$\alpha_4\beta_1$	
	$\alpha_5\beta_1$	
	$\alpha_6\beta_1$	
	$\alpha_7\beta_1$	
	$\alpha_5\beta_3$	
	$\alpha_4\beta_7$	

Cellular communication for cell-to-cell formation proceeds through specific markers exhibited by both neighboring cells. For instance, endothelial cells and cardiac fibroblasts have tight association in the coronary vasculature of mice due the communication by their gap junctions and ECM [43].

2.3. Printing of Tissue Precursors

In vitro printings of tissue precursors deem promising for the replacement or repair of tissues or organ structures. The main challenge is the ability to manufacture tissues that closely represent the native microarchitecture of tissues by utilizing multiple cell types with adequate

precision and resolution necessary to recapitulate biological functions. Successful realization of these printing techniques could bring about a transformational change in tissue engineering and regenerative medicine needed to prolong lives.

Table 2-4: Proteins and their corresponding integrin receptors

Cell type	Integrins	Ref.
Fibronectin	$\alpha_1\beta_1$	[44-46]
	$\alpha_3\beta_1$	
	$\alpha_4\beta_1$	
	$\alpha_5\beta_1$	
	$\alpha_8\beta_1$	
	$\alpha_v\beta_1$	
	$\alpha_v\beta_3$	
	$\alpha_v\beta_6$	
	$\alpha_4\beta_7$	
Collagen type I	$\alpha_1\beta_1$	[40, 44, 45, 47, 48]
	$\alpha_2\beta_1$	
	$\alpha_{10}\beta_1$	
	$\alpha_{11}\beta_1$	
	$\alpha_v\beta_8$	

2.3.1. Inkjet Bioprinting

Inkjet-based bioprinters are the most commonly used strategy for printing 3D tissues. Similar to conventional inkjet printer technology, the ink cartridges and paper are substituted in the bioprinters with biological relevant materials and a motorized stage for controlled delivery and assembly of cells. Either piezoelectric or thermal forces are used to eject liquid droplets from the nozzle to a target substrate in order to build the desired construct. Application of this technique has been used in regeneration of skin tissues, bone and cartilage constructs [49-52].

This strategy allows for printing with increased resolution and speed. The use of localized electrical heating > 200 °C at the printhead to generate the drops of liquid in thermal printers does not drastically affect cell viability and stability [53]. But the frequent exposure of cells to shear stresses, high heat, clogging of nozzles and inadequate directionality of inconsistent sized droplets imposes major drawbacks for this approach. On the other hand, piezoelectric printers eject droplets with an acoustic wave with adjustable pulses, droplet sizes, duration and rates [54]. Although the piezoelectric printers address some of the drawbacks experienced with thermal printers, the need for low viscous biological liquids and the applied frequencies pose a potential damage for occurrence of cell lysis and disruption of cell membrane [55]. Together the inkjet printing of mammalian cells are limited to low cell densities and unique cell types [53].

2.3.2. Microextrusion Bioprinting

Extrusion-based printers utilize mechanical or pneumatic extrusion systems to eject beads of biological materials onto a substrate by employing a computer aided software to direct a motorized stage. The use of intermediate materials such as hydrogels, cell suspensions and self-assembled spheroids is a requirement with these printers. Applications have been in fabrication of vascular trees and aortic valves [56-59].

This system allows for construction of complex tissue structures due to its controlled spatial distribution, which enables patterning of different cell types. Additionally, it is compatible with high viscosity materials that have shear thinning properties and allow deposition of high cell densities. The main drawbacks of this technique are the low resolution; print speed; and the low cell survival rates of 40-86% depending on the nozzle diameter and pressure of the extruder [60, 61].

2.3.3. Micro-contact Printing of Cells

Micro-contact printing (μCP) technique for printing of cells is a relatively new approach for fabrication of mini-tissue building blocks. Whitesides first established this technique in 1993 by using a polydimethylsiloxane (PDMS) elastomeric stamp consisting of bas-relief features [36]. The stamp is used to ink self-assembled (SAM) alkanethiol monolayers on gold surfaces with designed patterns at micron length scales. Employing a photolithography technique to develop the desired template of patterns controls spatial distribution of the deposited material. Although micro-contact printing technique was originally developed to pattern gold, numerous materials have now been patterned such as organic solvents, polymers, proteins, metals and cells [62-65]. Cell patterning with this technique is primarily by patterning proteins onto substrates for selective cell adhesion. No studies on direct printing of patterned cells have been revealed to date except in this dissertation.

The elastomeric stamp deforms macroscopically *via* mechanical compression allowing the protruding features to conform to the target substrate over large surface area. This deformable property of the stamp and its low surface energy enables instant inking of material to be transferred, printing to the target and instant removal without obstructing the patterned ink. To ensure successful printing, the target substrate must be more energetically favorable than the

stamp. Also transfer efficiency is determined by the surface chemistries of the stamp and target. The drawback of this technique is the deformability feature of the stamps, which poses a limit on the aspect ratios and resolution of the features. The failure events are typically sagging, lateral and buckle collapse of the stamp features.

2.4. Tissue Engineering Applications

2.4.1. Cell Culture, Recovery and Cell Sheet Engineering

Recovery of cultured cells by conventional means could be detrimental to the health of the cells. Traditional cell harvesting techniques involves either mechanical dissociation or proteolysis. A silicone rubber is used in the mechanical method to disaggregate cells, which could lead to loss of cell number and disrupted cell membranes [66]. The commonly used proteolysis, enzymatic digestion with trypsin-EDTA, suppresses expression of transmembrane proteins by down regulating proteins responsible for cell proliferation and metabolism while up regulating the apoptosis related proteins [67].

Recently, thermoresponsive pNIPAAM grafted surfaces have been proven as suitable systems for cell recovery through a mild temperature modulation without inducing any harsh treatment of the cells [68, 69]. Rather, cells are harvested as “cell sheets” with retained metabolism and functionality. This cell culture recovery system is termed “cell sheet engineering” as coined by Teruo Okano in the early 1990’s. Cells are cultured on the thermoresponsive surface at physiological temperature of 37 °C above its LCST until confluency is reached. At T < LCST, the surface becomes more hydrophilic resulting in a volume expansion, which initiates a spontaneous release of the attached cells as continuous confluent cell sheet. Compared to mechanical scraping and enzymatic digestion via trypsinization, pNIPAAm substrates provide a non-invasive approach for cell harvest since its basal surface ECM is

maintained and the cell-to-cell junctions are well preserved thus an intact monolayer of cell sheet is created, which is suitable for tissue transplantation [70, 71].

Temperature modulated cell culture recovery systems allow the use of harvested autologous cells for clinical regenerative therapies thereby reducing chances of inflammatory response or host rejection problems. This approach also allows for additive assembly of two dimensional (2D) cell sheets into 3D tissue constructs from multiple cell lines. Successful studies employing this technique include engineering of tissues such as periodontal ligament, corneal, renal, oesophageal ulceration, and myocardial tissues [72-76].

2.4.2. Cellular Organization on Patterned Surfaces

Cell microenvironment studies are important for regulating cellular behavior and functionality. Micropatterning of substrates for cell alignment studies provides the capacity to engineer organized patterned complex structures that mimic native tissues in order to reproduce their structural cues. Patterning of tissues is accomplished by culturing cells on surfaces with defined pattern geometry that can direct cell orientation and guide attachment. Surface patterning is commonly accomplished by employing micro-contact printing techniques or soft lithography [64, 65, 77, 78].

Regulation of cell orientation and its ECM *in vitro* is crucial for controlling tissue geometry when stacking tissue constructs in order to maintain tissue integrity or induce desirable biological response. In contrast, lack of topographical cues or structural organization may alter protein expression and cell functioning. For instance, innately organized interconnected cardiomyocytes were observed to form aligned fields of spontaneous synchronous beatings with neighboring patterned cells when cultured on protein patterned surfaces with defined width and spacing dimensions [62, 79]. Likewise anisotropy skeletal myoblast, which are natively

composed of parallel bundles of multinucleate muscle fiber, was found to re-orient the bottom layer of a thick unpatterned 4-layered cell sheets when stacked on the top sheet [80, 81].

Control of cytoskeleton components can be regulated by organization of cells on patterned surfaces. The significant orientation of actin filaments observed in cell layers of normal human dermal fibroblasts (NHDF) after few days on 50 μm patterns of pNIPAAm copolymer suggested that the cytoskeleton is controlled by the surface topography [82]. Limitations of micropatterning technique are loss of cell alignment, which could be dependent on cell phenotype expression or cell seeding densities.

2.4.3. Fabrication of 3D Tissues with Layer-by-layer Assembly

Construction of functional 3D tissues *in vitro* without the use of scaffolds is achievable by employing an automatic plunger-like cell sheet stacking manipulator system. This stacking process involves multiple layer-by-layer steps. Multiple cell culture dishes are maintained on pNIPAAm-grafted surfaces while gelatin or fibrin hydrogel is adhered to the bottom of the manipulator. The cell adhesive hydrogel manipulator is then brought in contact with a confluent cell layer at an incubation temperature of 20 °C. After an elapse time, the cell sheet is lifted off and stacked on another layer of sheets until the desired number of multilayered sheet is attained. Then the hydrogel is dissolved away leaving behind the multilayered construct [83, 84]. The resulting thickness for a five-layered tissue construct is approximately 80 μm which is fabricated in 100 minutes.

Application of this manipulator system has led to successful *in vitro* tissue model of tissue constructs for regenerative medicine such as cardiomyopathy, Type 1 diabetes and visual acuity [85-87]. The main challenge of this technique is the fabrications of cell dense pre-vascularize thick tissue grafts to recapitulate the complex microarchitecture of native tissues. In

general, co-cultures of endothelial cells with fibroblasts, myoblasts and cardiomyocytes have been used to control vascular network formation in vitro. Though endothelial cells are used as vascular precursors, the extent of vascular network formation is dependent on its patterning directionality, frequency of contacts and the spatial distribution of the cells between layers of the other cell types.

Long-term viability of transplanted tissue grafts requires adequate vascularization to promote angiogenesis *in vivo*. *In vivo* transplantation of patterned endothelial cells within fibroblast or myoblasts in nude rat showed sufficient connection to host vessels thereby resulting in viable grafts which promoted neovascularization [88, 89]. Similarly endothelial cells co-culture with myocardial tissues enhanced neovascularization and the spontaneously pulsated cardiac sheets improved cardiac function and in a rat infarction model [90, 91].

Limitations of the technique include limited thickness for *in vitro* static culture; possible tearing of cell sheets; inadequate weight of manipulator sufficient to adhere to cell sheets; and cold treatments at 20 °C for duration up to 60 minutes in the pre-cooling groups.

2.4.4. Myocardial Infarction

Cardiovascular disease is the leading cause of morbidity and mortality in developed nations. In the United States alone, over 300,000 people die each year from myocardial infarctions (MI) [92]. Myocardium in the left ventricle (LV) is responsible for the contractility and electrical conductivity of the heart. Impaired myocardial tissue is composed of terminally differentiated cardiac myocytes whose ability to self-regenerate is less than 1% per year [93]. Acute myocardial infarction commonly referred to as heart attack occurs due to prolonged ischemia or blocked lumen in the coronary artery which may lead to cell death of about one billion cardiomyocytes (CMs) [94]. Necrotic myocardium affects the remodeling activity of the

left ventricular. Increase in infarcted area could exert wall stress on the LV causing a significant reduction in wall thickness, dilatation and decreased contractile function while prolonged increase of the infarction eventually leads to chronic impaired LV [95]. The current treatments for chronic cardiac failures are LV assist devices or heart transplants. However, these treatments are limited by shortage of organ donors and resources. Therefore alternative therapeutic strategy to circumvent this deadly disease is of great need.

The challenges involved in myocardial tissue engineering are mainly three-fold. First is the ability to closely mimic the tissue microarchitecture specifically complex tissues. Normal LV myocardium consists of arrays of organized myocytes stacked in different circumferential orientations with a dense muscle mass thickness of approximately 12 mm [96]. The second challenge is engineering tissue constructs for cellular organization without compromising vascularization or thirdly, building sufficiently thick 3D tissues without risking the oxygen diffusion limitation of 200 μm for tissue depth [97].

Current strategies for repairing infarcted myocardium include direct injection of healthy cells into the infarcted zone; though this is a less invasive delivery, the amount of cell loss is huge and poor vascular integration is experienced [98]. Clinical use of biocompatible scaffolds is associated with inflammatory response, slow vascularization and selective perfusion [99, 100]. Recent applications of cell sheet based therapy from pNIPAAm surfaces seems more promising due to the high production of cell density and tailored cell organization, however vascularization and perfusion capabilities remain a challenge.

Engineered cardiac patches for infarcted heart was developed by seeding layers of CMs on thin grafted pNIPAAm surfaces. After few days, the layered CM sheets showed synchronized pulsation and adhesive junctions [22-24]. Co-culture of endothelial cells and CMs enhanced

neovascularization and angiogenesis in the ischemia hearts of rats [25]. Formation of an endothelial cell network improved the CMs survivability in 3D; promoted synchronized contraction and enhanced spatial organization by providing controlled gap junction proteins for diffusion of nutrients [26]. In attempt to overcome the diffusion limits imposed by insufficient thickness, a polysurgery of sequential assembly of ten tri-layer cardiac cell sheet grafts (~1000 μm thick) was conducted to produce thick vascularized tissues [27]. Though the multi-step transplantation of the tri-layer cardiac graft showed significant improvement in vascularization, the surgery required 1 or 2-day intervals between transplantation. This lag period and multiple transplantation surgeries is not feasible in humans therefore the need for perfuse thicker graft is important.

2.4.5. Congenital Heart Defects

Congenital heart defects (HD) is one of the leading cause of prolonged hospitalization of newborns after delivery. Though the mortality rates due to congenital HD have declined in the United States, the burden of the disease still remains high. Prevalence report indicates an estimate of 1% in live births and 1 in every 150 adults are expected to have some form of congenital HD [1]. The use of autologous tissues for transplantation will provide an alternative to current therapy of organ transplantation that is impinged on availability of donors and could also lead to organ rejection or inflammatory response. Regeneration of these cardiac tissues is challenging due to its complex 3D architecture and pertinent electrophysiological function. An ideal engineered cardiac tissue should possess the electrical conductivity and contractility properties of a normal myocardium to aid proper functioning and lower risks of arrhythmias or heart failures.

Recent studies with cell sheet technology show a promising alternative to organ transplantation, which could lead to a transformational change in regenerative therapies [2-4]. Tissue engineered autologous skeletal myoblasts sheets improved cardiac function in animals and even in a Japanese adult male both with different forms of cardiac anomalies [5]. While no increase in arrhythmias was observed in those studies, another group reported higher occurrence of arrhythmogenicity in their clinical trials [6]. Thus far, great strides are been made with pNIPAAm as culture platforms for these engineered tissues. Continuous and further exploration of other forms of pNIPAAm surfaces where heart tissues can be regenerated via engineered cardiac patches could lead to successful clinical trials.

CHAPTER 3: SHAPE-CHANGING HYDROGEL SURFACES TRIGGER RAPID RELEASE OF PATTERNED TISSUE MODULES[1]

3.1. Introduction

An emerging field known as modular tissue engineering employs a bottom-up approach that utilizes tissue building blocks as modular units to construct biological tissues with specific architectural features. As an example, modular tissues can be created using cell sheets and assembled through stacking of layers to enhance [1] formation of complex microstructural functional units such as microvascular networks, thereby augmenting integration and facilitating recovery [80, 101-103] . This bottom-up approach aims to develop biomimetic engineered tissues that effectively recapitulates native tissues [104, 105].

Recently, responsive materials have been used as a platform for generating tissue modules due to their convenient manipulation of cell-surface interactions on culture supports induced by an environmental cue such as temperature, pH, ionic strength, solvent, salt, surfactant, electric or magnetic field [8, 106, 107]. In particular, grafted films of poly (*N*-isopropylacrylamide) (pNIPAAm), a thermally responsive polymer, have attracted a great deal of attention for use as cell culture platforms for cell sheets because this polymer undergoes a sharp volume-phase transition due to thermally mediated changes in the hydrophilic and hydrophobic

---

[1]This chapter have been previously published in *Acta Biomaterialia*, 2015, 11: 96-103, and have been reproduced with permission from Elsevier. Permission is included in Appendix A.

interactions around its lower critical solution temperature (LCST) of 32°C [69, 107, 108]. In comparison to conventional enzymatic release of cells with trypsin and ethylene diamine tetraacetic acid (EDTA), the hydration of grafted pNIPAAm provides a slow, but non-destructive approach for tissue harvest so that intact monolayers of cells can be formed [68, 70, 71].

Rapid production, versatility and scalability are important factors for in vitro construction of tissues and organs. Herein, a shape-changing hydrogel cell culture platform that demonstrates these properties is described. This platform is based on patterned arrays of microscale protrusions (or microbeams) of cross-linked pNIPAAm [19]. Lateral swelling of the microbeams occurs upon thermal activation, expanding and distorting the surface of microbeams. Although several studies have shown release of tissue modules from two-dimensional (2D) grafted thin pNIPAAm films, the release of tissues from shape-changing 3D pNIPAAm hydrogels is unexplored. While thin films can be used to generate layered tissues from stacked cell sheets [73-75, 91, 95, 109], such substrates provide limited range in tissue geometries and slower cell release times.

Hence, developing an alternative method that enables faster cell detachment and allows for the fabrication of geometrical patterns of the hydrogel could facilitate the organization and rapid release of tissue modules. We hypothesized that rapid tissue module release occurs on shape-changing surfaces via mechanical mechanisms that are unique to patterned shape-changing cell culture supports. Furthermore, it is speculated this simple method can be used to form the diverse building blocks required for building robust multilayered tissues that are complex in architecture and may, for example, be used to enhance vascularization in thicker tissue grafts for organ repair or replacement.

The objective of this work is to demonstrate the feasibility of fabricating and harvesting tissue modules via a strain-mediated process and to study the mechanism that regulates rapid release from shape-changing biomaterials. We fabricated 3D pNIPAAm microbeams having various swelling ratios to investigate the effect of swelling-induced strain on tissue module release. We also examined the effect of cell density on cell detachment; and to understand the mechanism of tissue release from these shape-changing surfaces, we investigated the roles of metabolic activity and cytoskeletal contractility by probing the adhesive interface. Finally, we evaluated the viability of cells within the released tissue modules. The results described here provide the first steps toward fabricating and harvesting living tissue building blocks with intact organization and cell-cell connections that may ultimately be used to build complex 3D tissues via assembly of diverse tissue modules.

3.2. Materials and Methods

3.2.1. Materials

NIH/3T3 mouse embryonic fibroblast cells were purchased from the American Type Culture Collection. Dulbecco's modified Eagle's medium (DMEM), Dulbecco's phosphate buffered saline (DPBS), newborn calf serum (NCS), 0.25% trypsin EDTA (1X), Calcein AM, ethidium homodimer, penicillin and streptomycin were all obtained from Life Technologies. N-isopropylacrylamide (NIPAAm), 2-dimethoxy-2-phenylacetophenone (DMPA), N, N'-methylenebisacrylamide (MBAm), 3-(trichlorosilyl) propyl methacrylate (TPM), sodium azide (NaN_3), Rho-associated protein kinase (ROCK) inhibitor Y-27632, acetone, and carbon tetrachloride were all purchased from Sigma-Aldrich. Methacryloxyethyl thiocarbonyl rhodamine B (polyfluor® 570) was purchased from Polysciences. 3,3´-dithiobis-

sulfosuccinimidylpropionate (DTSSP) was obtained from Thermo Scientific. Silicone elastomer (PDMS) kits (Sylgard®184) were obtained from Dow Corning.

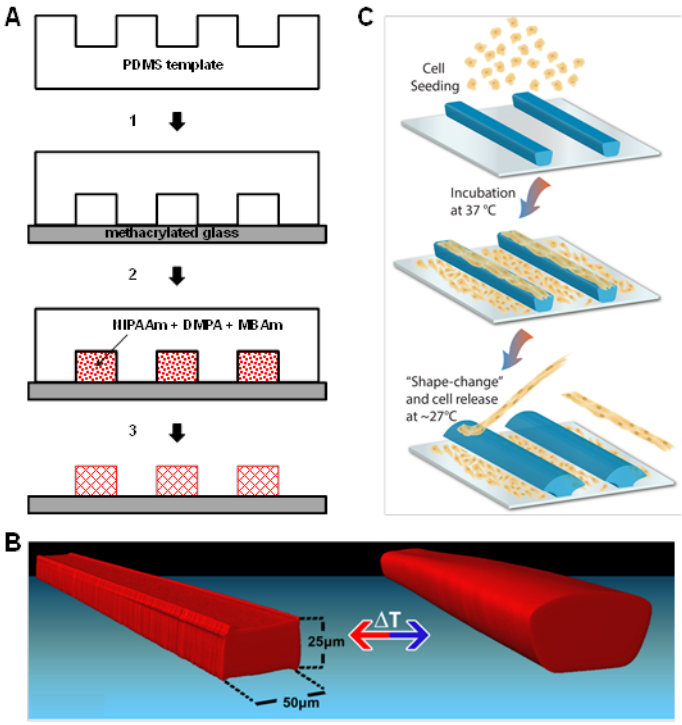

Figure 3-1: Shape-changing pNIPAAm hydrogel microbeams for tissue module. (A) Schematic of microbeam fabrication steps. (1) A PDMS template is placed on a methacrylated coverslip and (2) prepolymer solution is flowed into the recesses. (3) The hydrogel networks are polymerized with 350 nm UV light before the PDMS template is removed. (B) Three-dimensional reconstructions from z-stacks of images taken by confocal microscopy of a surface-confined microbeam of low aspect ratio (AR = 0.5) with a collapsed (37 °C) height of 25 μm and width of 50 μm (left) which transforms into a bulbous geometry (right) upon thermally intitated shape change at 27 °C. Note microbeams with AR < 1.0 were used in this study. (C) Schematic of formation and release of tissue modules from shape-changing hydrogel microbeams. (1) Cells adhered to and conformed to the shape of the microbeams, organizing into geometric tissue modules. (2) Tissue modules released from microbeams upon expansion beyond a critical lateral strain.

3.2.2. Preparation of Dynamic pNIPAAm Hydrogel Arrays

Patterns of crosslinked pNIPAAm hydrogel (50-100 μm width x 25 μm height x 5 mm length) microbeams were fabricated as described previously [19, 110] on 22 mm x 22 mm glass

coverslips (#1.5) using PDMS molds by employing the micromolding in capillaries (MIMIC) technique (Figure 3-1A). Briefly, the glass cover slip was surface modified with TPM in carbon tetra chloride. 1-4% MBAm crosslinker (5 mg/mL), 10% DMPA photo initiator (20 mg/mL) and 1% polyfluor® 570 (0.5 mg/mL) were added to a 250 mg/mL solution of NIPAAm in acetone. The resulting solution was introduced to the PDMS molds and polymerized with ultraviolet light (350 nm) for 4 minutes. The fabricated surfaces were sequentially rinsed with acetone, ethanol and water to remove unpolymerized monomer.

3.2.3. Cell Culture

NIH/3T3 mouse embryonic fibroblast cells were cultured in 10% NCS growth medium containing 1% antibiotics (10,000 units/mL penicillin and 10,000 units/mL streptomycin) at 37 °C in a humidified atmosphere of 5% CO_2. To prepare tissue modules, trypsinized fibroblasts were seeded onto the fabricated responsive hydrogel arrays at a density of 500 - 750 cells/mm^2 and cultured at 37 °C until confluence (24 - 48 h). Studies of release from low cell density (100 cells/mm^2) were cultured for 24 hours.

3.2.4. Release of Tissue Modules from Shape-changing Hydrogels

Rapid release of tissue modules was induced by thermally initiated swelling of the hydrogel beams. 2 mL of cold PBS (4 -10°C) was introduced 1 mL at a time into the seeded dish containing 2.5 mL of 37 °C medium resulting in cooling to approximately 27 °C. Cell release was monitored via time-lapse image acquisition on a microscope for at least 70 seconds.

3.2.5. Viability of Cells Released

A cell viability assay was performed on released cells by using a LIVE/DEAD kit (containing calcein AM and ethidium homodimer) following the commercially recommended protocol. Once the cells reached confluence on the hydrogel, the tissue modules were released

with fresh cold medium and plated onto a new tissue culture polystyrene (TCPS) dish. Following incubation for 24 or 48 hours at 37 °C, the cells were stained with 300 µl of 20 µM Calcein AM and 40 µM ethidium homodimer-1 solution. After 30 min, the dish was rinsed twice with warm PBS and replenished with fresh medium prior to imaging.

3.2.6. Mechanism of Tissue Module Detachment Studies

The mode of cell release from hydrogel surfaces was examined by separately treating seeded samples with agents that modulate metabolism, contractility or adhesion. 24 hours after after attachment to microbeams, cells were exposed to sodium azide, a compound known to block ATP production via inhibition of cytochrome C oxidase in mitochondoria [68, 111], Y-27632, a selective inhibitor of Rho-associated protein kinases [112, 113], or DTSSP, a homobifunctional crosslinker that fixes only integrins bound to the extracellular matrix [114, 115]. Briefly, samples were exposed to 2 mM sodium azide for 60 minutes or 50 µM Y-27632 or 2 mM DTSSP for 30 minutes prior to initiating tissue module release. To investigate the effect of surface strain on attached cells, the concentration of the network crosslinker (MBAm) in the prepolymer solution was varied from 1 to 4% before MIMIC processing. The one-dimensional width-wise strain in each microbeam was calculated from phase contrast micrographs as follows:

$$\varepsilon = \frac{\Delta w}{w_{collapsed}} = \frac{w_{swollen} - w_{collapsed}}{w_{collapsed}} \quad (1)$$

where ε is the Cauchy strain, $w_{collapsed}$ is the width of the hydrogel beam in the collapsed state and $w_{swollen}$ is the width of the hydrogel beam in the swollen state. Cell detachment was calculated as the percent of cells released from the microbeams within 3 minutes after thermal stimulation.

3.2.7. Microscopy

Video analysis (60 frames per second) and micrographs of samples were obtained using an Eclipse Ti-U (Nikon Instruments, Japan) fluorescent microscope equipped with a CCD camera (CoolSNAP HQ2, Photometrics, Tuscon). Cell images were analyzed with NIS-Elements advanced research software Ver. 4.20 (Nikon Instruments) and cell counting were performed in ImageJ (NIH, USA). Images were processed to overlay fluorescent channels on the phase-contrast channel for LIVE/DEAD analysis.

To capture x-y-z image stacks for 3D rendering of the microbeams, images were taken with a Leica TCS SP5 confocal laser scanning microscope (CLSM) equipped with 20X/0.7NA and 40X/1.25NA objectives (Leica Microsystems, Germany). An argon laser line, tuned to 543 nm, was applied to excite fluorescent microbeams and an Acousto Optical Beam Splitter was used to filter the emission. Image sections were taken at a constant z-spacing of 0.25 μm and were captured with photomultiplier detectors using the Leica Application Suite Advanced Fluorescence software version 2.1.0 (Leica Microsystems, Germany).

3.2.8. Statistical Analysis

Release data was collected with a sample size of $n \geq 5$ independent experiments for each case and reported as scatter plots. Statistical differences between treatment types were determined by performing a single factor ANOVA followed by Tukey's test for pairwise comparisons with $p < 0.05$ considered a significant difference.

3.3. Results

3.3.1. Surface-confined Stimuli-responsive Microbeams Swell Anisotropically

Shape-changing microbeams were fabricated by MIMIC and photopolymerization (Figure 3-1A). This process has previously been used to generate a range of initial geometries

and reversibly deforming structures [19]. For this investigation, rectangular prismatic microbeams with aspect ratios 0.25 to 0.5 were used to generate laterally straining surfaces in response to thermal activation. Under cell culture conditions at 37 ^{o}C, the microbeams were collapsed polymer networks forming a stable topography suitable for culturing cells. Thermal reduction of the aqueous medium to 27 ^{o}C caused swelling of the surface-confined microbeams. Covalent attachment to the underlying substrate prevented expansion of the microbeams adjacent to the surface and resulted in anisotropic shape changes. The crosslink density in the hydrogel determined the extent of swelling; increasing the concentrations of the crosslinker reduced swelling and therefore retarded the lateral strain.

3.3.2. Rapid Tissue Module Release via Surface Expansion of Shape-changing Surfaces

Model tissue modules were formed from interconnected mouse embryonic fibroblasts by seeding these cells at high density (500 cell/mm^2) onto arrays of microbeams crosslinked with 1% MBAm (*n = 5*) (Figure 3-1C). Seeded cells formed continuous multicellular monolayers that

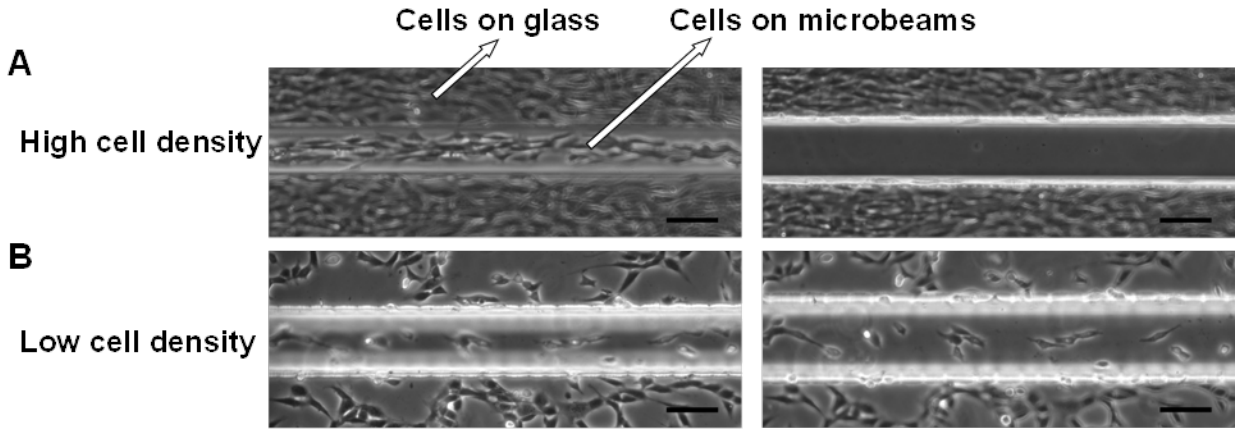

Figure 3-2: Phase contrast images of tissue modules. Shown are before (left) and after (right) microbeam expansion. (A) High cell density (ε = 0.33) and (B) low cell density (ε = 0.31) were compared for similar strains. Scale bars = 100 μm.

conformed to the microbeam's shape within 48 hours. Cells were observed to populate the top surface of the microbeams and the recessed spaces between the beams (Figure 3-2C).

The shape-changing property of these surface-confined microbeams was investigated as a method to harvest the attached tissue modules without disrupting their intercellular connections and organization. Thermal activation of these dynamic hydrogel arrays triggered rapid release of tissue modules following swelling-induced shape changes. Upon introduction of cold medium to reduce the temperature, the projected area of each microbeam increased as expansion occurred in the width-wise direction. Simultaneously, the confluent cells detached in aggregate from the microbeams as continuous tissue stripe modules (Figure 3-2A). Cell to cell connections in the released tissue modules appeared to remain intact while cells between the microbeams maintained attachment to the glass surface after the change in temperature. Release occurred rapidly as separation was observed within a few seconds of reducing the medium temperature to approximately 27 °C. Complete detachment of the overlying tissue was observed in less than 3 min.

3.3.3. Effects of Cell Density on Tissue Module Release

Cell to cell connections were found to be a requirement for inducing confluent cell stripes to release from shape-changing hydrogel surfaces. For low cell density, 100 cells/mm^2 were seeded on microbeams ($n = 5$) (Figure 3-2B) and compared to high cell density samples (500 cells/mm^2) with the same crosslink density (Figure 3-2A). Cells seeded at low density were predominantly adhered individually to the microbeams with cells interacting with very few neighboring cells after 24 hours of culture. Upon reducing the culture temperature, minimal detachment of cells was observed from low cell density microbeams (Figure 3-2B). In contrast, complete detachment of continuous tissue modules occurred within seconds to minutes when the

cells were connected atop the microbeams. A significant difference in the number of detached cells was observed between the high and low cell densities at 4 minutes after expansion ($p < 0.001$). The microbeams in these experiments were exposed to equal thermal stimuli and underwent similar lateral strains, indicating that the rapid release requires cell-to-cell connections and that the reduction in temperature alone does not induce tissue module release.

3.3.4. Mechanism of Tissue Release from Shape-changing Microbeams

Based on the cell density results, it was hypothesized that a mismatch between the expanding surface and the allowable stress or strain in the tissue module caused the detachment of interconnected cells. To determine the mechanism of detachment from the shape-changing microbeams, the mode of release was examined using four approaches. First, the degree of swelling of pNIPAAm hydrogels is dependent on the extent of available network crosslinks; increasing crosslinks reduces swelling. The concentration of MBAm crosslinker in the prepolymer solution was varied from 1 to 4%, which resulted in microbeams whose surface expansion caused a range of lateral strain, ε, from 0.05 to 1.2 (i.e., 5-120% increase in width). Cells seeded at high density formed morphologically similar tissue modules on all crosslinked hydrogel microbeams. Upon swelling, it was observed that lateral strain strongly regulated tissue release. Cells remained adhered and spread on microbeams with low strain; however, intact tissue modules were released above a threshold lateral strain of approximately 0.25 ($p < 0.001$) (Figure 3-3 & 3-4a).

Next, the role of processes requiring cellular metabolism for cell detachment were examined by treating the tissue modules with sodium azide [111], a potent inhibitor of ATP production, prior to microbeam swelling. Less than 20% of the cells detached when $\varepsilon < 0.25$ while more than 90% cell detachment was observed for $\varepsilon > 0.25$ (Figure 3-3 & 3-4b). This trend

was similar to untreated samples, indicating that inhibiting metabolic processes did not prevent cell release ($p < 0.001$).

Since it was hypothesized that the mismatch between compliance of the tissue modules and the underlying surface expansion may disrupt the adhesive interface and lead to release, intracellular tension was modulated. Actin-myosin contractility was inhibited with Y-27632 prior to microbeam swelling. It was observed that the cells primarily remained attached even after inducing large strains ($\varepsilon > 0.25$), implying that contractility is required for rapid tissue module detachment (Figure 3-3 & 3-4c). Moreover, instead of releasing from the surface, the contractility-inhibited cells expanded with the swelling surface.

Finally, attached cells were treated with DTSSP, a chemical crosslinker with a 12 Å spacer arm length which specifically crosslinks integrin receptors bound to extracellular matrix ligands [114, 115]. In this case, significant cell release was not observed within 5 minutes of initiating shape change, indicating that the disruption of integrin-mediated adhesion is required for release (Figure 3-3 & 3-4D). Together, these results suggest a mechanical mechanism triggers rapid tissue module release that is mediated by the lateral strain of the cell-surface interface provided by the shape-changing properties of the patterned, surface-confined hydrogels.

3.3.5. Strain Induced Release Does Not Reduce Cell Viability

To examine the fate of cells within released tissue modules, the multicellular stripes were harvested via lateral strain ($\varepsilon > 0.30$) and allowed to re-attach to tissue culture polystyrene (TCPS). Cell survival was observed over 48 hours. After 24 hours on TCPS, the organization of the tissue module was generally lost as the morphology became a loose aggregate of spreading cells, as expected for fibroblasts on TCPS (Figure 4-5A). After 48 hours, the cell number and area further increased (Figure 3-5B). A LIVE/DEAD viability assay indicated that the majority

(~94%) of the harvested and reattached cells remained viable after release from the shape-changing microbeams (Figure 3-5).

3.4. Discussion

The goal of this study was to demonstrate the feasibility of detaching cells from shape-changing surfaces and to investigate the mechanism of release. Toward this goal, we engineered surface-confined hydrogel structures that swell anisotropically when stimulated; in this case, when the environment drops below the transition temperature. Micromolding was used to form these structures because it is amenable to parallel fabrication of patterned structures with diverse geometries and lateral dimensions spanning micrometers to centimeters on the same array, thereby greatly expanding the range of possible tissue module shapes and scales beyond what is currently possible. For this study, rectangular beams were used to create cell stripes which facilitated the investigation of module release. Other tissue module geometries that have been fabricated include arbitrary 2D shapes as well as thin lines and arcs [110].

Fibroblast-based tissue modules with defined geometries formed spontaneously when cells were seeded at high density atop the patterned arrays. Once formed, the harvest of these tissue modules to enable subsequent processing or modular assembly was investigated. Release of tissue modules from pNIPAAm hydrogel microbeams occurred within seconds and was completed within 3 minutes after lowering the culture temperature to 27 °C as long as there were cell to cell connections present and the lateral strains exceeded 25%. This 25% strain minimum was found to be a threshold for triggering release of fibroblast-based tissue modules. An obvious comparison to this surface strain effect is cyclic stretching of cells on elastic substrates. Studies using these experimental systems do not report instantaneous cell release; however, uniaxial stretch is typically less than 20%, designed to mimic physiologic strains [115]. Unlike enzymatic

detachment techniques, the tissue modules released as single entities while unconnected individual cells remained attached to the microbeams. Decreasing the density of cells attached to the shape-changing microbeams significantly reduced cell release even after inducing large strain (≥ 50%). In contrast, cells seeded at high density to form confluent tissue modules detached rapidly and completely from microbeams subjected to similar laterals strains. These results show that the release of the cells depended on the cohesive support from neighboring cells suggesting that intercellular tension may play a significant role. This observation led to an in depth investigation of the mechanism that regulates rapid tissue module release from these shape-changing surfaces.

Importantly, the thermal stimulus used to actuate the pNIPAAm hydrogel was not the key factor in achieving rapid cell release from the shape-changing microbeams. When the amount of crosslinker was varied in the hydrogel network, the extent of bulk swelling and therefore surface expansion was modulated. It was observed that lateral strain greater than 25% was required to initiate confluent tissue module detachment despite all modules being exposed to the same temperature reduction (~10 °C). Thus, the mechanism of rapid release from shape-changing pNIPAAm hydrogels appears to be dominated by mechanical expansion of the surface rather than a change in temperature or hydrophobicity.

A few examples of using stimuli-responsive materials to release cells from surfaces have been successful. Most notably, work pioneered by Okano et al. in the early 1990's focused on the use of thin (~30 nm), grafted pNIPAAm films for cell sheet growth and release [69, 86, 116-122]. They observed that upon lowering the culture temperature below the demixing temperature (~32 °C), cell sheet lift-off occurred in response to the shift in physicochemical properties; specifically the transition of pNIPAAm from a hydrophobic state to a hydrophilic one [68].

However, this technique requires the temperature to be reduced to between 4 - 20 °C to trigger cell release [68, 116, 118]. Furthermore, the release from these surfaces typically takes 15 to 90 minutes raising concerns regarding long-term cellular biochemical disturbances and viability. Extended exposure of cells to low temperature, or hypothermic, environments can significantly impact cellular functions such as transcription, translation, metabolism, and cytoskeletal rearrangement [123-125]. When the mechanism of cell sheet lift-off was investigated, it was found that detachment from grafted pNIPAAm surfaces was reduced by approximately 50% in the presence of sodium azide [68], suggesting that metabolically driven processes are a key aspect to cell release from these surfaces. Additionally, both the depolymerization and stabilization of actin filaments reduced cell sheet detachment indicating that actin dynamics also plays an important role [28]. Based on these findings, it was proposed that cell detachment from grafted pNIPAAm surfaces due to a thermally induced shift in material properties was a two-step process: first, a passive detachment step which is a result in the change in the surface interactions between the pNIPAAm layer and the cell-matrix construct, and second, a metabolically active detachment step which requires cytoskeletal reorganization and intracellular signal transduction [28]. Thus, an alternative release technique that requires only a small temperature shift, or other harmless stimulus, to trigger tissue module detachment in only seconds is desirable; however such an approach would have to rely on a radically different mechanism of release.

In an effort to achieve faster release, another group demonstrated the release of an intact cell sheet from a different thermosensitive hydrogel, Tetronic-tyramine [126]. Release from this surface takes only 10 minutes, but a thermal shift from 37 °C to 4 °C is required. To control or accelerate cell detachment from pNIPAAm surfaces, others have altered the

hydrophilic/hydrophobic content of pNIPAAm by co-grafting with hydrophilic moieties or used approaches such as serum free media to completely recover attached cells [127-130].

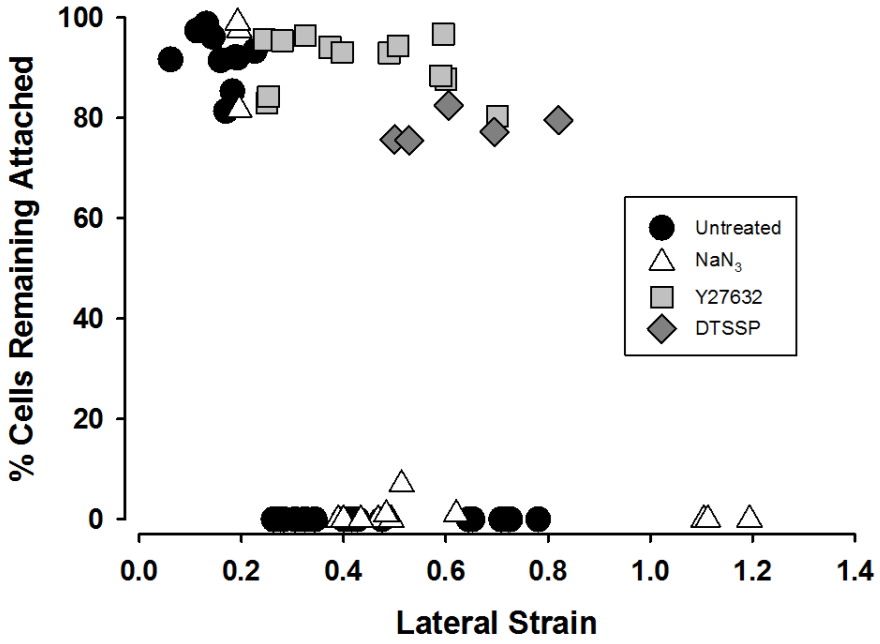

Figure 3-3: Surface strain regulates tissue detachment from pNIPAAm microbeams. Untreated, sodium azide (NaN_3), Y-27632, or DTSSP treated tissue modules were subjected to a range of lateral strain on shape-changing microbeams. Each data point represents one experiment. The vertical dashed line indicates the 25% strain threshold for releasing untreated tissue modules.

For the tissue modules formed on pNIPAAm microbeams, reducing metabolic activity by treatment with sodium azide had no detectable impact on tissue module detachment, in contrast to grafted pNIPAAm surfaces. Rather, the results suggest that the mechanism for detachment is strongly related to the degree of lateral strain from the anisotropic swelling of the hydrogel microbeams. It is noted that no significant lateral strain occurs in thin grafted pNIPAAm films. We thus hypothesized that this strain-dependent release occurs because the contractile forces within tissues and the stretching forces of the expanding surface were greater than the adhesion

forces, and consequently mechanical failure occurred at the interface between the cells and the surface bound matrix, resulting in detachment.

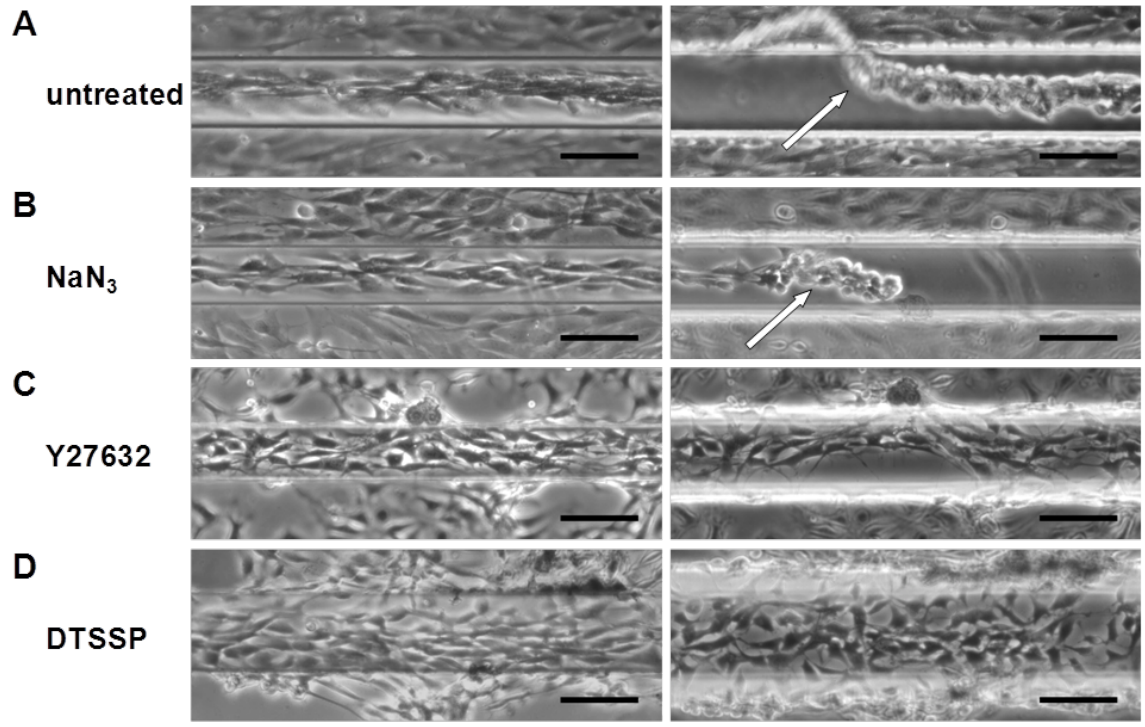

Figure 3-4: Phase contrast images of tissue modules before (left) and after (right) microbeam expansion (~3 min). (A) Untreated, ε = 0.35; (B) sodium azide (NaN_3), ε = 0.50; (C) ROCK inhibitor (Y27632), ε = 0.59 and (D) integrin crosslinked (DTSSP), ε = 0.71 treatments are shown. Arrows indicate detached tissue stripes. Scale bars = 100 μm.

To test this hypothesis, attached tissue modules were treated with Y-27632, an inhibitor of the p160ROCK Rho-associated protein kinase mediated actin-myosin contractility, or DTSSP, a homobifunctinal crosslinker that only links integrin receptors that are bound to their extracellular ligand. Both prevented tissue module detachment for all strains tested (Figure 3-3 and 3-4) suggesting that the mechanical behavior of the tissue plays a significant role in detachment [114, 131]. Image analysis of cells on swollen microbeams after treatment with Y-27632 showed that cells deformed with the surface as the strain was applied indicating greater compliance to stresses generated by the expansion of the underlying surface. Similarly,

examining the DTSSP-treated samples showed cells with crosslinked adhesion receptors remained attached to the microbeams under large strains indicating that release most likely occurs by breaking integrin-matrix adhesions. This is consistent with previous reports that indicate at least some of the extracellular matrix is retained on pNIPAAm surfaces after cell release [11, 71].

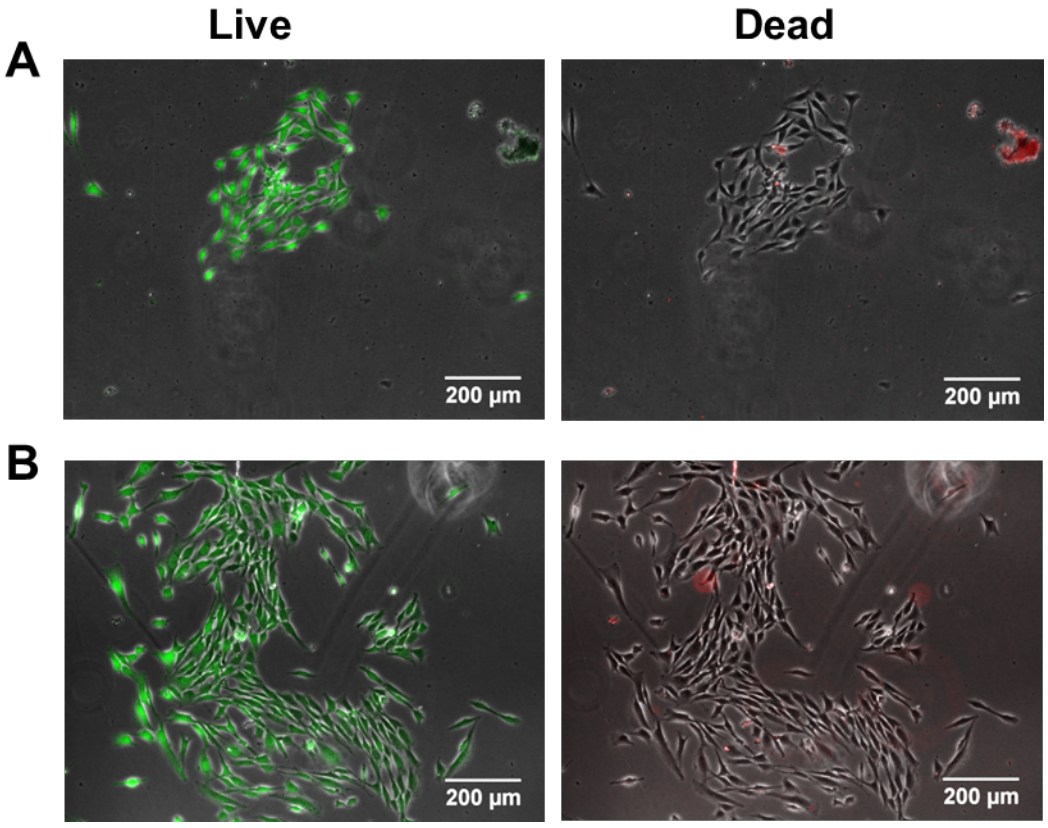

Figure 3-5: Phase contrast and fluorescence micrograph overlays of cells. (A) 24 hours and (B) 48 hours after release from pNIPAAm microbeams and precipitatation onto TCPS. Green indicates live cell staining (calcein AM, left) and red indicates dead cell staining (ethidium homodimer, right).

Together, these results reveal that the release of geometrically patterned tissue modules from shape-changing hydrogel arrays occurs within seconds via a critical strain of the microbeams. Cell-to-cell junctions and cytoskeletal tension are required for complete

detachment, and the separation occurs by disrupting adhesions between the fibroblast and the extracellular matrix. These findings support a novel mechanical release mechanism whereby strain disrupts the cell-matrix adhesive interface because inter- and intra-cellular tension prevents expansion of the tissue module with the swelling surface.

Finally, the small (≤ 10 °C) and brief (≤ 3 minutes) thermal shift of the culture media and the mechanical strain imposed on the tissue modules had minimal effect on cell integrity. Though some cells could have been lost during the transfer, a qualitative viability study following release showed that cells in large aggregates survive, adhere, spread and appeared to proliferate over 48 hours indicating that the rapid cooling and expansion of the support are not detrimental. Thus, the mechanically-driven mechanism for tissue module detachment from these shape-changing biomaterials is promising as it allows for rapid release without enzymatic digestion or extended hypothermic incubation steps, thereby preserving cell health and cell-cell connections. Additionally, it enables the exploration of harvesting tissue building blocks for assembly into complex 3D tissues.

3.5. Conclusion

A purely mechanical, strain-based mechanism of detaching intact tissue modules from patterned arrays of shape-changing hydrogel structures was demonstrated. The fabricated microbeams release cells organized into geometric tissue modules via large lateral strains utilizing the surface-confined hydrogel's anisotropic swelling properties. This mechanically induced method of rapid release is unique in comparison to thermally responsive films and coatings, and we believe is demonstrated for the first time. It is proposed that this mechanism could easily be extended to a variety of shape-changing material surfaces which would allow for controlled and rapid release initiated by stimuli other than temperature, thus providing enhanced

flexibility in the design of future tissue engineering platforms. This novel approach establishes a rapid method for recovery of tissue modules in an efficient manner which may be applicable for the modular, bottom up construction of tissues for organ models and regenerative therapies.

CHAPTER 4: MICRO-CONTACT PRINTING OF TISSUE PRECURSORS VIA GEOMETRICALLY PATTERNED SHAPE-CHANGING HYDROGELS

4.1. Introduction

In *vitro* tissue engineering could provide the needed breakthrough in engineering complex tissue structures such as the myocardium by allowing the construction of viable tissues to aid optimum nutrients and oxygen supply upon implantation. Current tissue printing approaches include inkjet and extrusion-based bioprinting technologies. Thermal or piezoelectric inkjet printers utilize heat or shear forces at the printhead nozzle, which could impair cell functionality and cause reduction in cell populations [53, 132, 133]. Although emerging studies are being conducted to improve cell survival but maintaining adequate cellular functionality and organization remain a challenge. The extrusion-based bioprinting techniques utilizes a "bio-ink" particle deposition method which incorporates either a cylindrical or spherical multicellular aggregates of specific composition and arrangements to aid printing of cells in a more physiological relevant environment by employing tissue fusion and cell sorting mechanisms [56, 57, 134, 135]. The use of cell suspension or hydrogel cell-laden in this approach creates additional intermediates that may impede productivity and also add cost to the preexisting cost-intensive printers. Moreover, these two printing approaches may be limited in terms of scalability, versatility and rapidity. An alternative approach to these two printing techniques is the self-assembly fabrication methods designed with stimuli responsive surfaces.

Recently, Okano and others have developed a tissue fabrication method whereby cells are assembled into sheets by a cell sheet manipulator technique using a temperature responsive polymer, poly-*N*-isopropylacrylamide (pNIPAAm) [84, 136]. Their technique have demonstrated the feasibility of constructing functional and transplantable thick tissues and have made remarkable advancement to promote provision of functionalize vasculatures [80, 89, 137], however the vascular supply is insufficient as the restraint of blood flow in *vivo* still remains tenuous. Herein, we demonstrate an alternative method to assembly of cells by employing the micro-contact printing technique.

Micro-contact printing (μCP) technology was developed over two decades ago for spatial patterning of gold onto surfaces at micron length scales [138]. However, this technique has since proven invaluable for patterning functionalization of biological relevant materials onto substrates to promote tailored cell adhesion. Researchers have printed single or multiple sized islands of self-assembled monolayers (SAMs) to promote adsorption of cell adhesive ECM proteins whereby cells are seeded onto to provide binding specificity to those locations [36, 139]. To our knowledge, μCP of cells directly onto substrates has yet to be illustrated to date. For the first time, we adapt the μCP technology to direct printing of live cells and demonstrate how viable tissues can be constructed in an attempt to design tissue constructs that could address the limited nutrient and oxygen supply challenges in tissue engineering. Though, vascularization studies would need to be conducted to demonstrate this ambitious goal, however this study elicits the basis. Previously, we demonstrated that attached tissue modules on shape-changing three-dimensional (3D) pNIPAAm hydrogel arrays are detached via a strain-mediated process [23]. In this study, we hypothesize that the combination of the shape changing hydrogel and μCP technique provides a reliable method in assembly of cells for use as a stackable device for

fabrication of functional tissue modules. To test this hypothesis, our objective is to show the feasibility of the contact printing process and the viability of the resulting tissues transferred. We first cultured fibroblasts on fabricated 3D patterned pNIPAAm hydrogels and then investigated the effects of contact printing on transferred tissues i.e. stamp force analysis, cell alignment and cell viability. We next examined the effects of cell adhesion promoters on target printing surface. Finally, we evaluated the metabolic activity of the cells printed. This study demonstrates promising results that could transform the field of *in vitro* tissue engineering.

4.2. Materials and Methods

4.2.1. Materials

NIH/3T3 cells were purchased from American Type Culture Collection. Dulbecco's Modified Eagles Medium (DMEM), Dulbecco's Phosphate buffered saline (DPBS), newborn calf serum (NCS), 0.25% trypsin EDTA (1X), penicillin, streptomycin, Calcein AM, ethidium homodimer, Alexa Fluor® 546 phalloidin, Hoechst 33342, goat anti-rabbit IgG secondary antibody and human plasma fibronectin were all from Life Technologies. N-isopropylacrylamide (NIPAAm), 2-dimethoxy-2-phenylacetophenone (DMPA), N, N'-methylenebisacrylamide (MBAm), 3-(trichlorosilyl) propyl methacrylate (TPM), acetone, carbon tetrachloride, Triton X-100, formaldehyde, sodium azide (NaN3) and poly-*l*-lysine were all purchased from Sigma-Aldrich. Tissue culture polystyrene (TCPS) dish was obtained from Fischer Scientific. Methacryloxyethyl thiocarbonyl rhodamine B (polyfluor® 570) was purchased from Polysciences. Silicone elastomer (PDMS) kits (Sylgard®184) were obtained from Dow Corning. Bovine collagen type 1 was obtained from Advanced BioMatrix. Anti-integrin Alpha 5 antibody, AB1928 was purchased from Merck Millipore.

4.2.2. Geometrical Patterned Shape-changing Hydrogel Preparation

Geometrical patterning of the shape-changing hydrogel arrays was fabricated as described previously [19, 23] using soft lithography. The resulting array dimensions had width spacing of 50, 75 or 100 μm covalently bound to a glass coverslip (22 mm x 22 mm).

In preparation for cell culture, the hydrogel arrays were coated with 50 μL of 0.1 mg/mL poly-*l*-lysine (PLL) for 5 minutes followed by a rinsing step in DPBS and then ambient drying in the biosafety hood for at least 2 hours.

4.2.3. Cell Culture

C2C12 skeletal myoblasts and NIH/3T3 mouse embryonic fibroblast cells were cultured in 15% or 10% NCS growth medium respectively, 84% or 89% DMEM and 1% antibiotics (10,000 units/mL penicillin and 10,000 units/mL streptomycin) at 37 °C in a humidified atmosphere of 5% CO_2.

To prepare tissue precursors, trypsinized cells were seeded onto the fabricated shape-changing hydrogel arrays at a density of 500 -750 cells/mm^2 and cultured at 37 °C until confluence.

4.2.4. Micro-contact Printing Process

Initiation of tissue printing occurs once cells seeded on the arrays have reach confluence, either 24 or 48 hours. The arrays are inverted like ink stamps and are placed on top of a target surface to transfer the attached tissues (Figure 4-1). Prior to printing, the target surface, a glass coverslip is coated with either of these three cell adhesion molecules (CAM); 10 μg/mL of human plasma fibronectin for 30 minutes, 100 μg/mL of bovine collagen type I for 3 hours, or 0.1 mg/mL of PLL for 5 minutes all at room temperature. To enable conformal contact to the target surface, a compressive load is applied to the back of the stamp. The sample is then

incubated at 37°C for 15 minutes and immediately placed in a 4°C environment for 5 minutes to initiate the release and printing of the tissues. Finally, the stamp is gently detached from the target surface leaving behind the tissues.

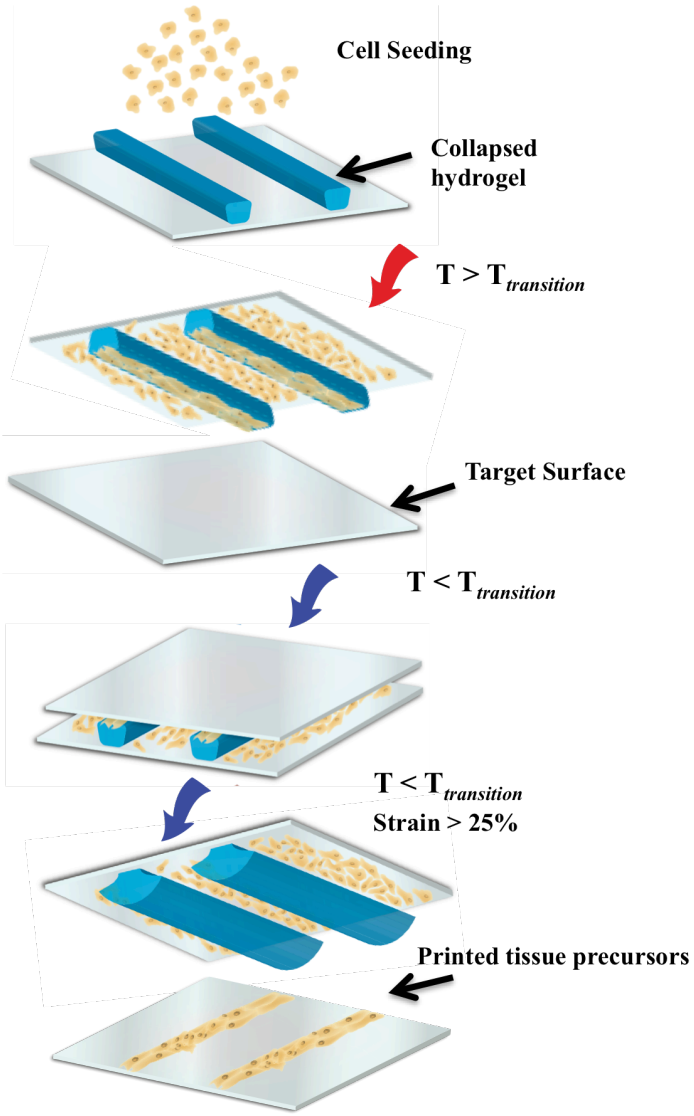

Figure 4-1: Schematic illustration showing the formation and release of tissue precursors (from shape-changing hydrogel micro arrays). Cells adhered to and conformed to the shape of the arrays, organizing into geometric tissue modules. Tissue precursors are then released from micro arrays upon expansion beyond a critical lateral strain of 25%.

4.2.5. Stamp Force Analysis

Compressive force analysis was determined as the amount of pressure applied to the hydrogel arrays (stamp) necessary to induce printing onto the target surface. To establish the optimum load required, calibration weights in 20g, 10g, 5g, 2g or 1g were independently applied to the backside of the stamp while in contact to the target to mate the two surfaces. The corresponding compressive pressure of each calibration weight on a 50 μm microbeam width stamp is 0.71, 1.45, 3.55, 7.10, 14.5 psi respectively. After a duration of 5 minutes at 4 °C, the load and stamp were removed and viability of the printed cells was examined.

4.2.6. Cell Viability Assay

Viability of printed cells was determined by using a LIVE/DEAD kit following the commercially recommended protocol. Briefly, cells were incubated in 200 μL of 20 μM Calcein AM and 40 μM ethidium homodimer-1 solution. Then the cells were rinsed twice with DPBS after 30 minutes and re-incubated in fresh serum containing medium prior to imaging.

4.2.7. Immunofluorescence Staining for Focal Adhesion Components

Printed tissue precursors were fixed in ice cold 3.7% formaldehyde for 5 minutes followed by permeabilization and stabilization of cytoskeletons (CSK) in ice cold CSK buffer with Triton X-100 for 10 minutes. Then a blocking buffer composed of 5% NCS and 0.01% NaN_3 in complete DPBS was used to block nonspecific adsorption for at least 1 hour. The sample was labeled with a primary antibody, polyclonal rabbit anti-integrin alpha 5 antibody diluted in blocking buffer at 1:100 for 1 hour, washed thrice with DPBS for 5 minutes each. Then incubated in goat anti-rabbit IgG secondary antibody conjugated with Alexa Fluor ® 488, Hoechst, phalloidin Alexa Fluor ® 568 diluted in blocking buffer for 1 hour at 1:100, 1:2000 and

1:50 dilutions respectively. Samples were rinsed three times with DPBS and twice with deionized water, sealed with mounting media, and then imaged.

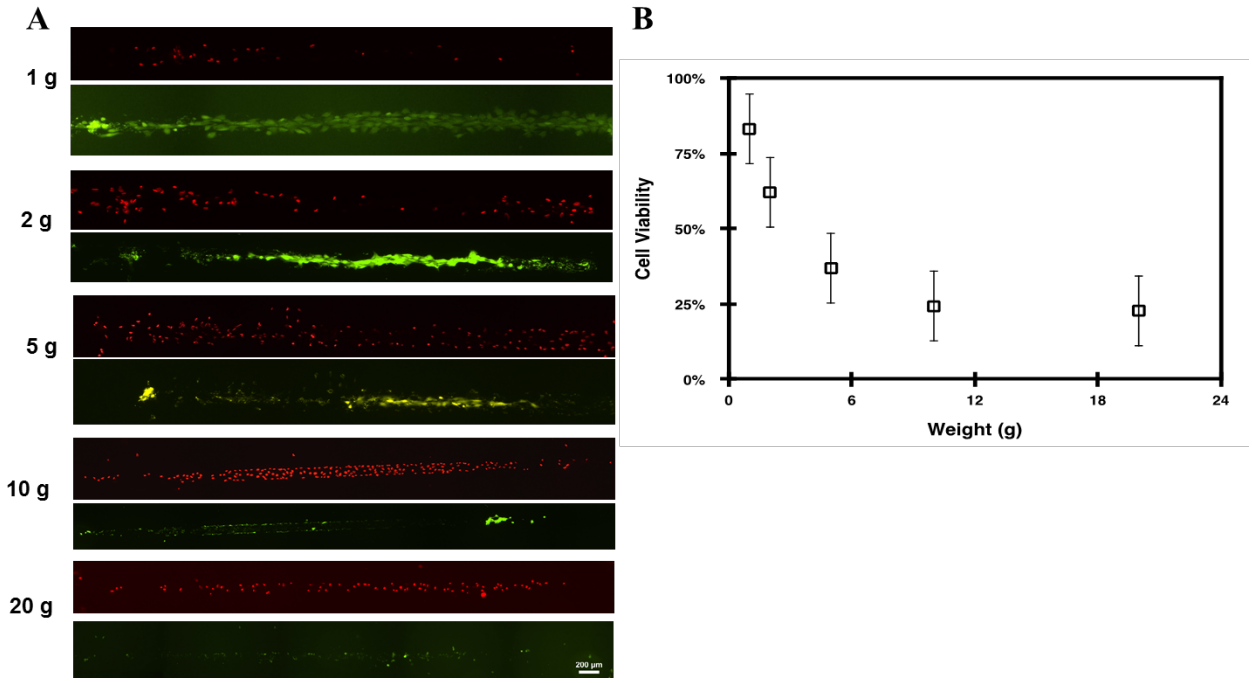

Figure 4-2: Viability of fibroblasts transferred from shape-changing hydrogel (different applied pressure ranging from 1 to 20 g weights). A: Fluorescence micrographs of fibroblast viability. Dead cells (red) and Live cells (green stain). B: Effects of applied pressured on cell viability. Bars represents standard error (SE) (n >3). Scale bar = 200 µm.

4.2.8. Cell Alignment and Orientation Analyses

Cell orientation of the printed tissue precursors and control samples were performed using ImageJ v1.49s (NIH, USA) with a sample size of $n \geq 3$. The angle between the cell morphology and the longitudinal direction of the micro array was measured. For the control samples (cells on non-patterned arrays), this angle was between the minor and major axis of the cells. The percentage of aligned cells was analyzed from the measured orientation distribution by using Excel Analysis toolpak. Cell alignment was determined as the average amount of cells

oriented within ± 20° of the preferred angle of orientation i.e. longitudinal axis of the hydrogel array.

4.2.9. Fluorescence Imaging and Analysis

Prepared samples were examined at ambient temperatures under a fluorescence microscope, Eclipse Ti-U (Nikon Instruments, Japan). The resulting cell images were then analyzed with NIS-Elements advanced research software Ver. 4.20 (Nikon Instruments) or Image J (NIH, USA).

4.2.10. Statistical Analysis

Pair-wise comparisons for cell viability, alignment and orientation data were performed using the two-tailed Student's t-test with $n \geq 3$, where $p < 0.05$ were considered statistically significant.

4.3. Results

4.3.1. Compressive Pressure Applied During Printing Affects Cell Viability

Viability of the printed tissue precursors were found to be predominantly correlated with the amounts of compressive pressure applied during printing. Cell survival was observed after 24 hours of printed tissues on polylysine coated target surfaces. To examine the adequate amounts of pressure necessary to print tissue modules, cells seeded on the shape-changing structures were subjected to pressures ranging from 0.71 to 14.5 psi and viability of the cells after transfer was analyzed. Calibration weights of 1-g, 2-g, 5-g, 10-g and 20-g were used to vary the amounts of pressure. A LIVE/DEAD viability assay determined that the lowest amount of pressure applied resulted in the most viable cells (~83% ± 3) of the (Figure 4-2). The number of

dead cells decreased as the amount of pressure applied was systematically reduced. A plot of the measured viable cells shows a power series regression model with an R-squared value of 95.9%.

4.3.2. Effect of Micro-contact Printing on Cell Adhesion Molecules Adsorbed Target Surfaces

Printing on target surfaces adsorbed with collagen type 1, fibronectin and polylysine did not show any statistical difference in cell viability. Viability of printed tissue precursors was reduced by 11, 22, and 7% for collagen, fibronectin and polylysine respectively in comparison to the control samples. Negative control consists of cells printed on plain glass surface and no cell transfer was observed to such surface while a positive control that include cells cultured on plain glass showed the highest number of viable cells. A single factor ANOVA test indicate a $P > 0.05$

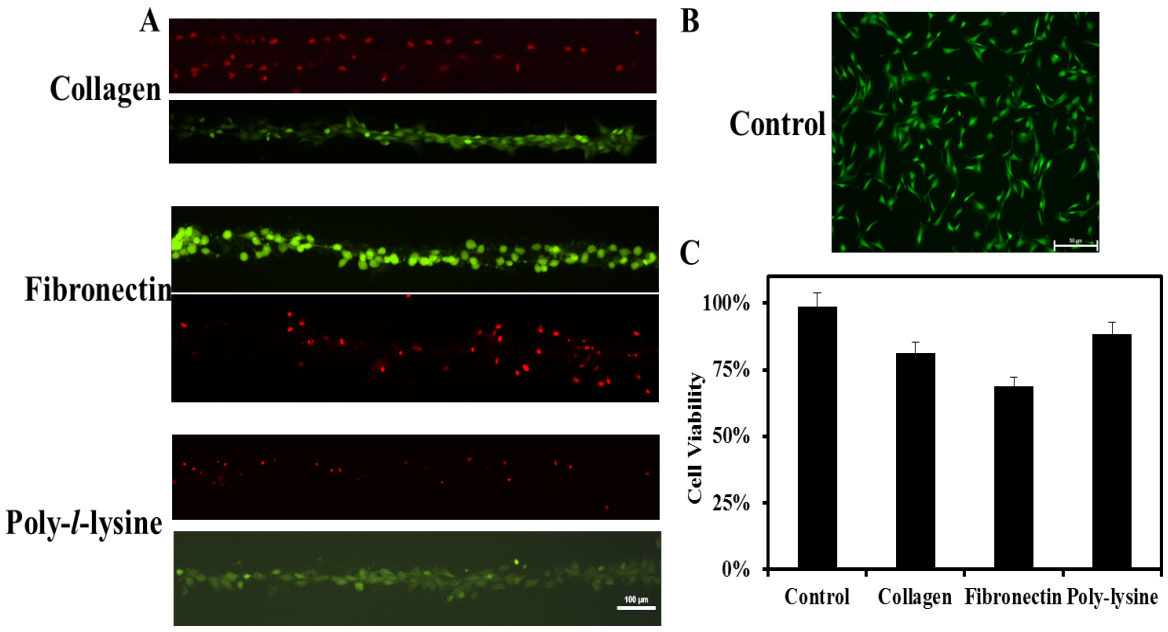

Figure 4-3: Viability of fibroblasts printed on cell adhesion promoters adsorbed target surfaces. A: Fluorescence images of printed tissue precursors on collagen, fibronectin and poly lysine surfaces. Dead cells (red) and Live cells (green stain). B: Positive control sample. Cells are seeded on plain glass coverslips. C: Bar charts representing the percentages of viable cells on the coated target surfaces. Bars represent standard deviation +/- 5 (SD) (n =3). Scale bar = 100 µm.

indicating no significant difference between the means. For subsequent printing, polylysine was selected as the CAM of choice for all target surfaces due to the ease of use and stability at ambient temperature.

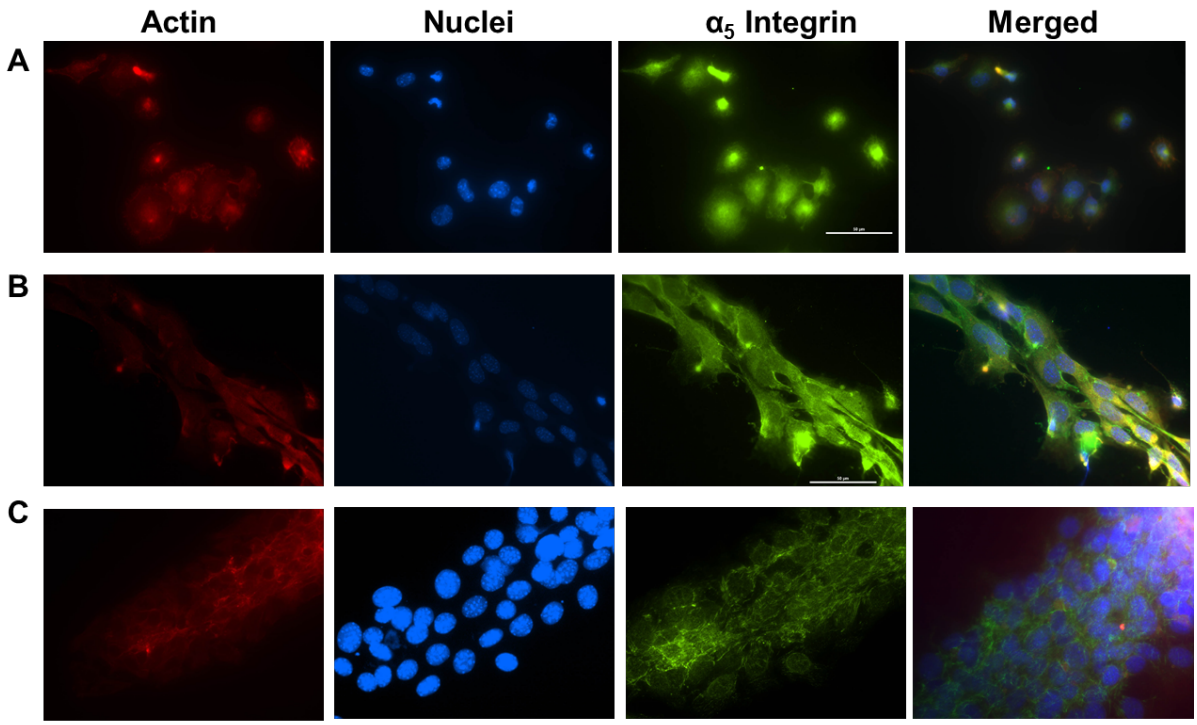

Figure 4-4: Structural components of fibroblast before and after printing with shape-changing hydrogel. Fluorescence micrographs of actin filament, nuclei and α_5 integrin A: After 2 hours of cell seeding on TCPS. B: Images of tissue precursors after 1 hour post printing. C: Printed fibroblasts showing formation of actin filaments, focal adhesion complexes and nuclei after 2 hours post printing. Cell nuclei (blue) were stained using Hoechst, actin filaments were stained with AF 568 phalloidin (red) and α_5 integrin were stained using polyclonal ab1928 (green). Scale bar = 50 μm.

4.3.3. Printed Tissue Precursors Reveal Preserved Focal Adhesion Components

To assess cellular morphology and metabolic activity, we compared printed cells to cells cultured on plain glass surface. An hour after printing, the actin stress fiber staining showed an elongated morphology compared to the rounded morphology seen in cells seeded on glass even

after 2 hours. To examine the cell-matrix adhesions, we stained the cell nucleus and the alpha 5 integrin an hour and 2 hours after printing. The results reveal emergence of physical integrin clustering at an hour after printing and enhanced clustering after 2 hours of printing indicating rapid reformation and recapitulation of focal adhesion components, which is attributed to the preserved cell morphology compared to the control samples (Figure 4-4).

4.3.4. Shape-changing Surface Provides Contact Guidance Cues for Cellular Organization

Analysis of cell orientation distribution revealed that cells elongated along the hydrogel pattern longitudinal direction well at 24 hours (Figure 4-5C, D). Spatial organization of printed cells showed a preferred orientation between 0° and 30° axis, compared to the random distribution observed in cells cultured on non-patterned pNIPAAm hydrogel after 24 hours (Figure 4-5A, B). Cell alignment calculations were made from the average cell orientation distribution values and the results indicate 90.8 % ± 0.11 of cells were aligned within ± 20° of the hydrogel array pattern direction.

Cellular organization was found to be dependent on the patterning of the hydrogel. Significant difference was observed between alignment of cells on non-patterned and patterned surfaces. Together these results indicate that the shape-changing hydrogel arrays provide contact guidance cues for spatial organization of cells depending on the width dimensions of the arrays.

4.3.5. Demonstration of Micro-contact Printing Technique on Other Cell Types

The micro-contact printing technique described here could be independent of cell types. C2C12 cells printed with shape-changing hydrogel stamps were observed to occur under the same conditions as the fibroblasts. Myoblasts tissue modules were incubated for 15 minutes at 37 °C and the tissue was completely transferrable under 1g weight to a target surface coated with polylysine within 5 minutes at 4 °C (Figure 4-6). However, the skeletal myoblasts were

observed to be more contractile so precautions were taken to avoid premature release. Viability of the myoblasts was determined as 89 %.

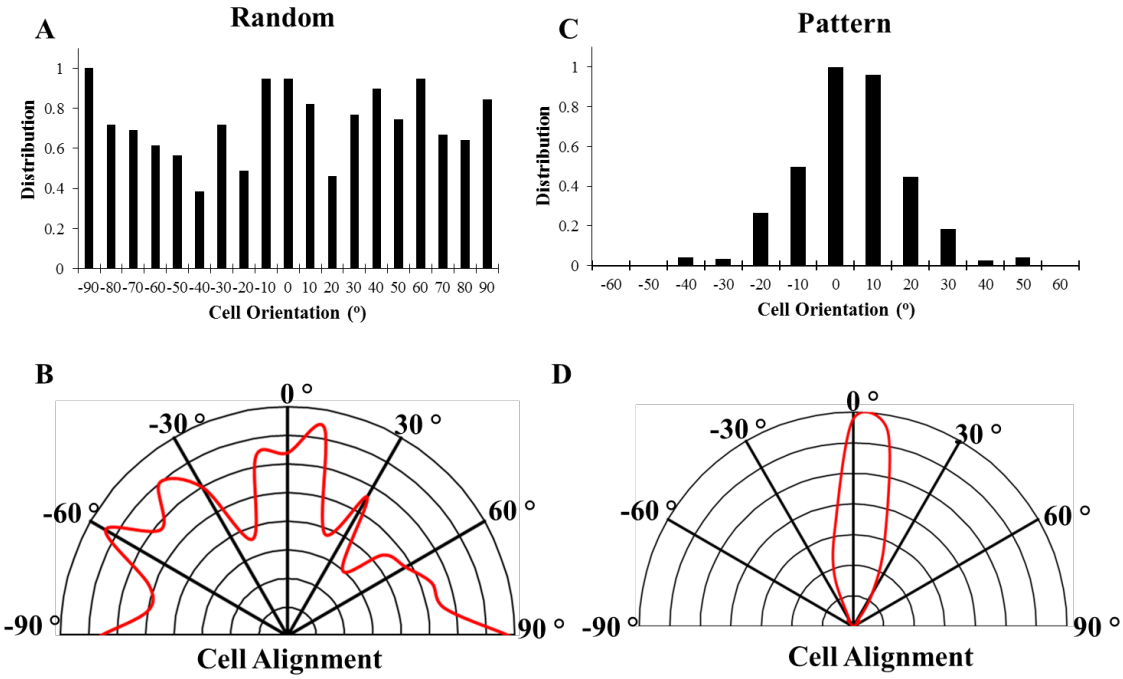

Figure 4-5: Cellular spatial organization before and after printing from shape-changing hydrogel. A & B: Distribution of cell orientation and polar plot on the control samples showing random organization. Cells were seeded on plain TCPS with no patterning for 24 hours. C & D: Distribution of cell orientation and polar plot on printed tissue precursors samples showing aligned organization governed by the hydrogel's pattern. Cells were seeded on patterned arrays for 24 hours with pattern direction at 0° axis. Sample size, $n \geq 3$.

4.4. Discussion

This research study aims to demonstrate the viability of fabricating tissue precursors from shape-changing surfaces by utilizing a micro-contact printing technique. Towards this goal, we cultured cells on previously developed surface confined poly-isopropylacrylamide hydrogel structures and then investigated the parameters to produce functional tissue modules. 3T3

fibroblasts were employed as a model cell type mainly to demonstrate the feasibility of printing due to its immortalized properties.

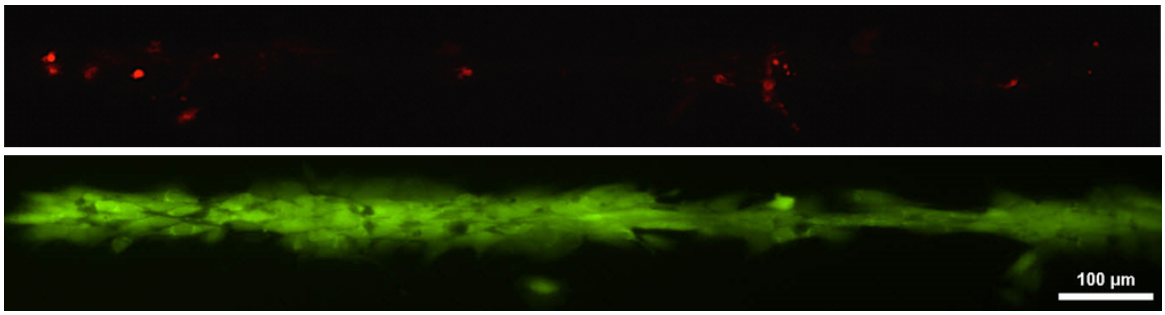

Figure 4-6: Murine skeletal C2C12 tissue precursors printed with shape-changing hydrogel. Fluorescence images of printed Myoblast tissue precursors on polylysine surfaces under applied pressure of 1g. Dead cells (red) and Live cells (green stain). Scale bar = 100 µm.

Notably other forms of printing tissues from stimuli responsive surfaces have developed functional transplantable tissue for repairs of corneal dysfunction, periodontal ligament to cardiac failure [74, 75, 117, 140]. However, their methods are limited to layer-by-layer assembly of tissues, which requires the use of longer incubation times up to 90 minutes at cold temperatures due to the hydration limitations of the nanoscale grafted brushes of the thermoresponsive surfaces used [141]. Other printing approaches that include inkjet printing and mechanical extruders bioprinting technologies seem promising for fabrication of solid organ structures owing to their high culture throughput, improved cell seeding densities and controlled spatial resolution [55, 56, 133, 135]. Boland and others used a commercial, thermal-based inkjet printer in printing Chinese Hamster Ovary (CHO) cells into pre-defined patterns and were able to show improved cell viability though patterning of the cells was not well maintained [53, 55, 142]. In these studies, requirements of cell suspension intermediates; loss of cell viability; need for low viscosity solutions to prevent clogging during droplet generation; maintaining cell

morphology and organization of cell patterning; and the relatively high cost of printers still remains a challenge. An alternative approach is the use of a nozzle-free acoustic ejector to overcome clogging [134]. Hydrogel droplet based systems or cell-suspension intermediates were found to address some of these challenges. Demirci and others developed a cell-laden hydrogel droplet deposition system for printing bladder smooth muscle cells and showed microscale spatial resolution while maintaining long-term cell viability [143]. Though the applications of the described systems are relevant to tissue engineering and regenerative medicine, an alternative approach that addresses rapid formation of tissues and that can retain cell morphology without the use of any intermediates between the cells and target substrate is of great benefit.

In this study, we demonstrate for the first time the feasibility of printing cells from a simple and direct contact printing method that may overcome these challenges. Similar to conventional micro-contact printing process whereby the stamp, typically a PDMS template, deforms while transferring the material of interest to its target, herein the stamp is a shape-changing structure that laterally expands around its transition temperature during cell printing. This expanding surface allows the stamp to be lifted off the target gradually without smearing or distorting the patterned tissues. Cells grown on such surfaces were recently reported to detach as intact tissue stripes by an applied strain of at least 25% as a result of lower adhesion strength between the ECM and shape-changing surface compared to the stronger bond between cell and its ECM [23]. Additionally, failure events common in conventional μCP are similar to our setup. Though sagging or roof collapse as commonly reported in μCP [77] are not experienced in this particular setup, surface chemistries of the target substrate and the amounts of compressive pressure applied during transfer was found to be significant for successful printing.

Fabrication of functional tissues via a printing mechanism requires processes that are not detrimental to the health of the cells but rather promotes growth and preserves functionality *in vivo*. Pressures < 1 psi was found to yield approximately 83% in cell viability (Figure 4-2). Pressures lower than 0.71 psi impeded cell transfer due to insufficient conformal contact to the target surface.

In an attempt to optimize the cell viability and to understand which surface is more energetically favorable for cell binding, we studied the effects of protein or CAM adsorbed to the target surface using a compressive pressure of 0.71 psi. All tissues were printed within 5 minutes. Collagen type 1 and human plasma fibronectin were selected based on their relative abundance physiologically. While polylysine, a chemically synthesized positively charged amino-acid was selected to promote cell binding to culture surfaces by electrostatic interactions with the negative charged ions of the cells. No statistically significant difference in cell viability was observed between the CAMs tested though the polylysine target surface showed higher amounts (Figure 4-3). Hence, all studies utilized polylysine for its ease of use and stability.

Cellular organization is crucial for controlling microarchitecture and biological functions of tissues so we evaluated the alignment and orientations of printed cells as well as the effects of pattern width of the hydrogel. Cells proliferated randomly on non- patterned hydrogel. Meanwhile, preservation of spatial organization of cells was apparent after printing from the hydrogel arrays indicating that the arrays provide contact guidance cues for cells to orient. The percentage of cells that oriented along the longitudinal axis of the shape-changing array differs depending on the width of the arrays, a result consistent with other findings. A 50 μm pattern width significantly showed increased alignment with 3T3 fibroblasts and normal human dermal fibroblasts than wider patterns [82, 144]. Patterning dimensions for cell functionality is important

and necessary for promoting cell-to-cell communication in cardiomyocytes as reported by McDevitt [79]. A specified width dimension of < 30 μm was observed to induce synchronous beatings in cardiomyocytes, an electrical coupling property necessary for fabrication of functional myocardial constructs.

Importantly, examination of the focal adhesion complexes of the printed tissue precursors was noticeable shortly after printing. These results suggest that μCP printing technique does not hinder the normal regulation of cell binding and signaling activities. The actin filaments and alpha 5 integrin markers were observed to be significantly oriented in the cells compared to the control samples suggesting that the cytoskeleton of the cell is also regulated by the hydrogel array patterning (Figure 4-4). Interestingly, this preservation of the cell-matrix adhesion domains allows for assembly of subsequent tissue stripes thus enabling construction of 3D tissues.

Finally, we assessed the possibility of extending our simple μCP method to another cell type. We chose C2C12 cells for potential applications in skeletal muscle tissue engineering. This myoblast demonstrated similar detachment and printing times with the exceptions of the high contractility nature of the cell type, which was expected. The cells stripes were observed to readily detach while pulling along neighboring cells at higher tension than the fibroblast (data not shown). This cell type would be further explored for our sequential stacking of 3D cell stripe layers.

To our knowledge, μCP of cells directly unto a surface without the need of an intermediate has been demonstrated for the first time. Functional tissue precursors can be printed within 5 minutes with stamps constructed from a shape-changing hydrogel of poly-*N*-isopropylacrylamide. The stamps provide contact guidance cues for tissue spatial organization as observed by the cellular organization along the major axis of the hydrogel array. Formation of

focal adhesion complexes is prominently observed within a short time after printing. Tissue printing developed by a combination of shape-changing surfaces and μCP technique provides an alternative approach to other printing techniques allowing for faster production and preserved organization. In addition, this process could be optimized to allow printing of unique shapes of tissues to aid vascularization upon tissue implantation. Future studies would include fabrication of different geometries of the hydrogel arrays to provide contact guidance cues for assorted tissue formation.

4.5. Conclusions

Micro-contact printing of organized tissue modules from patterned arrays of shape changing hydrogel structures was demonstrated for the first time. Tissues are printed under low compressive pressures onto preferred target substrate without distorting the cell morphology or organization while still preserving its cellular functions. This simple method is easy to use and adaptable since no elaborate equipment is required and therefore allows for translation to other forms of stimuli responsive systems.

Future efforts will include optimization and automation of the printing system to enable higher printing resolution and culture throughput while exploring printing of versatile patterns for development of tissues that have complex organized microarchitecture *in vivo*. This direct method of printing cells without the need of cell suspension intermediates provides a powerful tool for investigation of tissue morphogenesis *in vitro*.

CHAPTER 5: ASSEMBLY OF PRINTED TISSUE PRECURSORS INTO THREE-DIMENSIONAL STRUCTURES

5.1. Introduction

Engineering robust biomimetic three-dimensional (3D) tissue structures is crucial in order to facilitate the repair of diseased tissues and organs. In tissue engineering, an ideal tissue construct should be able to recapitulate the functions of complex tissue micro architecture found in native tissues. Construction of 3D tissues *in vitro* creates an effective design model to systematically study a variety of cell types by manipulating cell interactions through tissue assembly, patterning or geometry.

Functioning of tissues is well correlated with the anatomic structure. Mechanical functioning of skeletal muscles is sustained by its vasculature, which is anisotropic in nature when fusion between muscle fibers and myoblasts occurs. In the organs, the structural network of liver facilitates transportation of waste and products. Each of the lobules in the liver is made up of plate-like assemblies of hepatic cells. Similarly, the highly oriented cyto-architecture found in myocardial tissues is important for the proper electromechanical functioning of the cardiomyocytes.

Previous studies have fabricated patterned 3D tissue structures *in vitro* by employing bioprinting techniques, inkjet printers and a cell sheet stacking manipulator method [56, 84, 142]. The most prevalent challenge encountered in these techniques is the need to enhance

prevascularization in the engineered tissues. The common strategy is to engineer dual cell types in different orientations to induce structural organization and promote formation of vascular networks upon tissue implantation [80, 145]. Though their results are promising, an alternative method that could give rise to rapid production of organized tissue precursors with different sizes and geometry is beneficial.

Recently, shape-changing hydrogel consisting of poly-*N*-isopropylacrylamide (pNIPAAm) molecules was shown to trigger release of intact tissue modules within 3 minutes [23]. Harvested cells from the substrate had > 90% in viability and re-plated cells continued to proliferate. The micron scale features of the pNIPAAM hydrogel promoted super hydration of the elongated chains and allowed for the fast detachment of tissues without the need for metabolic mechanism. Cell detachment occurred quickly at approximately 27 °C, a minor shift below the relevant physiologically temperature of 37 °C thus preserving the biological activity of the cells.

Herein, the lateral expansion capability of the shape-changing poly-*N*-isopropylacrylamide hydrogel is used to guide the orientation of cells into a well-organized 3D structure. The ability to print tissues into multiple layers and geometry were explored. The hypothesis is that the micro-contact technique enables assemblies of viable tissue precursors into well-organized 3D structures and that the use of shape-changing surfaces directs formation of tissue constructs into diverse geometries, size and organization. To test this hypothesis, the objective is to mimic native tissue cell orientation by fabricating tissue modules composed of fibroblasts and myoblasts in two orientations through the use of shape-changing hydrogel and a micro-contact printing technique.

5.2. Materials and Methods

5.2.1. Materials

The materials for this chapter are the same as in section 4.2.1 previously described.

5.2.2. Preparation of Patterned Stamps

The fabrications of patterned stamps are the same as in sections 3.2.2 and 4.2.2 previously described. In addition, closely spaced arrays of 10 µm x 2µm x 10 µm (wide x height x spacing) were fabricated using a mask containing the defined dimensions and photo-lithography was also employed.

5.2.3. Cell Culture

The cell culture method for this chapter are the same as in section 4.2.3 previously described.

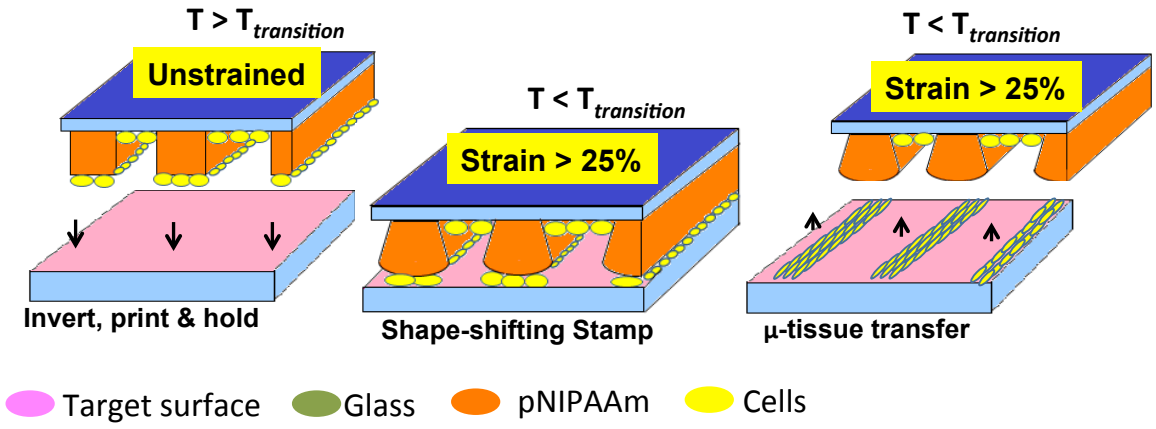

Figure 5-1: Schematic diagram of micro-contact printing technique. Cells are cultured on shape-changing stamp; the stamp is inverted and placed in contact with a target surface to facilitate cell adhesion; a thermal shift induces swelling which causes rapid detachment of the tissue modules from the stamp, transferring the pattern cells to the target surface.

5.2.4. Micro-contact Printing of Cells

Figure 5-1 shows the schematic diagram of the micro-contact printing technique. Pre-stained cells (see Appendix B.1.2) with density > 500 cells/mm^2 is seeded on polylysine coated patterned arrays of the shape-changing hydrogel. After 24 to 48 hours, the stamp containing confluent cells is inverted and placed in contact with a target surface to facilitate cell adhesion. Then a 1 or 2 gram calibration weight is taped to the back of the seeded stamp and placed on the target surface (monolayer of cells or pre-coated TCPS) in medium. The sample is then incubated for 15 minutes at 37 °C and immediately transferred to 4 °C chamber for 5 minutes. Then the weight is gradually lifted off the target surface leaving behind a cell stripe while no cells are left on the stamp. The temperature reduction causes swelling of the hydrogel arrays inducing detachment of the tissue modules from the stamp to the target surface.

5.2.5. Assembly of Multilayered Patterned Cells

Two sets of double layer sheets were assembled on an unstained monolayer of confluent cells. Patterned stripes of myoblasts were directly printed on the two dishes of monolayer of fibroblasts. Collagen solution was cured on one of the monolayers. 100 μg/mL of bovine collagen type I with a pH of 7.3 was prepared by following commercially recommended protocol. 2 mL of the collagen solution was gradually added to a confluent cell culture dish after the medium was removed. The solution was then allowed to cure for 90 minutes at 37 °C.

Triple-layer assembly of tissue precursors were constructed by stacking patterned myoblast in between a patterned fibroblast and a monolayer of confluent fibroblast. The patterned fibroblast and myoblast were pre-stained with cell tracker orange and green respectively and stacking was oriented 90 °C from each other.

5.3. Results

5.3.1. Formation of Fibroblasts and Myoblasts Tissue Modules

Shape-changing hydrogel from pNIPAAm arrays is use to fabricate tissue modules of multiple cell types by employing the micro-contact printing technique. Cells printed from arrays of the shape-changing structures maintained their cell orientations either when printed on protein coated surfaces or a monolayer of cells (Figures 5-2 & 5-3). No observable differences were seen in the printing mechanism of the two cell types. Both cells released from the hydrogel in 5 minutes at 4 °C under a compressive pressure of 1g calibration weight. However, myoblast cells seem to elongate more along the longitudinal axis of the arrays compared to fibroblasts.

5.3.2. Multilayered Assembly of Tissue Modules

Multilayered structures were achieved by stacking tissue modules onto pre-existing layer or layers of cells. Figure 5-4 shows the assembly of two layers of cells. A fibroblast cell stripe transferred onto a monolayer of fibroblast cells was first observed to print on the monolayer, as the cells in that layer seem to pave a pathway for the cell stripe (Figure 5-4 A & B). This occurrence was due to the lateral volume expansion of the hydrogel and the amount of compressive pressure on the arrays. Swelling of the hydrogel which is induced by the reduction in temperature at 4 °C could expand the beam by a factor of 0.5 of its original size [110]. The expansion in the hydrogel array is the observed print on the monolayer of cells at the top and bottom sides of the tissue array. Reduction in the compressive pressure to 1g-calibration weight improved the transfer of the cell stripe (Figure 5-4 C & D). Printing a myoblast cell stripe on a monolayer of fibroblast did not influence the printing resolution or outcome compared to the fibroblast cell stripe onto fibroblasts monolayer (Figure 5-4 D & E). Printing of intact tissue modules is attained on a 3-layered structure (Figure 5-5). The myoblast cell stripe is printed

between a layer of fibroblast cell stripe and its monolayer. The 3-layer tissue module structure is located where the three boxes overlap.

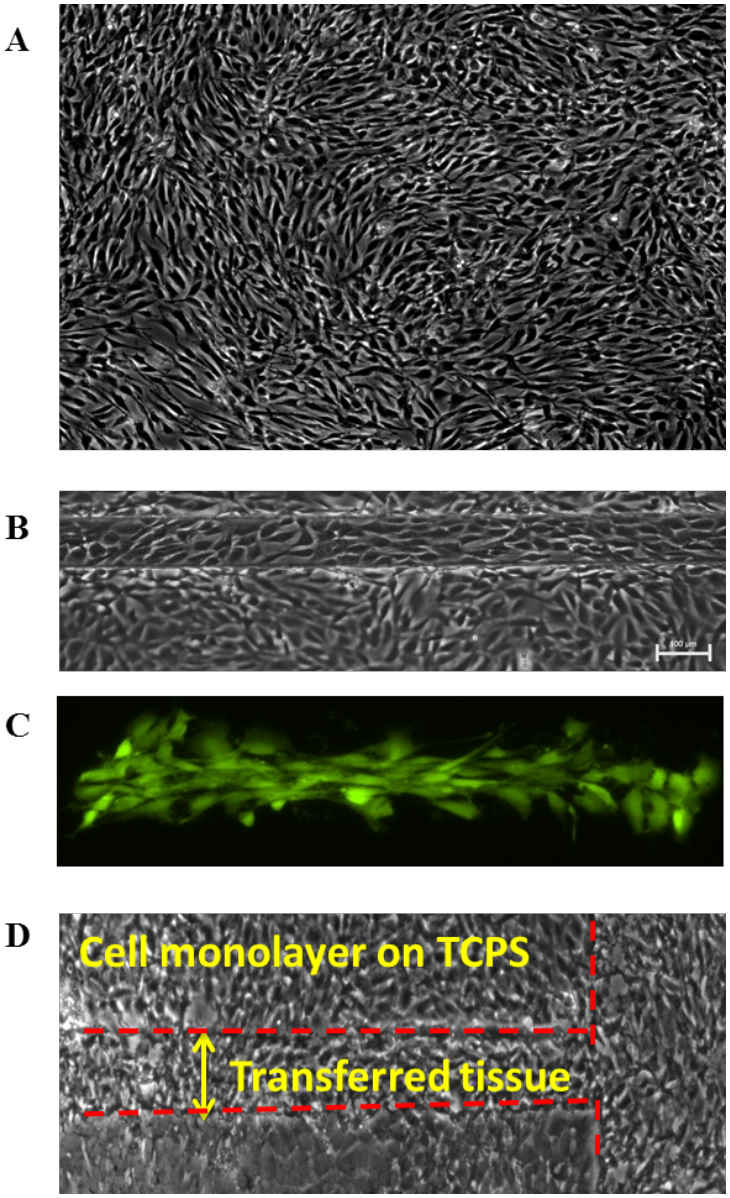

Figure 5-2: Fabrication of fibroblast tissue modules. (A) Confluent monolayers of cells cultured on TCPS after 24 hours. (B) Cells cultured on 100 µm wide arrays of shape-changing hydrogel. (C) Tissue modules printed on polylysine coated TCPS stained with cell tracker green. (D) Printed tissue modules on monolayer of cells.

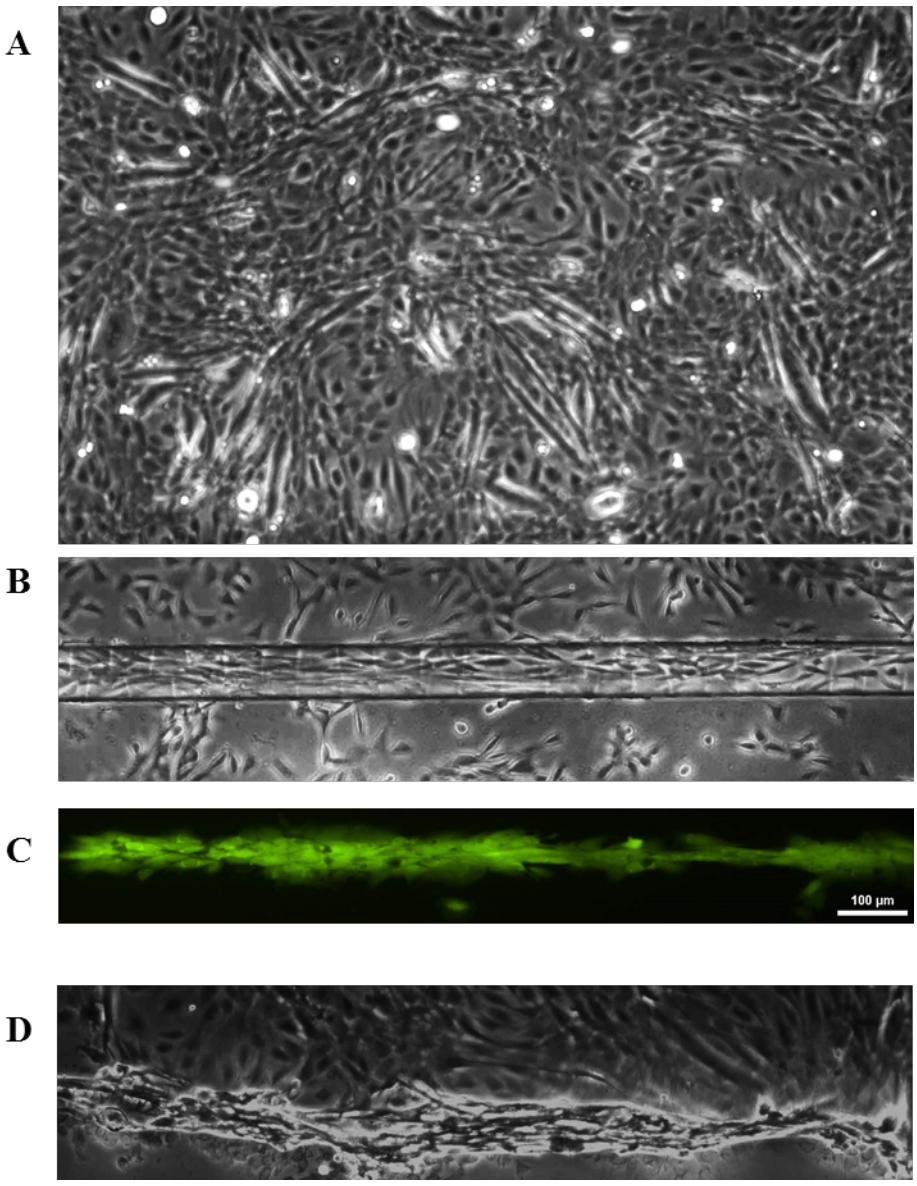

Figure 5-3: Fabrication of myoblast tissue modules. (A) Confluent monolayers of cells cultured on TCPS after 48 hours. (B) Cells cultured on 100 µm wide arrays of shape-changing hydrogel. (C) Tissue modules printed on polylysine coated TCPS stained with cell tracker green. (D) Printed tissue modules on monolayer of cells.

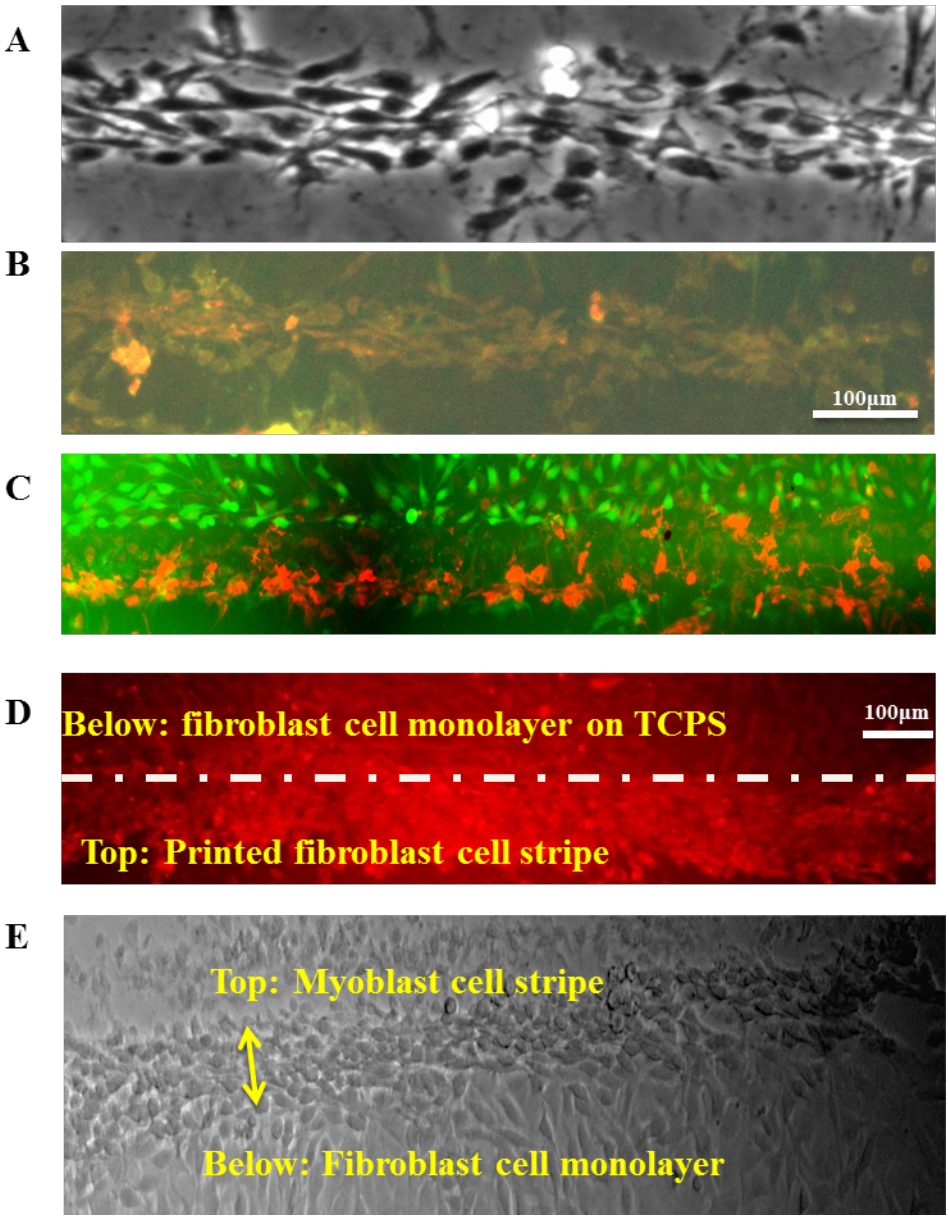

Figure 5-4: Assembly of 2-layer tissue modules. (A) Printed fibroblast tissue modules on monolayer of fibroblast cells in phase contrast with conformal printing pressure of 2 grams. (B) Printed fibroblast tissue modules (red stain) on monolayer of fibroblast cells (green stain), fluorescent images. (C) Printed fibroblast tissue modules on monolayer of fibroblast cells with cell tracker red staining on both layers with conformal printing pressure of 1 gram. (D) Printed myoblast tissue modules on monolayer of fibroblast cells in phase contrast.

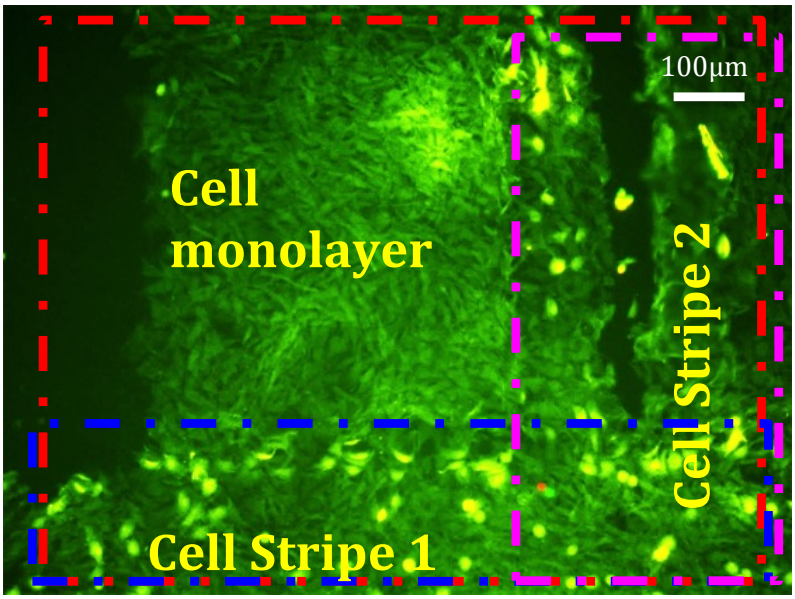

Figure 5-5: Assembly of 3-layer tissue modules. Monolayer of fibroblast cells (unstained) are cultured for 48 hours then myoblast cells (stained green) are printed along the horizontal axis of the monolayer as cell stripe 1 while an array of fibroblast cells (stained red) are printed on top the cell stripe 1 along the vertical axis of the monolayer as cell stripe 2.

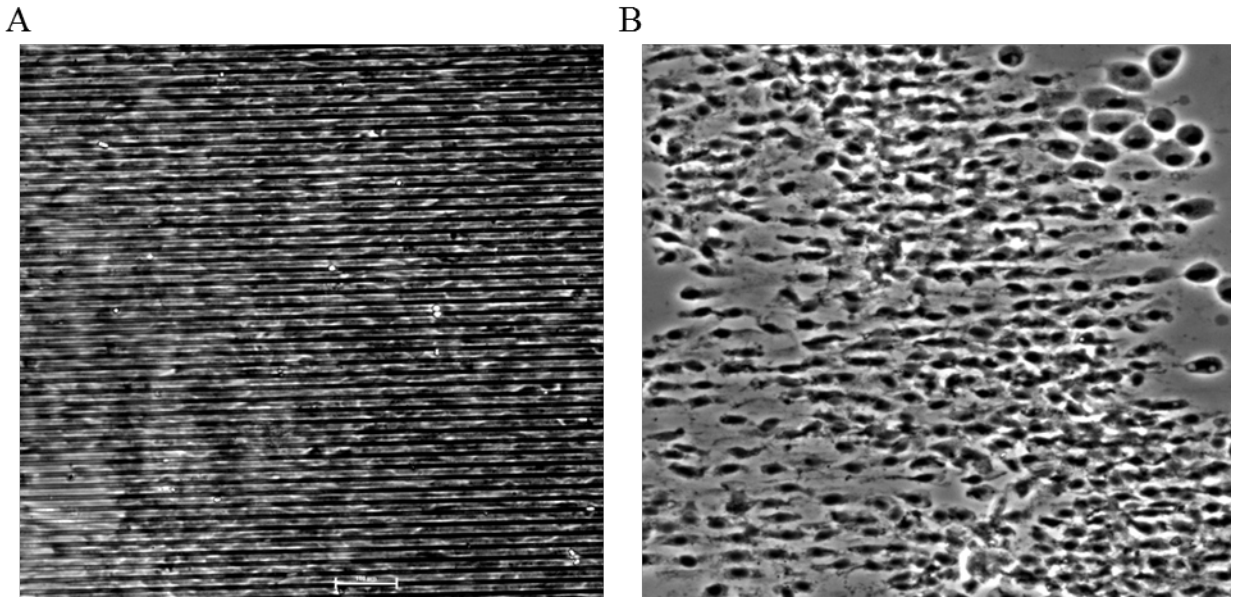

Figure 5-6: Fabrication of cells from closely spaced arrays of the shape-changing hydrogel. (A) Fibroblasts are cultured on 10 µm wide by 10 µm spacing arrays of the microbeams for 24 hours. (B) Printed cells from the 10 µm by 10 µm arrays onto a polylysine coated TCPS.

5.3.3. Formation of Diverse Tissue Modules

Arrays of the shape-changing hydrogel allows for printing of tissue modules with different geometries and/or spacing. Fibroblasts cultured on stamps fabricated with closely spaced arrays of the microbeams maintained cell orientation along the long axis of the beams (Figure 5-6). To our surprise, tissue module released from a 75 μm beam array resulted in a buckled structure when printed the protein adsorbed TCPS (Figure 5-7). Cells seeded on arrays with aspect ratios > 1.0 is expected to buckle due to conformance to the final structure of the hydrogel array in the swollen state [110]. These results suggest that patterning of the hydrogel may be used to direct cellular organization of diverse forms.

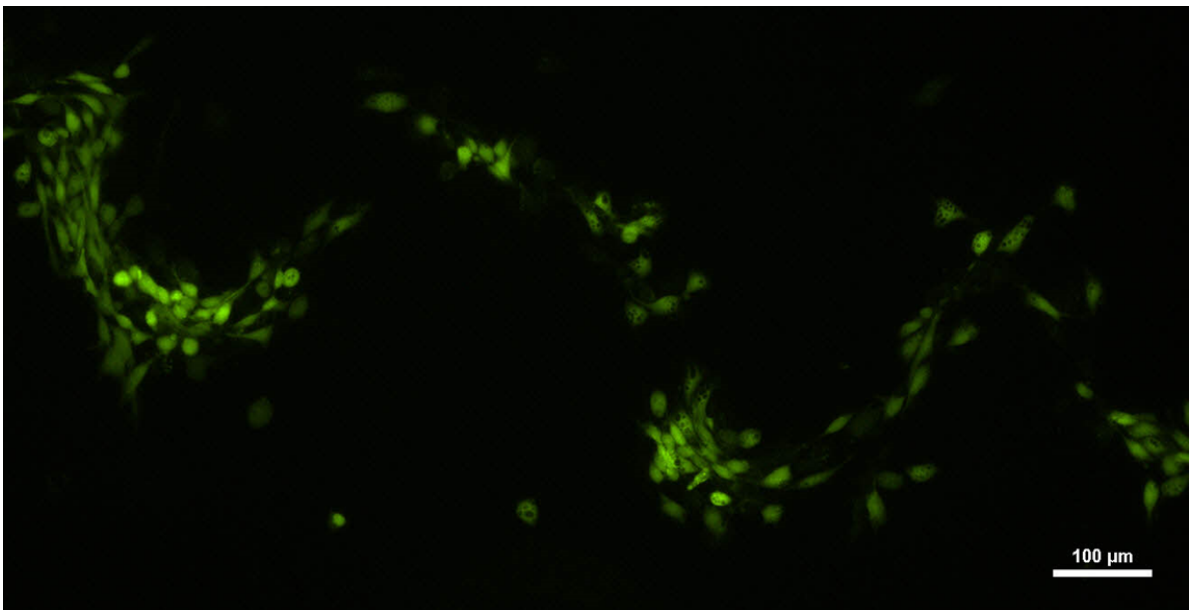

Figure 5-7: Fabrication of buckled tissue modules from 75 μm wide arrays of the shape-changing hydrogel. (A) Printed tissue modules on polylysine coated TCPS, calcein staining (B) Live (green) /Dead (red) staining of the buckled tissue module.

5.4. Discussion

The goal of this study is to demonstrate the versatility of the micro-contact printing technique for printing cells from patterned arrays of shape-changing hydrogel. To investigate how this technique can be used to build functional three-dimensional tissues, fibroblast and myoblast cells were cultured independently on the microbeams of the shape-changing hydrogel while micro-contact printing technique was used to transfer the organized tissue modules into parallel and perpendicular orientations. The possibility of forming diverse tissues was also introduced. This study provides knowledge on how to build and control tissue structures that are complex in nature.

Cellular behavior is influenced by response to surface geometry and co-culture with other cell types. Cell reorganization and formation of vascular networks were observed when stripe-patterned endothelial cells are sandwiched between parallel oriented sheets of normal human dermal fibroblasts (NHDF) [80]. However, a perpendicular orientation of the NHDF sheets did not reorganize the cells.

In this study, tissue modules transferred to protein adsorbed TCPS maintained their cellular organization (Figures 5-2 & 5-3). The morphology of the cells was the same before and after printing. Myoblast cells were more elongated depicting its normal anisotropic orientation *in vivo* while the fibroblast cells align along the longitudinal axis of the hydrogel array suggesting that the patterning of the hydrogel provide contact guidance cues for cell orientation. This organized cell orientation was however more unobtrusive in the multilayered construct (Figure 5-4 & 5-5). The 3-layered construct showed a change in cell morphology of the two cell stripes printed on the cell monolayer though the basal cells maintained its cell organization. Cell

reorganization in a multilayered system is commonly observed with multicellular systems indicating that the geometry of the base surface can be used to dictate cellular behavior [146].

While assembly of tissue modules *via* micro-contact printing technique is attainable with a shape-changing surface, there were some challenges encountered during the printing process. In figure 5-4D, the staining color for both cell layers is uniform; this was due to the infiltration of dye solution from the top to the bottom cell monolayer. To address this, concentration of the staining solution was significantly lowered and mild improvement was observed. Then a solution of collagen was introduced between the layers to prohibit the infiltration. This change only significantly distorted the organization of the top cells. Finally, pre-staining the cells prior to culturing significantly improved the individual visualization of the cell layers. Most importantly, tissues printed from this shape-changing platform with micro-contact printing technique retained their biological activity as demonstrated in section 4.4.

The feasibility of printing tissues with different geometry was revealed. Cells printed from closely spaced arrays of 10 μm (Figure 5-6) maintained their cell organization while surprisingly cells detached from a 75 μm wide microbeam (Figure 5-7) showed a well-defined buckled tissue structure. These results suggest that different patterning geometries of the shape-changing hydrogel could direct tissue structures into diverse multipurpose configurations.

In order to control cell organization in the 3D multilayered tissue construct, future studies will include investigating the underlying mechanisms of cell reorientation by examining the effect of cell reorientation duration, influence of cell types, morphology and increased cell density. Confocal imaging will be adapted for evaluating the cross section of the multilayered tissue construct. Also, different geometries of the shape-changing hydrogel will be fabricated to induce printing of tissues with diverse geometries for tissue engineering applications.

5.5. Conclusions

A micro-contact printing technique was for the first time employed in assembly of tissues in an additive manner to create multicomponent spatially controlled three-dimensional functional tissues. A novel concept for fabricating multilayered tissues with the flexibility of forming diverse tissue structures was introduced. The combination of shape-changing hydrogel and micro-contact printing techniques allowed for a well-organized and rapid printing of tissue modules that can aid formation of native tissues with complex microarchitecture for regenerative medicine.

CHAPTER 6: CONCLUSIONS AND FUTURE WORK

6.1. Conclusions

The key findings in this dissertation are summarized as follows:

- Release of tissue modules from shape-changing hydrogel occurs with a small thermal reduction by 10 °C below the physiological temperature.
- Complete detachment of tissue modules occurred as continuous tissue stripes in less than 3 minutes.
- Cells without cell-to-cell contacts did not detach from the hydrogel suggesting that the cohesive strength between the cell contacts plays a significant role during detachment.
- A lateral strain of at least 25% is necessary to detach cells that have cell-to-cell contacts from the hydrogel array. The mechanism of cell release was primarily a mechanically driven process compared to the metabolic driven process reported with the grafted pNIPAAm nanoscale films. The difference is attributed to the micron scale features of the shape-changing hydrogel array that allows for more hydration of the long chained three-dimensional arrays of the pNIPAAm molecules.
- For the first time, micro-contact printing technique was used to print cells directly onto target surfaces without the need of any intermediates.
- Cell survival after cell printing depended on the type of target surface, release time, temperature and the amounts of conformal pressure applied.

- Printed cells oriented along the longitudinal axis of the hydrogel arrays suggesting that the shape-changing hydrogel provides contact guidance cues for cell alignment.
- Printing conditions of myoblast and fibroblast cells were the same. The cells printed under 5 minutes at 4 °C.
- The combination of the shape-changing hydrogel and micro-contact printing technique allowed for modular assemblies of tissue modules into 2-layered and 3-layered structures.

The research outcomes discussed in this dissertation provide a novel approach to modular assemblies of tissue structures for the advancement of engineering diseased or damaged tissues and organs.

6.2. Future Directions

The objective of this proposed future work is to increase the experimental knowledge of the design and development of functional complex tissues. Thus, this study is designed to provide understanding to the fundamental principles governing assembly of organized 3D cardiac tissues that closely represents the native myocardium. The successful realization of this proposed study should provide a viable construct suitable for improving cardiac function by overcoming these key obstacles; vascular integration, diffusion, blood perfusion and new capillary formation *in vivo* thus revolutionize regenerative therapies.

6.2.1. Establish an Automated Micro-contact Printing Mechanism

The mechanics of micro-contact printing biochemical inks to pattern surfaces is well established [63, 147, 148]. However, printing tissues without disrupting the cellular membrane or organization is a challenge. Dissertation research studies demonstrate the procedure suitable for printing cells; though the global organization and cell-to-cell junctions are sometimes not fully retained when transferred to the target surface depending on the physical stability of the operator.

The ability to control multi-cellular local and global organization is significant for producing 3D tissue constructs; thus it is imperative to further investigate a robust method for reliable printing of functional cardiac tissues independent of the operator.

Create an automated device: Automation of the micro-contact printing of cells cultured on shape-changing stamps will enhance productivity and reduce errors caused by shearing of the cells during placing or removing stamp from the target surface. An enclosed motorized stage with heating and cooling chamber should be built for the contact printing of cells. LabView software can be used to record the printing parameters.

Assess the main effects of contact printing parameters: A micro-contact printing mechanism is governed by having conformal contact between a stamp and its target whereby cells efficiently transfer to the target with preserved cell viability and organization. The printing parameters include the contact time, release temperature, applied pressure, and the surface chemistry of the target. These parameters all play a significant role in maintaining the intact cell stripe during and after transfer. The main effects of these factors should be evaluated by conducting a 2-level factorial design of experiments (DOE). The measurable outcome will be the percentage of remaining attached cells on the stamp after transfer. An optimum printed tissue will be a fully viable tissue module with the shortest amount of contact time independent of the aspect ratio or geometry of the patterned hydrogel.

Evaluate cell morphology, organization and viability of μ-tissue transferred: To confirm the formation of intercalated discs, i.e. the adhering structure responsible for synchronized contraction of the myocardium, immunostain the cardiac tissues for desmosomes, cadherins and connexins, the cell-to-cell junctions. Transmission electron microscopy (TEM) should be used to examine the intercellular junctions that indicate tissue formation. Video via optical microscopy

should be used to monitor changes in cell morphology while the NIH Image J software should be used to analyze cell alignment and orientation. Cytotoxicity assay containing Calcein AM and ethidium homodimer should be used to evaluate cell viability.

6.2.2. Optimize the Design Parameters of the Stamp

Cells are known to respond to their microenvironment therefore the patterning of the shape-changing hydrogel must be well characterized in order to fabricate functional 3D cardiac tissues. The width and spacing of laminin patterns were found to affect the alignment and orientation of contractile myofibrils, and the formation of cell-to-cell junctions [62, 78]. Adherent cardiomyocytes (CMs) on narrowly spaced patterns of 10μm and widths < 20μm were found to maintain cell alignment and also yield synchronized contractions on laminin coated surfaces. Dissertation research studies show that closely spaced arrays (10 μm) of the shape-changing arrays yield aligned tissue modules along the longitudinal axis of the target surface (Figure 5-6). To determine myofibril alignment and synchronous beatings of CMs, the optimal adhesive domain geometry for cellular organization should be evaluated. In addition, cell morphology, organization and formation of myofibrils are influenced by the rigidity of the substrate; the stiffness of the substrate can drive the tension forces between cells [149-151]. Thus, the need to evaluate the optimal hydrogel properties by varying the densities of crosslink is important. Lower crosslink density gels are softer and do have more degrees of freedom to swell leading to more rapid cell sheet recovery. However, a high crosslink density gel may induce the stiffness required for the normal mechanical workload of the myocardium. Since organization of CM is geometric and substrate stiffness dependent the effects of PNIPAAm array spacing and crosslink density should be studied.

Assess the effect of array spacing and modulus on the organization, rate of release and pulsation of cardiomyocytes: Photolithography should be used to fabricate master molds with new sets of array spacing. The aspect ratio of the arrays should remain constant while the spacing and crosslink densities should vary from 5-20μm and 1-4% respectively. Atomic force microscopy should be used to evaluate the mechanical force of the arrays. Primary cardiac myocytes should be cultured on these arrays and their local and global organization should be examined over a prolonged culture using fluorescence microscopy and the NIH image J software for analysis. The ease of rapid tissue transfer should be assessed by studying the release kinetics induced by a 10°C shift below the culture temperature. The release kinetics should be monitored on a video via confocal microscopy. Electrocardiogram (ECG) should be used to evaluate the synchronous beating of the engineered CMs. Knowledge gained in this study will establish the optimal PNIPAAm patterns required to direct myocytes organization and regulate their contractions.

Evaluate the cell morphology and expression of myofibrils: To assess cytoskeletal organization and expression, immunofluorescence staining with actin phalloidin, cell nuclei stain-Hoechst 33342, and antibodies to myosin should be conducted. To confirm the formation of intercalated discs, the optimal cardiac tissue should be immunostained for desmosomes, cadherins and connexins, the cell-to-cell junctions responsible for synchronized contraction of the myocardium. TEM should be used to characterize the myofibril structure and the cell junction morphologies.

6.2.3. Construct Functional Three-dimensional Tissues

Since there are no successful clinical trials for regenerating an infarcted heart due to the complexity of the organ tissue and vascularization issues then the need to develop a viable tissue

construct is of great need. Prevascularization of thick grafts has been shown to promote *in vivo* perfusion, neovascularization and angiogenesis in myocardial ischemia and infarction of rats [89, 91, 100, 137]. Using the cell-sheet engineering technology, diffusion of nutrients is limited to a graft thickness of 80 μm. Multiple surgeries were used to overcome this drawback [137]. However, the act of repeated surgeries (~10 times) within 48 hours is not feasible for humans. As a result, an alternative strategy to enhance diffusion is necessary. Human umbilical vein endothelial cells (HUVEC) can differentiate into beating CMs when co-cultured with neonatal rat cardiomyocytes with high efficiency (11 ± 0.5%) [90]. Thus, the feasibility of stacking HUVEC between cardiomyocytes to promote neovascularization should be investigated (Figure 6-1).

Fabricate myocardium-like tissues: Assembly of 3D cardiac tissues should be accomplished by sequential printing of HUVEC between layers of CMs via the contact printing procedure. The CMs should be cultured on the optimal narrowly spaced arrays while the HUVEC should be on widely spaced arrays to support vascular lumen formation. To promote diffusion, we will study different stacking orientations (parallel and perpendicular) and ratios (CM :HUVEC :CM = 3:1:3, 3:2:3, 3:3:3, 4:2:4). Confocal microscopy should be used to analyze the corresponding thickness and examine the formation of cell-to-cell junctions between layers of adjacent cells. CellTracker dyes should be used to differentiate between layers. The engineered 3D construct should be maintained in static cultures for up to 2 weeks with daily monitoring and examination of physical properties.

Evaluate the therapeutic potential: Immunohistology assays should be used to examine the expressed cardiac markers, cell viability, organization, morphology and vasculogenesis of the tissue construct. To stimulate cardiac neovascularization perfusion culture with growth factors

supplements should be conducted. This culture should be monitored in a custom-built flow chamber with the suspended tissue aligned parallel to the flow. Pulsation is crucial for cardiac function, as the heart beats ~100,000 times daily [152]. Native myocardium undergo repetitive forces during contraction, hence the tissue construct should be able to withstand compressive forces up to 3 mN/mm^2 [153]. Atomic force microscopy should be used to analyze the engineered tissue compressive forces. And an electrocardiogram should be employed to assess the synchronous contraction of the engineered cardiac muscle.

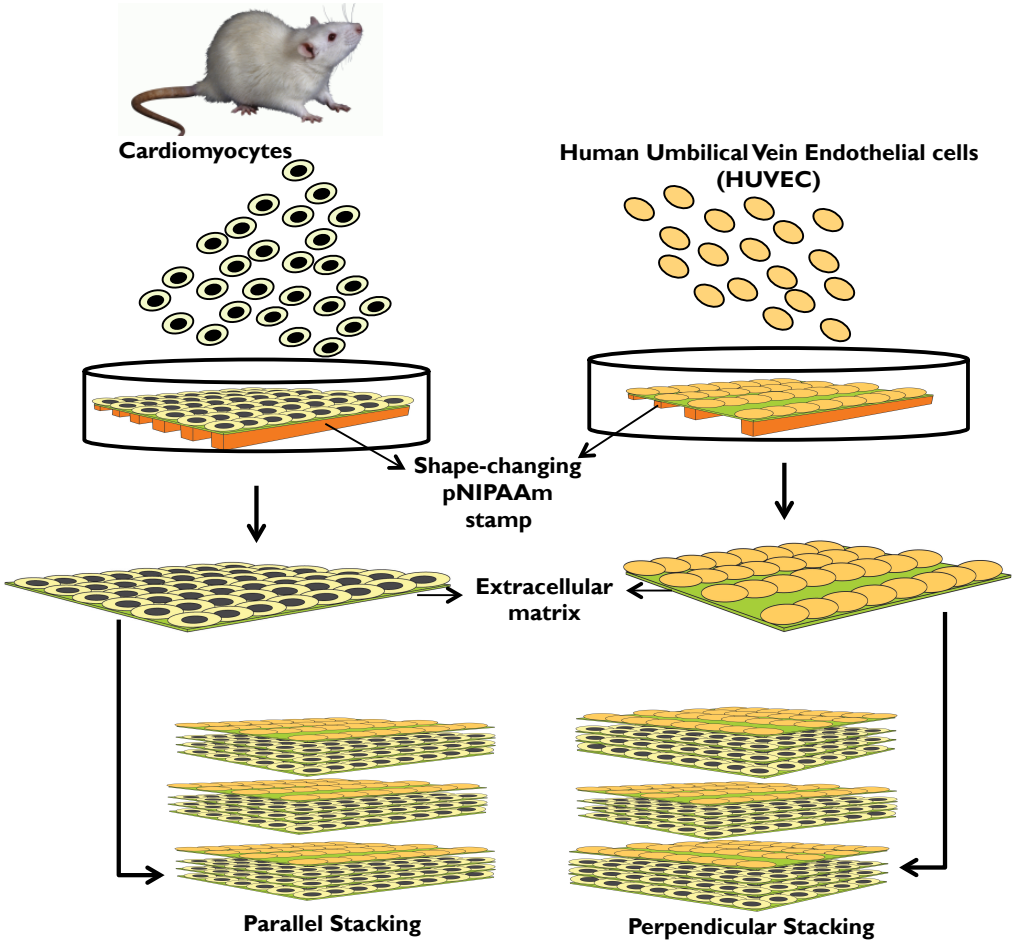

Figure 6-1: Schematic diagram of proposed future work. Neonatal rat cardiomyocytes are cultured on shape-changing poly-(*N*-isopropylacrylamide) constructs concurrently with endothelial cells for formation of intact aligned micro-tissues. Layers of tissues are then stacked into parallel or perpendicular orientations to promote diffusion of nutrients.

REFERENCES

[1] Go AS, Mozaffarian D, Roger VL, Benjamin EJ, Berry JD, Blaha MJ, et al. Heart disease and stroke statistics--2014 update: a report from the American Heart Association. Circulation 2014;129:28-292.

[2] Ju X, Pi S, Xie R, Guo X, Liu J, Yu Y, et al. Comprehensive Alcohol-/Ion-Responsive Properties of Poly(N-Isopropylacrylamide-co-Benzo-18-Crown-6-Acrylamide) Copolymers. Chinese Journal of Chemical Engineering 2014;22:1038-45.

[3] Wang YM, Ju XJ, Liu Z, Xie R, Wang W, Wu JF, et al. Competitive molecular-/ion-recognition responsive characteristics of poly(N-isopropylacrylamide-co-benzo-12-crown-4-acrylamide) copolymers with benzo-12-crown-4 as both guest and host units. Macromol Rapid Commun 2014;35:1280-6.

[4] Schmaljohann D. Thermo- and pH-responsive polymers in drug delivery. Advanced drug delivery reviews 2006;58:1655-70.

[5] Namkung S, Chu CC. Partially biodegradable temperature- and pH-responsive poly(N-isopropylacrylamide)/dextran-maleic acid hydrogels: formulation and controlled drug delivery of doxorubicin. Journal of biomaterials science Polymer edition 2007;18:901-24.

[6] Filipcsei G, Csetneki I, Szilágyi A, Zrínyi M. Magnetic Field-Responsive Smart Polymer Composites. Oligomers - Polymer Composites - Molecular Imprinting: Springer Berlin Heidelberg; 2007. p. 137-89.

[7] Frimpong RA, Hilt JZ. Poly(n-isopropylacrylamide)-based hydrogel coatings on magnetite nanoparticles via atom transfer radical polymerization. Nanotechnology 2008;19:175101.

[8] Kumar A, Srivastava A, Galaev IY, Mattiasson B. Smart polymers: Physical forms and bioengineering applications. Progress in Polymer Science 2007;32:1205-37.

[9] Fukumori K, Akiyama Y, Kumashiro Y, Kobayashi J, Yamato M, Sakai K, et al. Characterization of Ultra-Thin Temperature-Responsive Polymer Layer and Its Polymer Thickness Dependency on Cell Attachment/Detachment Properties. Macromolecular Bioscience 2010;10:1117-29.

[10] Akiyama Y, Kikuchi A, Yamato M, Okano T. Ultrathin Poly(N-isopropylacrylamide) Grafted Layer on Polystyrene Surfaces for Cell Adhesion/Detachment Control. Langmuir : the ACS journal of surfaces and colloids 2004;20:5506-11.

[11] Canavan HE, Cheng X, Graham DJ, Ratner BD, Castner DG. Surface characterization of the extracellular matrix remaining after cell detachment from a thermoresponsive polymer. Langmuir : the ACS journal of surfaces and colloids 2005;21:1949-55.

[12] Canavan HE CX, Graham DJ, Ratner BD, Castner DG. . A plasma-deposited surface for cell sheet engineering: Advantages over mechanical dissociation of cells. Plasma Process Polymer 2006;3:516-23.

[13] Mizutani A, Kikuchi A, Yamato M, Kanazawa H, Okano T. Preparation of thermoresponsive polymer brush surfaces and their interaction with cells. Biomaterials 2008;29:2073-81.

[14] Halperin A. Polymer Brushes that Resist Adsorption of Model Proteins: Design Parameters. Langmuir : the ACS journal of surfaces and colloids 1999;15:2525-33.

[15] Xue C, Yonet-Tanyeri N, Brouette N, Sferrazza M, Braun PV, Leckband DE. Protein Adsorption on Poly(N-isopropylacrylamide) Brushes: Dependence on Grafting Density and Chain Collapse. Langmuir : the ACS journal of surfaces and colloids 2011;27:8810-8.

[16] Li L, Zhu Y, Li B, Gao C. Fabrication of Thermoresponsive Polymer Gradients for Study of Cell Adhesion and Detachment. Langmuir : the ACS journal of surfaces and colloids 2008;24:13632-9.

[17] Moran MT, Carroll WM, Gorelov A, Rochev Y. Intact endothelial cell sheet harvesting from thermoresponsive surfaces coated with cell adhesion promoters. Journal of the Royal Society, Interface / the Royal Society 2007;4:1151-7.

[18] Nash ME, Healy D, Carroll WM, Elvira C, Rochev YA. Cell and cell sheet recovery from pNIPAm coatings; motivation and history to present day approaches. Journal of Materials Chemistry 2012;22:19376-89.

[19] DuPont Jr SJ, Cates RS, Stroot PG, Toomey R. Swelling-induced instabilities in microscale, surface-confined poly(N-isopropylacryamide) hydrogels. Soft Matter 2010;6:3876-82.

[20] Matsuda T. Poly(N-isopropylacrylamide)-grafted gelatin as a thermoresponsive cell-adhesive, mold-releasable material for shape-engineered tissues. Journal of Biomaterials Science, Polymer Edition 2004;15:947-55.

[21] Duarte AR, Mano JF, Reis RL. Thermosensitive polymeric matrices for three-dimensional cell culture strategies. Acta Biomater 2011;7:526-9.

[22] Moran MT, Carroll WM, Selezneva I, Gorelov A, Rochev Y. Cell growth and detachment from protein-coated PNIPAAm-based copolymers. Journal of biomedical materials research Part A 2007;81:870-6.

[23] Akintewe OO, DuPont SJ, Elineni KK, Cross MC, Toomey RG, Gallant ND. Shape-changing hydrogel surfaces trigger rapid release of patterned tissue modules. Acta Biomater 2015;11:96-103.

[24] Buck CA, Horwitz AF. Cell surface receptors for extracellular matrix molecules. Annual review of cell biology 1987;3:179-205.

[25] Garcia AJ, Vega MD, Boettiger D. Modulation of cell proliferation and differentiation through substrate-dependent changes in fibronectin conformation. Molecular biology of the cell 1999;10:785-98.

[26] Gumbiner BM. Regulation of cadherin-mediated adhesion in morphogenesis. Nature reviews Molecular cell biology 2005;6:622-34.

[27] Borghi N, Lowndes M, Maruthamuthu V, Gardel ML, Nelson WJ. Regulation of cell motile behavior by crosstalk between cadherin- and integrin-mediated adhesions. Proceedings of the National Academy of Sciences of the United States of America 2010;107:13324-9.

[28] Masayuki Yamato MO, Fumiko Karikusa, Akihiko Kikuchi, Yasuhisa Sakurai, Teruo Okano. Signal transduction and cytoskeletal reorganization are required for cell detachment from cell culture surfaces grafted with a temperature-responsive polymer. J Biomed Mater Res 1999;44:8.

[29] Juliano RL. Signal transduction by cell adhesion receptors and the cytoskeleton: functions of integrins, cadherins, selectins, and immunoglobulin-superfamily members. Annual review of pharmacology and toxicology 2002;42:283-323.

[30] Klebe RJ. Isolation of a collagen-dependent cell attachment factor. Nature 1974;250:248-51.

[31] Grinnell F, Feld MK. Adsorption characteristics of plasma fibronectin in relationship to biological activity. Journal of Biomedical Materials Research 1981;15:363-81.

[32] Quinton PM, Philpott CW. A role for anionic sites in epithelial architecture. Effects of cationic polymers on cell membrane structure. The Journal of cell biology 1973;56:787-96.

[33] Thomas CH, McFarland CD, Jenkins ML, Rezania A, Steele JG, Healy KE. The role of vitronectin in the attachment and spatial distribution of bone-derived cells on materials with patterned surface chemistry. J Biomed Mater Res 1997;37:81-93.

[34] Tegoulia VA, Cooper SL. Leukocyte adhesion on model surfaces under flow: Effects of surface chemistry, protein adsorption, and shear rate. Journal of Biomedical Materials Research 2000;50:291-301.

[35] Lewandowska K, Pergament E, Sukenik CN, Culp LA. Cell-Type-Specific adhesion mechanisms mediated by fibronectin adsorbed to chemically derivatized substrata. Journal of Biomedical Materials Research 1992;26:1343-63.

[36] Singhvi R, Kumar A, Lopez GP, Stephanopoulos GN, Wang DI, Whitesides GM, et al. Engineering cell shape and function. Science 1994;264:696-8.

[37] Lewandowska K, Balachander N, Sukenik CN, Culp LA. Modulation of fibronectin adhesive functions for fibroblasts and neural cells by chemically derivatized substrata. Journal of cellular physiology 1989;141:334-45.

[38] Shelton RM, Rasmussen AC, Davies JE. Protein adsorption at the interface between charged polymer substrata and migrating osteoblasts. Biomaterials 1988;9:24-9.

[39] Keselowsky BG, Collard DM, Garcia AJ. Surface chemistry modulates fibronectin conformation and directs integrin binding and specificity to control cell adhesion. Journal of biomedical materials research Part A 2003;66:247-59.

[40] Mineur P, Guignandon A, Lambert CA, Amblard M, Lapière CM, Nusgens BV. RGDS and DGEA-induced [Ca2+]i signalling in human dermal fibroblasts. Biochimica et Biophysica Acta (BBA) - Molecular Cell Research 2005;1746:28-37.

[41] van der Flier A, Sonnenberg A. Function and interactions of integrins. Cell Tissue Res 2001;305:285-98.

[42] Gullberg D, Velling T, Lohikangas L, Tiger CF. Integrins during muscle development and in muscular dystrophies. Front Biosci 1998;3:D1039-50.

[43] Souders CA, Bowers SL, Baudino TA. Cardiac fibroblast: the renaissance cell. Circulation research 2009;105:1164-76.

[44] Tzu J, Marinkovich MP. Bridging structure with function: structural, regulatory, and developmental role of laminins. The international journal of biochemistry & cell biology 2008;40:199-214.

[45] Letourneau PC, Condic ML, Snow DM. Extracellular matrix and neurite outgrowth. Current opinion in genetics & development 1992;2:625-34.

[46] Altankov G, Groth T, Krasteva N, Albrecht W, Paul D. Morphological evidence for a different fibronectin receptor organization and function during fibroblast adhesion on hydrophilic and hydrophobic glass substrata. Journal of biomaterials science Polymer edition 1997;8:721-40.

[47] Adams JC. Cell-matrix contact structures. Cellular and molecular life sciences : CMLS 2001;58:371-92.

[48] Hidalgo-Bastida LA, Cartmell SH. Mesenchymal stem cells, osteoblasts and extracellular matrix proteins: enhancing cell adhesion and differentiation for bone tissue engineering. Tissue engineering Part B, Reviews 2010;16:405-12.

[49] Skardal A, Mack D, Kapetanovic E, Atala A, Jackson JD, Yoo J, et al. Bioprinted amniotic fluid-derived stem cells accelerate healing of large skin wounds. Stem Cells Transl Med 2012;1:792-802.

[50] Cui X, Breitenkamp K, Finn MG, Lotz M, D'Lima DD. Direct human cartilage repair using three-dimensional bioprinting technology. Tissue engineering Part A 2012;18:1304-12.

[51] Xu T, Binder KW, Albanna MZ, Dice D, Zhao W, Yoo JJ, et al. Hybrid printing of mechanically and biologically improved constructs for cartilage tissue engineering applications. Biofabrication 2013;5:015001.

[52] De Coppi P, Bartsch G, Jr., Siddiqui MM, Xu T, Santos CC, Perin L, et al. Isolation of amniotic stem cell lines with potential for therapy. Nat Biotechnol 2007;25:100-6.

[53] Xu T, Jin J, Gregory C, Hickman JJ, Boland T. Inkjet printing of viable mammalian cells. Biomaterials 2005;26:93-9.

[54] Murphy SV, Atala A. 3D bioprinting of tissues and organs. Nat Biotech 2014;32:773-85.

[55] Cui X, Boland T, D'Lima DD, Lotz MK. Thermal Inkjet Printing in Tissue Engineering and Regenerative Medicine. Recent patents on drug delivery & formulation 2012;6:149-55.

[56] Jakab K, Norotte C, Damon B, Marga F, Neagu A, Besch-Williford CL, et al. Tissue engineering by self-assembly of cells printed into topologically defined structures. Tissue engineering Part A 2008;14:413-21.

[57] Jakab K, Norotte C, Marga F, Murphy K, Vunjak-Novakovic G, Forgacs G. Tissue engineering by self-assembly and bio-printing of living cells. Biofabrication 2010;2:022001.

[58] Duan B, Hockaday LA, Kang KH, Butcher JT. 3D bioprinting of heterogeneous aortic valve conduits with alginate/gelatin hydrogels. Journal of biomedical materials research Part A 2013;101:1255-64.

[59] Norotte C, Marga FS, Niklason LE, Forgacs G. Scaffold-free vascular tissue engineering using bioprinting. Biomaterials 2009;30:5910-7.

[60] Smith CM, Stone AL, Parkhill RL, Stewart RL, Simpkins MW, Kachurin AM, et al. Three-dimensional bioassembly tool for generating viable tissue-engineered constructs. Tissue engineering 2004;10:1566-76.

[61] Chang R, Nam J, Sun W. Effects of dispensing pressure and nozzle diameter on cell survival from solid freeform fabrication-based direct cell writing. Tissue engineering Part A 2008;14:41-8.

[62] Todd C. McDevitt JCA, Marsha L. Whitney, Hans Reinecke, Stephen D. Hauschka,, Charles E. Murry PSS. In vitro generation of differentiated cardiac myofibers on micropatterned laminin surfaces. J Biomed Mater Res 2001;60:8.

[63] Gallant ND, Charest JL, King WP, Garcia AJ. Micro- and nano-patterned substrates to manipulate cell adhesion. Journal of nanoscience and nanotechnology 2007;7:803-7.

[64] Shen K, Qi J, Kam LC. Microcontact Printing of Proteins for Cell Biology. Journal of Visualized Experiments : JoVE 2008:1065.

[65] Kaufmann T, Ravoo BJ. Stamps, inks and substrates: polymers in microcontact printing. Polymer Chemistry 2010;1:371-87.

[66] Fujioka N, Morimoto Y, Takeuchi K, Yoshioka M, Kikuchi M. Difference in infrared spectra from cultured cells dependent on cell-harvesting method. Appl Spectrosc 2003;57:241-3.

[67] Huang HL, Hsing HW, Lai TC, Chen YW, Lee TR, Chan HT, et al. Trypsin-induced proteome alteration during cell subculture in mammalian cells. J Biomed Sci 2010;17:36.

[68] Okano T, Yamada N, Okuhara M, Sakai H, Sakurai Y. Mechanism of cell detachment from temperature-modulated, hydrophilic-hydrophobic polymer surfaces. Biomaterials 1995;16:297-303.

[69] Okano T, Yamada N, Sakai H, Sakurai Y. A novel recovery system for cultured cells using plasma-treated polystyrene dishes grafted with poly(N-isopropylacrylamide). J Biomed Mater Res 1993;27:1243-51.

[70] Lee EL, von Recum HA. Cell culture platform with mechanical conditioning and nondamaging cellular detachment. Journal of Biomedical Materials Research Part A 2010;93:411-8.

[71] Canavan HE, Cheng X, Graham DJ, Ratner BD, Castner DG. Cell sheet detachment affects the extracellular matrix: a surface science study comparing thermal liftoff, enzymatic, and mechanical methods. Journal of biomedical materials research Part A 2005;75:1-13.

[72] Kubo H, Shimizu T, Yamato M, Fujimoto T, Okano T. Creation of myocardial tubes using cardiomyocyte sheets and an in vitro cell sheet-wrapping device. Biomaterials 2007;28:3508-16.

[73] Yang GP, Soetikno RM. Treatment of oesophageal ulcerations using endoscopic transplantation of tissue-engineered autologous oral mucosal epithelial cell sheets in a canine model. Gut 2007;56:313-4.

[74] Hasegawa M, Yamato M, Kikuchi A, Okano T, Ishikawa I. Human periodontal ligament cell sheets can regenerate periodontal ligament tissue in an athymic rat model. Tissue engineering 2005;11:469-78.

[75] Hayashida Y, Nishida K, Yamato M, Yang J, Sugiyama H, Watanabe K, et al. Transplantation of tissue-engineered epithelial cell sheets after excimer laser photoablation reduces postoperative corneal haze. Investigative ophthalmology & visual science 2006;47:552-7.

[76] Sekine H, Shimizu T, Yang J, Kobayashi E, Okano T. Pulsatile myocardial tubes fabricated with cell sheet engineering. Circulation 2006;114:I87-93.

[77] Alom Ruiz S, Chen CS. Microcontact printing: A tool to pattern. Soft Matter 2007;3:168-77.

[78] Todd C. McDevitt KAW, 2 Stephen D. Hauschka,3 Charles E. Murry,4, Stayton1 PS. Spatially organized layers of cardiomyocytes on biodegradable polyurethane films for myocardial repair. J Biomed Mater Res 2003;66:10.

[79] McDevitt TC, Angello JC, Whitney ML, Reinecke H, Hauschka SD, Murry CE, et al. In vitro generation of differentiated cardiac myofibers on micropatterned laminin surfaces. Journal of Biomedical Materials Research 2002;60:472-9.

[80] Muraoka M, Shimizu T, Itoga K, Takahashi H, Okano T. Control of the formation of vascular networks in 3D tissue engineered constructs. Biomaterials 2013;34:696-703.

[81] Nagamori E, Ngo TX, Takezawa Y, Saito A, Sawa Y, Shimizu T, et al. Network formation through active migration of human vascular endothelial cells in a multilayered skeletal myoblast sheet. Biomaterials 2013;34:662-8.

[82] Takahashi H, Nakayama M, Itoga K, Yamato M, Okano T. Micropatterned thermoresponsive polymer brush surfaces for fabricating cell sheets with well-controlled orientational structures. Biomacromolecules 2011;12:1414-8.

[83] Haraguchi Y, Shimizu T, Sasagawa T, Sekine H, Sakaguchi K, Kikuchi T, et al. Fabrication of functional three-dimensional tissues by stacking cell sheets in vitro. Nature protocols 2012;7:850-8.

[84] Kikuchi T, Shimizu T, Wada M, Yamato M, Okano T. Automatic fabrication of 3-dimensional tissues using cell sheet manipulator technique. Biomaterials 2014;35:2428-35.

[85] Haraguchi Y, Shimizu T, Yamato M, Okano T. Regenerative therapies using cell sheet-based tissue engineering for cardiac disease. Cardiology research and practice 2011;2011:1-8.

[86] Elloumi-Hannachi I, Yamato M, Okano T. Cell sheet engineering: a unique nanotechnology for scaffold-free tissue reconstruction with clinical applications in regenerative medicine. Journal of internal medicine 2010;267:54-70.

[87] Matsuda N, Shimizu T, Yamato M, Okano T. Tissue Engineering Based on Cell Sheet Technology. Advanced Materials 2007;19:3089-99.

[88] Kim DW, Jun I, Lee TJ, Lee JH, Lee YJ, Jang HK, et al. Therapeutic angiogenesis by a myoblast layer harvested by tissue transfer printing from cell-adhesive, thermosensitive hydrogels. Biomaterials 2013;34:8258-68.

[89] Sasagawa T, Shimizu T, Sekiya S, Haraguchi Y, Yamato M, Sawa Y, et al. Design of prevascularized three-dimensional cell-dense tissues using a cell sheet stacking manipulation technology. Biomaterials 2010;31:1646-54.

[90] Condorelli G, Borello U, De Angelis L, Latronico M, Sirabella D, Coletta M, et al. Cardiomyocytes induce endothelial cells to trans-differentiate into cardiac muscle: implications for myocardium regeneration. Proceedings of the National Academy of Sciences of the United States of America 2001;98:10733-8.

[91] Sekine H, Shimizu T, Hobo K, Sekiya S, Yang J, Yamato M, et al. Endothelial cell coculture within tissue-engineered cardiomyocyte sheets enhances neovascularization and improves cardiac function of ischemic hearts. Circulation 2008;118:S145-52.

[92] Roger VL, Go AS, Lloyd-Jones DM, Benjamin EJ, Berry JD, Borden WB, et al. Heart disease and stroke statistics--2012 update: a report from the American Heart Association. Circulation 2012;125:1-223.

[93] Bergmann O, Bhardwaj RD, Bernard S, Zdunek S, Barnabe-Heider F, Walsh S, et al. Evidence for cardiomyocyte renewal in humans. Science 2009;324:98-102.

[94] Andreas Soejitno DMW, R.A. Tuty Kuswardhani. Clinical Applications of Stem Cell Therapy for Regenerating The Heart. Acta Med Indones-Indones J Intern Med 2010;42:243-57.

[95] St John Sutton M, Lee D, Rouleau JL, Goldman S, Plappert T, Braunwald E, et al. Left ventricular remodeling and ventricular arrhythmias after myocardial infarction. Circulation 2003;107:2577-82.

[96] Matthew W. Curtis MBR. Cardiac Tissue Engineering. Journal of Cardiovascular Nursing 2009;24:6.

[97] Milica Radisic JM, Eric Epping, Wenliang Geng, Robert Langer and Gordana Vunjak-Novakovic. Oxygen gradients correlate with decrease in cell density and viability in engineered cardiac tissue. Biotechnology and bioengineering 2006;93:332-43.

[98] Teng CJ, Luo J, Chiu RC, Shum-Tim D. Massive mechanical loss of microspheres with direct intramyocardial injection in the beating heart: implications for cellular cardiomyoplasty. The Journal of thoracic and cardiovascular surgery 2006;132:628-32.

[99] Qingen Ke YY, Jamal S. RANA, CHEN Yu, James P. MORGAN, XIAO Yong-Fu. Embryonic stem cells cultured in biodegradable scaffold repair infarcted myocardium in mice. Acta Physiologica Sinica 2005;57:673-81.

[100] Ishii O, Shin M, Sueda T, Vacanti JP. In vitro tissue engineering of a cardiac graft using a degradable scaffold with an extracellular matrix-like topography. The Journal of thoracic and cardiovascular surgery 2005;130:1358-63.

[101] Elbert DL. Bottom-up tissue engineering. Current Opinion in Biotechnology 2011;22:674-80.

[102] McGuigan AP, Sefton MV. Design and fabrication of sub-mm-sized modules containing encapsulated cells for modular tissue engineering. Tissue engineering 2007;13:1069-78.

[103] Nichol JW, Khademhosseini A. Modular Tissue Engineering: Engineering Biological Tissues from the Bottom Up. Soft Matter 2009;5:1312-9.

[104] Furth ME, Atala A, Van Dyke ME. Smart biomaterials design for tissue engineering and regenerative medicine. Biomaterials 2007;28:5068-73.

[105] da Silva RMP, Mano JF, Reis RL. Smart thermoresponsive coatings and surfaces for tissue engineering: switching cell-material boundaries. Trends in biotechnology 2007;25:577-83.

[106] Roy I, Gupta MN. Smart Polymeric Materials: Emerging Biochemical Applications. Chemistry & Biology 2003;10:1161-71.

[107] Klouda L, Mikos AG. Thermoresponsive hydrogels in biomedical applications. European Journal of Pharmaceutics and Biopharmaceutics 2008;68:34-45.

[108] Shibayama M, Tanaka T. Volume phase transition and related phenomena of polymer gels. In: Dušek K, editor. Responsive Gels: Volume Transitions I: Springer Berlin Heidelberg; 1993. p. 1-62.

[109] Kolettis TM, Vilaeti,A. Dimos, K. ,Tsitou, N., and Agathopoulos, S. Tissue Engineering for Post-Myocardial Infarction Ventricular Remodeling. Mini-Reviews in Medicinal Chemistry 2011;11:8.

[110] Dupont SJ. Shape-shifting Surfaces For Rapid Release and Direct Stamping of Organized Micro-tissues. Disserstation, University of South Florida, Tampa, Florida 2012:217.

[111] Palmieri F, Klingenberg M. Inhibition of respiration under the control of azide uptake by mitochondria. European journal of biochemistry / FEBS 1967;1:439-46.

[112] Ishizaki T, Uehata M, Tamechika I, Keel J, Nonomura K, Maekawa M, et al. Pharmacological properties of Y-27632, a specific inhibitor of rho-associated kinases. Molecular pharmacology 2000;57:976-83.

[113] Dumbauld DW, Shin H, Gallant ND, Michael KE, Radhakrishna H, Garcia AJ. Contractility modulates cell adhesion strengthening through focal adhesion kinase and assembly of vinculin-containing focal adhesions. Journal of cellular physiology 2010;223:746-56.

[114] Gallant ND, Michael KE, Garcia AJ. Cell adhesion strengthening: contributions of adhesive area, integrin binding, and focal adhesion assembly. Molecular biology of the cell 2005;16:4329-40.

[115] Wang JC, Thampatty BP. An Introductory Review of Cell Mechanobiology. Biomech Model Mechanobiol 2006;5:1-16.

[116] Ohashi K, Yokoyama T, Yamato M, Kuge H, Kanehiro H, Tsutsumi M, et al. Engineering functional two- and three-dimensional liver systems in vivo using hepatic tissue sheets. Nature medicine 2007;13:880-5.

[117] Yang J, Yamato M, Shimizu T, Sekine H, Ohashi K, Kanzaki M, et al. Reconstruction of functional tissues with cell sheet engineering. Biomaterials 2007;28:5033-43.

[118] Kwon OH, Kikuchi A, Yamato M, Sakurai Y, Okano T. Rapid cell sheet detachment from poly(N-isopropylacrylamide)-grafted porous cell culture membranes. J Biomed Mater Res 2000;50:82-9.

[119] Masuda S, Shimizu T, Yamato M, Okano T. Cell sheet engineering for heart tissue repair. Advanced drug delivery reviews 2008;60:277-85.

[120] Shimizu T, Yamato M, Kikuchi A, Okano T. Two-dimensional manipulation of cardiac myocyte sheets utilizing temperature-responsive culture dishes augments the pulsatile amplitude. Tissue engineering 2001;7:141-51.

[121] Shimizu T, Yamato M, Kikuchi A, Okano T. Cell sheet engineering for myocardial tissue reconstruction. Biomaterials 2003;24:2309-16.

[122] Yamato M, Okano T. Cell Sheet Engineering. Materials Today 2004;7:6.

[123] Fujita J. Cold shock response in mammalian cells. Journal of molecular microbiology and biotechnology 1999;1:243-55.

[124] Sonna LA, Fujita J, Gaffin SL, Lilly CM. Invited review: Effects of heat and cold stress on mammalian gene expression. Journal of applied physiology (Bethesda, Md : 1985) 2002;92:1725-42.

[125] Al-Fageeh MB, Marchant RJ, Carden MJ, Smales CM. The cold-shock response in cultured mammalian cells: harnessing the response for the improvement of recombinant protein production. Biotechnology and bioengineering 2006;93:829-35.

[126] Kim SJ, Jun I, Kim DW, Lee YB, Lee YJ, Lee J-H, et al. Rapid Transfer of Endothelial Cell Sheet Using a Thermosensitive Hydrogel and Its Effect on Therapeutic Angiogenesis. Biomacromolecules 2013;14:4309-19.

[127] Hyeong Kwon O, Kikuchi A, Yamato M, Okano T. Accelerated cell sheet recovery by co-grafting of PEG with PIPAAm onto porous cell culture membranes. Biomaterials 2003;24:1223-32.

[128] Hou Y, Matthews AR, Smitherman AM, Bulick AS, Hahn MS, Hou H, et al. Thermoresponsive nanocomposite hydrogels with cell-releasing behavior. Biomaterials 2008;29:3175-84.

[129] Haraguchi K, Takehisa T, Ebato M. Control of cell cultivation and cell sheet detachment on the surface of polymer/clay nanocomposite hydrogels. Biomacromolecules 2006;7:3267-75.

[130] Reed JA, Lucero AE, Cooperstein MA, Canavan HE. The effects of cell culture parameters on cell release kinetics from thermoresponsive surfaces. Journal of applied biomaterials & biomechanics : JABB 2008;6:81-8.

[131] Gallant ND, Garcia AJ. Quantitative analyses of cell adhesion strength. Methods in molecular biology (Clifton, NJ) 2007;370:83-96.

[132] Xu T, Zhao W, Zhu JM, Albanna MZ, Yoo JJ, Atala A. Complex heterogeneous tissue constructs containing multiple cell types prepared by inkjet printing technology. Biomaterials 2013;34:130-9.

[133] Lorber B, Hsiao W-K, Hutchings IM, Martin KR. Adult rat retinal ganglion cells and glia can be printed by piezoelectric inkjet printing. Biofabrication 2014;6:015001.

[134] Demirci U, Montesano G. Single cell epitaxy by acoustic picolitre droplets. Lab on a chip 2007;7:1139-45.

[135] Lee V, Singh G, Trasatti JP, Bjornsson C, Xu X, Tran TN, et al. Design and fabrication of human skin by three-dimensional bioprinting. Tissue engineering Part C, Methods 2014;20:473-84.

[136] Kushida A, Yamato M, Konno C, Kikuchi A, Sakurai Y, Okano T. Temperature-responsive culture dishes allow nonenzymatic harvest of differentiated Madin-Darby canine kidney (MDCK) cell sheets. J Biomed Mater Res 2000;51:216-23.

[137] Shimizu T, Sekine H, Yang J, Isoi Y, Yamato M, Kikuchi A, et al. Polysurgery of cell sheet grafts overcomes diffusion limits to produce thick, vascularized myocardial tissues. FASEB journal : official publication of the Federation of American Societies for Experimental Biology 2006;20:708-10.

[138] Kumar A, Whitesides GM. Features of gold having micrometer to centimeter dimensions can be formed through a combination of stamping with an elastomeric stamp and an alkanethiol ‘‘ink’’ followed by chemical etching. Applied Physics Letters 1993;63:2002-4.

[139] Jang M, Nam Y. Aqueous micro-contact printing of cell-adhesive biomolecules for patterning neuronal cell cultures. BioChip J 2012;6:107-13.

[140] Matsuura K, Haraguchi Y, Shimizu T, Okano T. Cell sheet transplantation for heart tissue repair. Journal of Controlled Release 2013;169:336-40.

[141] Tang Z, Akiyama Y, Okano T. Temperature-Responsive Polymer Modified Surface for Cell Sheet Engineering. Polymers 2012;4:1478-98.

[142] Boland T, Xu T, Damon B, Cui X. Application of inkjet printing to tissue engineering. Biotechnology journal 2006;1:910-7.

[143] Moon S, Hasan SK, Song YS, Xu F, Keles HO, Manzur F, et al. Layer by layer three-dimensional tissue epitaxy by cell-laden hydrogel droplets. Tissue engineering Part C, Methods 2010;16:157-66.

[144] Aubin H, Nichol JW, Hutson CB, Bae H, Sieminski AL, Cropek DM, et al. Directed 3D cell alignment and elongation in microengineered hydrogels. Biomaterials 2010;31:6941-51.

[145] Wüst S, Müller R, Hofmann S. Controlled Positioning of Cells in Biomaterials—Approaches Towards 3D Tissue Printing. Journal of Functional Biomaterials 2011;2:119-54.

[146] Takahashi H, Nakayama M, Shimizu T, Yamato M, Okano T. Anisotropic cell sheets for constructing three-dimensional tissue with well-organized cell orientation. Biomaterials 2011;32:8830-8.

[147] Gallant ND, Capadona JR, Frazier AB, Collard DM, García AJ. Micropatterned Surfaces to Engineer Focal Adhesions for Analysis of Cell Adhesion Strengthening. Langmuir : the ACS journal of surfaces and colloids 2002;18:5579-84.

[148] Elineni KK, Gallant ND. Regulation of cell adhesion strength by peripheral focal adhesion distribution. Biophysical journal 2011;101:2903-11.

[149] Choi YS, Vincent LG, Lee AR, Kretchmer KC, Chirasatitsin S, Dobke MK, et al. The alignment and fusion assembly of adipose-derived stem cells on mechanically patterned matrices. Biomaterials 2012;33:6943-51.

[150] Engler AJ, Rehfeldt F, Sen S, Discher DE. Microtissue Elasticity: Measurements by Atomic Force Microscopy and Its Influence on Cell Differentiation. In: Yu-Li W, Dennis ED, editors. Methods in Cell Biology: Academic Press; 2007. p. 521-45.

[151] Engler AJ, Griffin MA, Sen S, Bonnemann CG, Sweeney HL, Discher DE. Myotubes differentiate optimally on substrates with tissue-like stiffness: pathological implications for soft or stiff microenvironments. The Journal of cell biology 2004;166:877-87.

[152] Jawad H, Lyon AR, Harding SE, Ali NN, Boccaccini AR. Myocardial tissue engineering. British medical bulletin 2008;87:31-47.

[153] Zimmermann WH, Schneiderbanger K, Schubert P, Didie M, Munzel F, Heubach JF, et al. Tissue engineering of a differentiated cardiac muscle construct. Circulation research 2002;90:223-30.

APPENDIX A: COPYRIGHT PERMISSIONS

A.1. Permission to Use Published Contents in Chapter 3

ELSEVIER LICENSE
TERMS AND CONDITIONS

May 26, 2015

This is a License Agreement between Olukemi O Akintewe ("You") and Elsevier ("Elsevier") provided by Copyright Clearance Center ("CCC"). The license consists of your order details, the terms and conditions provided by Elsevier, and the payment terms and conditions.

All payments must be made in full to CCC. For payment instructions, please see information listed at the bottom of this form.

Supplier	Elsevier Limited The Boulevard,Langford Lane Kidlington,Oxford,OX5 1GB,UK
Registered Company Number	1982084
Customer name	Olukemi O Akintewe
Customer address	12118 Fern Haven Ave GIBSONTON, FL 33534
License number	3624391049074
License date	May 08, 2015
Licensed content publisher	Elsevier
Licensed content publication	Acta Biomaterialia
Licensed content title	Shape-changing hydrogel surfaces trigger rapid release of patterned tissue modules
Licensed content author	None
Licensed content date	1 January 2015
Licensed content volume number	11
Licensed content issue number	n/a
Number of pages	8
Start Page	96
End Page	103
Type of Use	reuse in a thesis/dissertation
Portion	full article
Format	both print and electronic
Are you the author of this Elsevier article?	Yes

Will you be translating?	No
Title of your thesis/dissertation	Fabrication of Tissue Precursors induced by Shape-Changing Hydrogel
Expected completion date	Aug 2015
Estimated size (number of pages)	120
Elsevier VAT number	GB 494 6272 12
Permissions price	0.00 USD
VAT/Local Sales Tax	0.00 USD / 0.00 GBP
Total	0.00 USD
Terms and Conditions	

INTRODUCTION

1. The publisher for this copyrighted material is Elsevier. By clicking "accept" in connection with completing this licensing transaction, you agree that the following terms and conditions apply to this transaction (along with the Billing and Payment terms and conditions established by Copyright Clearance Center, Inc. ("CCC"), at the time that you opened your Rightslink account and that are available at any time at http://myaccount.copyright.com).

GENERAL TERMS

2. Elsevier hereby grants you permission to reproduce the aforementioned material subject to the terms and conditions indicated.

3. Acknowledgement: If any part of the material to be used (for example, figures) has appeared in our publication with credit or acknowledgement to another source, permission must also be sought from that source. If such permission is not obtained then that material may not be included in your publication/copies. Suitable acknowledgement to the source must be made, either as a footnote or in a reference list at the end of your publication, as follows:

"Reprinted from Publication title, Vol /edition number, Author(s), Title of article / title of chapter, Pages No., Copyright (Year), with permission from Elsevier [OR APPLICABLE SOCIETY COPYRIGHT OWNER]." Also Lancet special credit - "Reprinted from The Lancet, Vol. number, Author(s), Title of article, Pages No., Copyright (Year), with permission from Elsevier."

4. Reproduction of this material is confined to the purpose and/or media for which permission is hereby given.

5. Altering/Modifying Material: Not Permitted. However figures and illustrations may be altered/adapted minimally to serve your work. Any other abbreviations, additions, deletions and/or any other alterations shall be made only with prior written authorization of Elsevier Ltd. (Please contact Elsevier at permissions@elsevier.com)

6. If the permission fee for the requested use of our material is waived in this instance, please be advised that your future requests for Elsevier materials may attract a fee.

APPENDIX B: EXPERIMENTAL METHODS

B.1. Cell Culture

Murine skeletal C2C12 myoblasts (American Type Culture Collection) and NIH/3T3 mouse embryonic fibroblast cells (American Type Culture Collection) were cultured in 15% or 10% newborn calf serum (NCS) growth medium respectively, 84% or 89% Dulbecco's Modified Eagle's Medium (DMEM) and 1% antibiotics (10,000 units/mL penicillin and 10,000 units/mL streptomycin) at 37 °C in a humidified atmosphere of 5% CO_2. All culture growth medium materials were purchased from Life Technologies.

C2C12 cells were maintained in culture up to passage number 15 while fibroblasts were used up to passage 25. Daily examination of the medium was performed to ensure normal growth rate, cell morphology and density. Cells were harvested either every 2 days or once the population density has reached 70% for C2C12 or 80% for fibroblast, whichever comes first. Harvesting of cells is performed in a laminar flow hood by decanting the old media with a sterile glass pipette into a waste collection container. Adherent cells were then rinsed with 10 mL of pre-warmed Dulbecco's phosphate buffered saline without Ca^{++} and Mg^{++} ions. 2 mL of cell dissociation agent, tryspin-EDTA (Ethylene diamine tetraacetic acid) was added and incubated for up to 10 minutes at 37°C to enzymatically release cells from the TCPS surface. Complete detachment of the cells is confirmed with an examination under an inverted optical microscope (NIKON 100X magnification). For a 1: 3 split, 4 mL of fresh medium was added to the cells and

immediately mixed in the fluid by pipetting up and down for at least 5 times to dislodge any aggregates of cells. 2 mL each of the cell suspension was dispensed into three 60 mm tissue culture polystyrene dish (Fischer Scientific). Then the dishes were incubated at 37 °C in a humidified atmosphere of 5% CO_2 until the next 2 days or experimental use.

B.1.1. Cell Counting

A Neubauer chamber hemocytometer (Celeromics, Grenoble, France) was employed for counting the cell population in each dispensed 35 mm sample-containing dish. 10 µL each was removed from the 100 µL of the stored cell suspension (see section B.1) and loaded into the chamber cavity on both ends without introducing bubbles or moving the chamber top glass cover. The center and four corners of the chamber squares were then counted on both sides to make a final count of 10 squares. The number of cells per volume in a sample dish was calculated as follows in equation 1.

$$\text{Concentration (cells/mL)} = \frac{\#\ \text{of cells x } 10^4}{\#\ \text{of squares} \times \text{dilution}} \quad (1)$$

B.1.2. Cell Seeding on Stamps

For experimental use, once the attached cells have been released from the TCPS surface, the 2 mL of trypsin-EDTA was removed and transferred into a 50 mL conical tube. Fresh medium was then added into the flask to make a total 10 mL. For multiple dishes of cells, the total medium in the tube changes by 8 mL from the total number of cell suspension. The tube is then centrifuged at 1000 RCF for 2.5 minutes. The supernatant fluid was gently decanted by using a pipette and fresh medium was added to the tube in the hood. Then immediately pipette the cells up and down until the cell pellet was completely dislodged. For cell counting purposes, a 100 µL of the cell suspension was placed into a micro-centrifuge tube and stored until use.

While the remaining cell suspension was dispense in samples of 2.5 mL each in a 35 mm TCPS. Cells are seeded onto fabricated shape-changing hydrogel arrays at a density of 500 -750 cells/mm^2 and cultured at 37 °C until confluence, typically 24 to 48 hours.

B.2. Fabrication of Geometrically Patterned Shape-Changing Hydrogel Stamps

Geometrical patterning of shape-changing hydrogel is prepared by implementing three main steps; 1) Development of master mold, 2) Silanization of glass substrate and 3) Polymerization of shape-changing stamps.

B.2.1. Development of Master Mold

A mask with different length and width dimensions was designed with AutoCAD and a mask aligner (Karl Suss model no.) is used to develop a negative template by employing soft lithography technique (Figure 3-1). A 4-inch silicon wafer was cleaned with acetone followed by methanol, water and then dried with nitrogen gas. The cleaned wafer was then solvent bake at 150 °C for 5 minutes and plasma cleaning for 5 minutes at 150 watts to promote efficient adhesion to photoresist. Then a SU-8 2025 negative photoresist was gently cast onto the center of the wafer after being placed on a spin coater (Laurel WS400A). The spinner was set to 500 rpm for 10 seconds in step 1 and 4000 rpm for 30 seconds in step 2. After spinning, the wafer was prebaked at 65 °C for 1 minute and then 95 °C for 5 minutes with 2 to 3 minutes of dwell time subsequently. The prebaked wafer was mounted to the Karl Suss mask aligner with a setting of 150 mJ/cm^2 and an exposure time of 5 seconds. Then post bake at 65 °C for 1 minute and then 95 °C for 4 minutes followed by turning off the heat source to gradually cool wafer. The exposed wafer was then submerged in a developer and gently swirled for 5 minutes to dissolve the resist. Then the wafer was rinsed with isopropanol and nitrogen dry. The template was then examined under an optical microscope to verify proper transfer of features from the mask and adjustments

were made accordingly either to the exposure time and energy or develop time. A profilometer (Tencor Alpha-step 200) was then used to measure the resulting height of the features on the template. Finally, the wafer was hard baked at 95 °C for 5 minutes prior to casting polydimethylsiloxane (PDMS) for the master mold. To prepare the master molds, approximately 12 g of Silicone elastomer kits (Sylgard®184) was mixed at 10:1 and completely de-aerated. The degassed mixture was then cast onto the developed wafer and cures at 65 °C for at least 1 hour.

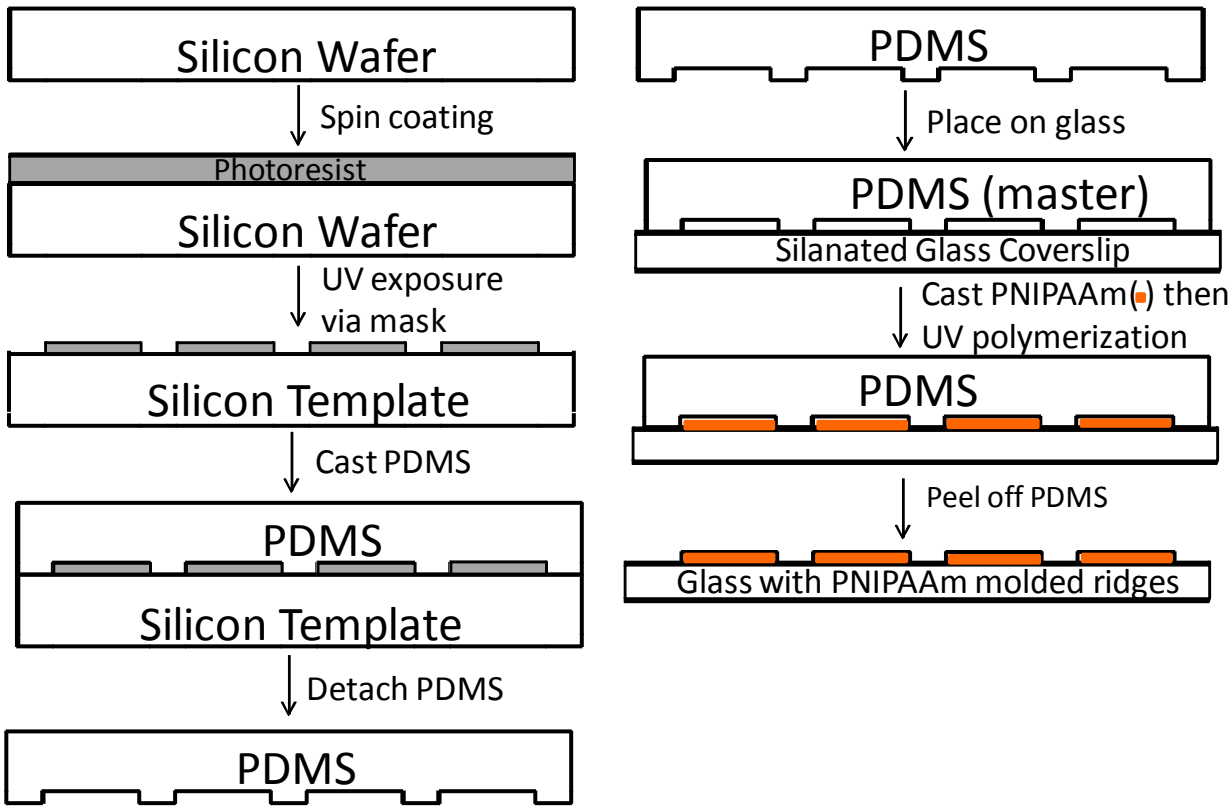

Figure B-1: Fabrication of shape-changing stamps via soft lithography technique.

B.2.2. Silanization of Glass Substrates

Glass coverslips (22 mm x 22 mm, #1.5) were used as substrates to create covalent attachment to the shape-changing hydrogel. The glass coverslips were plasma treated at 100 W

for 5 minutes in an oxygen plasma chamber (Plasma Etch, PE 50) and then submerged in a solution containing 1mM of 3-(trichlorosilyl)propyl methacrylate (Sigma Aldrich), added to a 4:1 ratio of heptane and carbon tetrachloride under a oxygen free environment. After 8 minutes in the solution, the coverslips were removed and rinsed in hexane and deionized water subsequently for 5 minutes each. The glass substrates were then nitrogen dried and stored in a desiccator until use.

B.2.3. Polymerization of Shape-changing Stamps

Fabrication of the shape-changing stamp (Figures B-2) was prepared by employing the micromolding in capillaries (MIMIC) method and photo-polymerization process (Figures B-1). Prepolymer solution was prepared by mixing 1-4% crosslinker (5 mg/mL), 10% 2-dimethoxy-2-phenylacetophenone (20 mg/mL) photo initiator in 250-mg/mL solution of N-isopropylacrylamide in acetone. All materials were purchased from Sigma Aldrich. Under nitrogen environment, the solution was cast into a precut PDMS template (section B.2.2) by placing the template with desired dimension on the silanated glass coverslip with the features face down. 30 μL of the solution was then pipetted into the side channel of the mold. An alternative to the MIMIC method was to use a compression mold method whereby the solution was first added to the glass while the mold was gently compressed on top. Immediately, the solution was crosslinked at 350 nm of ultra violet light for 4 minutes. The PDMS mold was detached from the glass surface by gently pulling off and the resulting fabricated pNIPPAAm arrays were then sequentially rinsed with acetone, ethanol and water to remove any unpolymerized monomer.

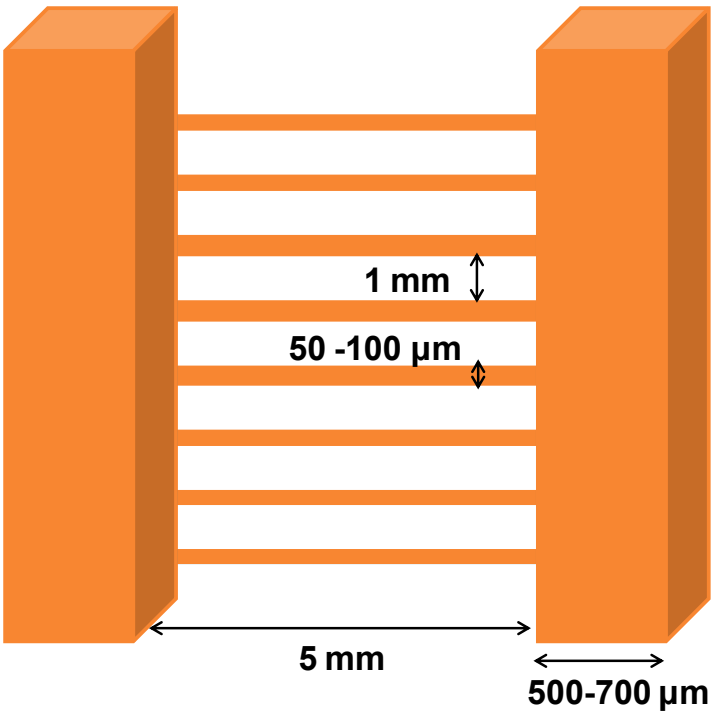

Figure B-2: Shape-changing stamp fabricated from poly-*N*-isopropylacrylamide.

B.3. Preparation of Stamps for Cell Seeding

Fabricated arrays of the shape-changing hydrogel were prepared for cell culture by adsorbing a cell adhesion promoter to the surfaces. 50 µL of 0.1 mg/mL of polylysine (PLL) solution (Sigma-Aldrich) was added to the stamps for 5 minutes, aspirated and then rinsed twice in DPBS. Then the surfaces were air-dried in a laminar hood for at least 2 hours prior to cell seeding.

A sterilization process is performed for re-used stamps. Stamps with pre-detached cells were sterilized by submerging in 70:30 ethanol-water mixtures for 5 minutes. Stamp was then allowed to stand for 20 to 30 minutes to evaporate the residual ethanol followed by a 2X rinse in DPBS with Ca^{++} and Mg^{++} ions. Then the stamps were re-coated with the polylysine solution.

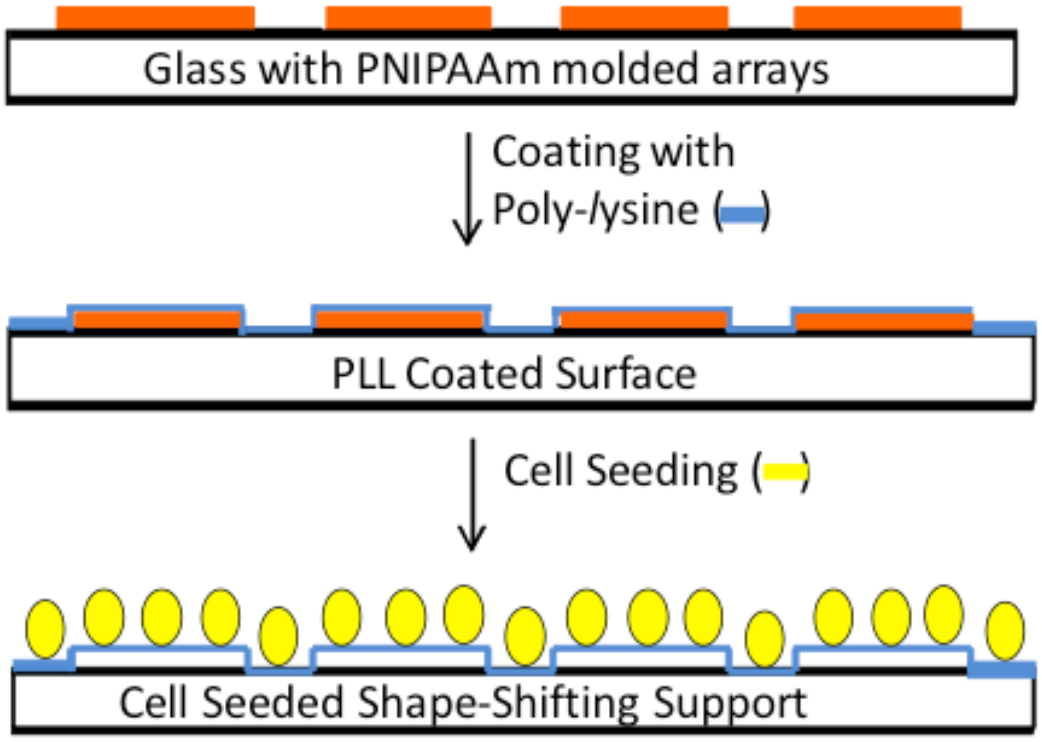

Figure B-3: Preparation of shape-changing stamps for cell culture.

B.3.1. Analysis of Stamp Arrays for Residual Adsorbed Protein

Arrays of polyisopropylacrylamide hydrogel (stamps) were coated with 1 mg/mL of PLL FITC labeled (MW 15,000-30,000, Sigma-Aldrich). FITC-PLL solution was adsorbed on 4 stamps for 5 minutes, rinsed twice with PBS and allowed to air dry for 2 hours. Two stamps were then seeded with NIH/3T3 fibroblast cells (~500 cells/mm^2) while the others were incubated in the plain standard growth medium without cells. After 24 hours of incubation at 37 °C, the media from all four samples were replaced with warm PBS and allowed to incubate for at least 30 minutes. Warm PBS in all samples were removed and stored while a cold PBS (~10°C) was added to initiate expansion of the arrays and thus release cells from the 2 samples followed by an incubation for 30 minutes at 4°C. Samples with released cells were centrifuged and the supernatant was stored. The removed medium and PBS supernatant before and after swelling

were examined with a NanoDrop 1000 spectrophotometer (Thermo Fisher Scientific) for presence of the poly-*l*-lysine FITC labeled biomolecule.

B.4. Method of Cell Release from Stamps

Detachment of tissue modules from shape-changing hydrogel occurs by a reduction of the stamp temperature, which induces a strain on the hydrogel causing a lateral swelling of the microbeams. A strain of at least 25% (section 3.3.4) was necessary to induce sufficient amounts of lateral force required to detach the tissues. Rapid release of the modules occurs almost instantaneously when the hydrogel was brought in contact with cold DPBS. 2 mL of a 4-10 °C DPBS was introduced into the culture dish at 1 mL at a time to give a final temperature of approximately 27 °C. A time-lapse image acquisition was used to monitor the cell release.

B.5. Micro-contact Printing of Tissue Modules

Printing of cells onto a target surface was conducted by adapting the micro-contact printing technique established by Whitesides [36].

B.5.1. Preparation of Target Surface

The target surface could be a layer of cell sheet or a plain glass surface. In the case of glass target, the surface was prepared to promote successful cell transfer by adsorbing cell adhesion promoters. A circular glass coverslip (25 mm, #1.0) was plasma treated at 100 W for 5 minutes and then either 10 μg/mL of human plasma fibronectin (Life Technologies) was adsorbed for 30 minutes or 100 μg/mL of bovine collagen type I (Advanced BioMatrix) for 3 hours, or 0.1 mg/mL of PLL for 5 minutes and then air dry for 2 hours in ambient. Immediately after the time point, the protein solutions were rinsed twice with DPBS and stored in the incubator at 37 °C until use.

A cell sheet target surface involves adsorption of a protein layer after a confluent cell sheet has been achieved. A 3D collagen gel was prepared by slowly adding 1 part of 10X PBS with 8 parts cold collagen solution at 3 mg/mL with gentle swirling for 30 seconds. Gradually added 700 mL of 0.1 M of sodium hydroxide (NaOH) in 100 mL increments until a pH of 7.3 was achieved. Slowly 50 mL of deionized water was added to adjust the final volume to a total of 10 parts. 1 mL of the collagen solution was then added to a 35 mm cell culture dish containing confluent cells with media removed and rinsed with DPBS. To form gel, the dish was cured at 37 °C for 90 minutes, while the remaining batch of collagen solution was stored at 4°C until use.

B.5.2. Printing of Cells on Target Surfaces

Once cells on the stamps were confluent (section B.1.2) typically within 24 to 48 hours, the glass coverslip containing the covalently bound pNIPPAAm arrays (Shape-changing hydrogel) were gently removed from the medium and a known weight was adhered to the backside with a double-sided tape. To promote proper adhesion, the back of the glass was dried off with a Kleenex wipe. The added weight allows conformal contact to the target surface. The glass was then gently placed on top of the target surface, which contains 1 mL of media. Immediately the mated surfaces were placed incubated at 37 °C for 15 minutes to stabilize the cells on the target surface. Printing of the cells occurs by subjecting the mated surfaces to a rapid cold environment at 4°C for 5 minutes. The weight with the stamp was gradually lifted off the target surface while the tissue was printed on the target surface. Due to the temperature change below the stamp-hydrogel lower critical solution temperature (LCST), a lateral expansion occurs sufficient enough to disrupt the bond between the extracellular matrices (ECM) from the surface of the stamp. And the tissue module was successfully printed on the target surface.

B.5.3. Stamp Force Analysis

A force analysis was conducted to examine the appropriate compressive pressure necessary to induce an optimum viable cell. This analysis was determined by varying the amount of pressure applied to the stamp during printing onto the target surface. To establish the optimal load required, calibration weights in 20g, 10g, 5g, 2g or 1g were separately applied to the backside of the stamp while in contact to the target. After duration of 5 minutes at 4 °C, the load and stamp was gently removed and viability of the printed cells was assessed as described in section B.6.1. The corresponding compressive load applied is tabulated in Table B-1.

Table B-1: Compressive pressure applied during printing of tissues

Weight (g)	**Force** (N)	**Pressure** (N/mm^2)	**Force** (lbf)	**Pressure** (psi)
1	0.01	0.005	0.0022	0.71
2	0.02	0.01	0.0045	1.45
5	0.05	0.025	0.011	3.55
10	0.1	0.05	0.022	7.10
20	0.2	0.1	0.045	14.5

Surface area of stamp: 8 beams by 50 μm width by 5 mm long = 2 $mm^2 \approx 0.0031$ in^2

B.6. Cell Analysis

The viability and metabolic activity of the tissue modules were analyzed before and after printing to evaluate cell fate.

B.6.1. Evaluation of Cell Viability

A combined Live/Dead kit containing two components, calcein AM and ethidium homodimer-1 (Molecular Probes, Invitrogen) fluorescent molecules were used to assess the viability of cells. The staining stock solution diluted in PBS for a final concentration of 40 μM for calcein AM and 20 μM for ethidium homodimer and then vortex for thorough mixing. A 150 to 300-μL of the working solution was directly added to a rinsed surface of a cell sheet (control samples) and/or printed cells such that the cells are completely in contact with the dye solution. The cells were then incubated for 15-30 minutes at 37 °C followed by a rinse with warm PBS and a fresh warm medium was added. The stained sample was then viewed under a fluorescence microscope. Cells with red fluorescence indicate dead cells while green cells represent the live cells. The number of viable cells per sample was determined using the equation 2.

$$\text{Viability of cells (\%)} = \frac{\#\text{ of live cells}}{\text{total }\#\text{ of cells (live+ dead)}} \times 100 \quad (2)$$

B.6.2. Preparation of Cell Tracker Probes

Fluorescent cell tracker probes, Green CMFDA and Orange CMTMR (Molecular Probes, Invitrogen) were used to trace live cells. A working solution was prepared by separately diluting each probe in PBS to give a final concentration of 5 μM. Cells were stained either in suspension or attached to the 35mm dish. For cells in suspension, cells were centrifuged at 1000 RCF for 2.5 minutes and the supernatant is aspirated while the cells are resuspended in pre-warmed working solution. While for adherent cells, the medium was replaced with pre-warmed working solution. The cells were then incubated for 30 minutes at 37 °C. The dye solution was replaced with serum free medium and incubated for another 30 minutes at 37 °C to allow secretion of the

chloromethyl groups from the cells. Then the cells were rinsed with PBS and resuspended in standard growth medium until imaging.

B.6.3. Immunofluorescence

Tissue modules were examined for preserved cellular physiology by staining cells with immunofluorescence molecules after fixation. Control and test samples were washed twice with PBS then fixed in ice-cold 3.7% formaldehyde (Sigma-Aldrich) for 5 minutes followed by a permeabilization step in cold cytoskeleton buffer (CSK) with Triton X-100 (Sigma-Aldrich) and protease inhibitors for 10 minutes. Non-specific adsorption was prevented by adding a blocking buffer that was composed of 5% NCS and 0.01% sodium azide (NaN_3, Sigma-Aldrich) in complete DPBS for at least 1 hour. Then cells were incubated cells with 1: 100 primary antibodies diluted in blocking buffer for an hour. The cells were washed three times with DPBS for 5 minutes each followed by incubation in a blocking buffer solution of Alexa Fluor 488 secondary antibodies, 1:200 or 1:100 goat anti-rabbit IgG secondary antibodies conjugated and 1: 50 Alexa Fluor 568 phalloidin and 1:2000 Hoechst 33342. The samples were then covered in a dark place for an hour and then rinsed three times with DPBS for 5 minutes each followed by another rinsing step in deionized water to prevent salt crystallization. The samples were then mounted on No. 1.5 glass slide with mounting media and the edges were sealed with clear nail polish to prevent drying and air bubbles.

B.6.4. Imaging and Analysis

Micrographs and time lapse video images (60 fps) of the cell morphology, release and viability were all captured by an Elipse Ti-U microscope (Nikon Instruments) equipped with a CCD camera (CoolSNAP HQ2, Photometrics, Tuscon) and a 10X, 40X and 60X objective lens

using either a phase contrast or DIC filter. The images were analyzed with NIS Elements advanced research software version 4.20 (Nikon Instruments).

ImageJ v1.49s (NIH, USA) was employed for cell counting and orientation analysis. For printed patterned cells, the orientations of cells were obtained by measuring the angle between the cell morphology and the reference origin, typically the longitudinal axis. While in the control samples in which the cells were randomly distributed, the angle between major and minor axis of the cells were measured.

B.6.5. Data Analysis

Minitab statistical tools were used for data analysis. For pairwise comparison, either a two-tailed Student's t-test or a single factor ANOVA test was used followed by Tukey's test where $p < 0.05$ was considered statistically significant. In general, a sample size of $n \geq 3$ was used in all experiments.

Cell alignment data was determined from the orientation distribution values as the average amount of cells oriented within ± 10° of the preferred angle of orientation i.e. longitudinal axis of the hydrogel array.

ABOUT THE AUTHOR

Olukemi “Kemi” was born in Washington, D.C and raised in Lagos, Nigeria. She earned her Bachelors of Engineering degree in Chemical Engineering at the City College of New York (CCNY) of the City University of New York (CUNY) in 2002. She went on to receive her Masters in Materials Science and Engineering at The Ohio State University (OSU) in 2005. She worked as an adjunct faculty in the department of Biological & Physical Sciences at the Columbus State Community College (CSCC) for about a year. She was then employed as a U.S. defense contractor for 4 years in Wausau, Wisconsin and then Orange, Virginia before pursuing her doctorate’s degree in Chemical Engineering at the University of South Florida (USF).

During her tenure at USF, she led STEM tours for younger students K-12 for the Girls Inc. of Pinellas County, National Girls Collaborative Project of Florida and MOSI’s Summer Science Camp. She also mentored high school student for the TRIO Upward Bound program and a number of USF undergraduates. She is the co-founder and president of the American Association of University Women (AAUW) STEM chapter at USF, an organization formed by female doctoral graduate students to foster a sense of community among their peers.

Kemi has been awarded an NIH-funded postdoctoral fellowship in the NHLBI-sponsored Multidisciplinary Research Training Program at the Whitaker Cardiovascular Institute of the Boston University School of Medicine. Her career mission is to become an emerging leader in the field of tissue engineering while serving as an educator who can inspire the next generation of scientists and engineers.